The Mechanism of Endoplasmic Reticulum Oxidoreductase α (Ero1α) Inactivation

Colin Shepherd BSc (Hons) Biochemistry

Supervisor: Prof. Neil Bulleid

Submitted in fulfilment of the requirements for the Degree of Doctor of Philosophy

Institute of Molecular, Cell and Systems Biology

University of Glasgow

April 2012

Summary

Ero1α is a resident ER oxidase and is an important member of the oxidative protein folding machinery. It generates disulphide bonds *de novo* and donates them to protein disulphide isomerase (PDI), which in turn oxidises nascent substrate proteins within the ER. Ero1 activity must be tightly regulated for two key reasons: (i) it must maintain the balance of oxidised PDI to ensure oxidative protein folding can occur, but cannot be so active that the ER becomes hyperoxidising and dysfunctional, and (ii) Ero1 activity must be regulated to prevent the accumulation of hydrogen peroxide, a reactive oxygen species (ROS), within the ER. The regulation of Ero1α comes principally from 3 intramolecular disulphide bonds which are reduced by substrate upon activation, and re-oxidised upon inactivation by an unknown mechanism. Using an SDS-PAGE based assay we tested three hypotheses: that sulphenylation by Ero1α-produced hydrogen peroxide could induce re-oxidation; that an internal disulphide exchange mechanism could generate and distribute disulphide bonds within Ero1α; and that ER oxidoreductases could act to inactivate Ero1α. Having successfully expressed, purified and characterised a recombinant version of Ero1α, this was tested in a number of assays to address the above hypotheses.

In vitro findings show that Ero1α is specifically and rapidly oxidised by ERp46 and PDI. Sulphenylation and internal disulphide exchange-mediated oxidation of Ero1α provided a comparatively slow and incomplete method of re-oxidation. *In vivo* results suggest that ERp46 and PDI may have implications in Ero1α activity regulation. Overexpression of several ER oxidoreductases had no effect on Ero1α re-oxidation after DTT challenge, whereas Ero1α oxidation was impaired slightly in PDI- ERp46 double knockdown cells. Depletion of PDI from cells results in the DTT-resistance of Ero1α, suggesting that Ero1α, PDI and glutathione are involved in an intricate mechanism of sensing and reacting to ER redox conditions.

Two key ER oxidoreductases, PDI and ERp57, are oxidised in semi-permeabilised cells. Oxidation coincides with permeabilisation of the plasma membrane and the removal of cytosolic glutathione, directly implicating glutathione in the maintainence of the redox states of ER oxidoreductases. Oxidation during the permeabilisation of cells is an enzymatic process which is mediated in part by Ero1α. Semi-permeabilised cells harbour a more oxidising environment than do microsomes.

This study contributes significantly to the research field by complementing several previously reported findings, as well as providing a novel investigation into the molecular regulation of Ero1α and its relationship with PDI and glutathione in the cell.

Table of Contents

List of Figures

Acknowledgement

Firstly, I must state my thanks and deep appreciation to my supervisor, Professor Neil Bulleid, who designed this study and gave his time, effort, equipment and much of his sanity to help me with the techniques and assays throughout. He was constantly available to help with problems, discussions and ideas and pushed me to see through the experiments and this thesis. I must also express my gratitude to Prof. Bulleid for giving me the opportunity to work with him on this project and the chance to begin a (hopefully) long and successful career in the ever more challenging and competitive field of academic research. Indeed, my future career in any vocation will be as a result of Prof. Bulleid's guidance during the last three and a half years. My gratitude cannot be overstated.

Secondly, this study would not have been possible without the help and guidance of Prof. Bulleid's talented postdoctoral research assistants and technicians – Dr. Ojore Oka, Dr. Zhenbo Cao, Dr. Marcel van Lith, Dr. Jana Rudolf, Marie-Anne Pringle and Donna McGow. Dr. Oka's and Dr. Cao's help and advice were invaluable throughout my studies, from molecular biology techniques to protein purification and cell assays. Indeed, a number of purified proteins were gifts of Dr. Oka and Dr. Cao. Not all of their advice was useful, though, as the Fantasy Football table might suggest...

Dr. Timothy Tavender, a former postdoctoral research assistant of Prof. Bulleid, also provided reagents for use in this study. I must thank each of the above, in addition to Rachael Martin and Greg Poet, for their help and advice throughout my time as a student, and for making my time in the lab enjoyable.

Thank you also to Professors Gordon Lindsay, Bill Cushley, Richard Cogdell and Gwyn Gould, who each instilled within me a passion and interest in science during my four years of undergraduate study. If it wasn't for them, I would not have undertaken a Ph.D.. Thank you for making learning enjoyable.

I must also thank my family for their support and hard work for countless years, allowing me to pursue my studies and for being such great role models. I hope that I have made you both proud.

Last but not least, thank you to Lauren who has helped me through the last year and made it bearable. Without such a mischevious wee monkey I'd have been lost. Thank you for being so generous and I will repay the favour soon! I promise!

Author's declaration

I declare that, except where explicit reference is made to the contribution of others, this thesis is the result of my own work and has not been submitted for any other degree at the University of Glasgow or any other institution.

Colin Shepherd

April 2013

Abbreviations, units and symbols

α - alpha

β - beta

ºC – degrees centigrade

µg - microgram

µl - microlitre

µM - micromolar

µm – micrometre

% - percent

BSO – buthionine sulphoximine

Cys - cysteine

dH_2O – distilled water

DNA – deoxyribonucleic acid

DTT - Dithiothreitol

DPS - 2, 2'-Dithiopyridine

EDTA – ethylenediaminetetraacetic acid

ER - endoplasmic reticulum

FAD - flavin adenine dinucleotide

g – grams

g/l – grams/litre

x g – times standard gravitational force

GSH – glutathione (reduced)

GSSG – glutathione (oxidised)

IPTG – isopropyl β-D-1-thiogalactopyranoside

kDa - kiloDalton

Da - Dalton

l - litre

LB – Luria-Bertani (medium)

M - molar

mg - milligram

min - minutes

ml - millilitre

mM - millimolar

mRNA – messenger ribonucleic acid

NAC – N-acetylcysteine

nm - nanometer

nM - nanomolar

ROS - reactive oxygen species

RNA- ribonucleic acid

rpm – revolutions per minute

SDS – sodium dodecylsulphate

SDS-PAGE – sodium dodecylsulphate – polyacrylamide gel electrophoresis

TEMED – N, N, N’, N’ – tetramethylethylenediamine

UPR – Unfolded protein response

v/v – volume/volume

w/v – weight/volume

WT – wild type

CHAPTER 1.0
Introduction

Proteins are essential to the workings of cells and biological processes. They perform a variety of functions and roles, from providing physical strength and support in the case of actin, myosin and tubulin, to carrying oxygen around the body in the case of haemoglobin. Integral to the functioning of a protein is its native three-dimensional structure – this must be adopted otherwise enzymatic activity is abolished. The primary structure of proteins initially has no defined secondary or tertiary structure and is deemed to be in a random coil state. Hydrogen bonding between amino acids in the polypeptide backbone is facilitated by multiple C=O and N-H groups and this form of bonding gives the primary sequence a degree of rigidity and stability. Hydrogen bonding in the backbone can result in α-helical (Pauling and Corey, 1951a), or β-sheet structure (Pauling and Corey, 1951b). These structures, termed secondary structure, contribute to the natively folded protein. A further driving force in protein folding is hydrophobicity. Hydrophobic amino acids favour an environment free of water and so tend to cluster together in the middle of the protein where hydrophobic interactions stabilise the conformation, allowing hydrophilic amino acids to interact with the water-based surrounding environment. These interactions drive the folding of proteins and allow the adoption of their unique tertiary and quaternary structure, thus facilitating functionality.

Disulphide bonds provide an extra degree of structural stabilisation and form between the side chain sulphydryl groups of two cysteine residues. Disulphide bonds also help proteins form tertiary and quaternary structure, effectively pinning parts of the molecule together. Many disulphide-containing proteins will not function until the correct disulphide bonds are formed within the molecule; an indication of their importance. Furthermore, studies have shown that cells deficient in disulphide formation are sensitive to stresses. Disulphide bonds are formed in proteins destined for life in the extracellular environment or within the plasma membrane. Due to their covalent nature they have increased stability and specialised function compared to hydrogen bonding or hydrophobic interactions. Disulphides are introduced into proteins in a specific process called oxidative protein folding; a pathway involving many enzymes which are conserved in eukaryotes. A number of diseases, such as ischemia, Parkinson's, Creutzfeldt-Jakob disease (CJD) and various forms of Alzheimer's, are linked to the misfolding of proteins. It is therefore crucial that proteins are folded and function correctly to avoid these debilitating diseases.

1.1 Oxidative protein folding

1.1.1 Disulphide bond formation.

Disulphide bond formation in proteins was first discovered to be a product of air oxidation (Anfinsen et al., 1961). Anfinsen used the model protein ribonuclease to investigate disulphide bond formation after treatment with β-mercaptoethanol and urea. This treatment leaves the enzyme in a reduced and denatured state with no ribonuclease activity. After removal of the reducing and denaturation agents, activity of the enzyme was followed as an indication of the folding status. The study showed that ribonuclease activity returns slowly over the course of 10-20 hours, suggesting that the native disulphide bonds have re-formed. Considering the kinetic data collected in this study, the authors concluded that disulphides can form by air oxidation and that the rearrangement of incorrectly formed, or non-native, disulphides is driven thermodynamically. However, in reality this mechanism of disulphide bond formation is too slow given the particular demands placed on the endoplasmic reticulum within secretory cells and tissues. The cell has therefore evolved a highly efficient and extremely specialised oxidative protein folding pathway which can provide the disulphide bonds, and proteins, required to allow the cell to survive and thrive in its environment, while at the same time maintaining fidelity. This function is provided by the endoplasmic reticulum (ER).

1.1.2 Oxidative protein folding; the role of the ER.

Secretory proteins differ from cytosolic proteins in that they need an extra degree of folding and stability to survive in the harsh extracellular environment. Secretory proteins usually contain an N-terminal signal sequence which directs them to the ER. This N-terminal signal sequence is hydrophobic in nature and binds to the signal recognition particle (SRP). SRP stalls translation and chaperones the ribosome-mRNA complex to the ER membrane where it interacts with the Sec translocon. Here SRP dissociates, translation re-starts and the nascent protein is co-translationally translocated through the Sec translocon pore into the ER lumen (Swanton and Bulleid, 2003). The ER is a highly specialised compartment which promotes protein folding and ensures that proteins exiting this organelle are folded correctly and appropriately glycosylated before being released from the cell.

One particular property of the ER that contributes significantly to the protein folding process and differentiates this compartment from the cytosol is the physico-chemical composition. The ER environment is considerably more oxidising due to the glutathione composition and contains a relatively high concentration of calcium. Calcium is known to be stored within the ER at high concentrations of up to 1mM (Somlyo et al., 1985,

Meldolesi and Pozzan, 1998), and is actively pumped into the ER by calcium ion pumps (reviewed by (Moller et al., 2010)). Calcium is essential for the correct folding of many proteins within the ER such as the asialoglycoprotein receptor (Lodish et al., 1992) and α-1 antitrypsin (Cooper et al., 1997, Lodish and Kong, 1990). With a perturbed calcium content, these proteins are misfolded and do not move through the secretory pathway. Many of the resident chaperones and protein folding enzymes contained within the ER have been shown to bind calcium; GRP94 is thought to have 15 calcium binding sites (Van et al., 1989). The binding of calcium triggers a conformational change which is thought to regulate its activity (Van et al., 1989). Other ER resident proteins known to bind calcium include GRP78/BiP, p50, PDI, ERp72, and calreticulin (Nigam et al., 1994). In a low calcium environment calreticulin is susceptible to proteolysis which indicates that calcium is needed for the enzyme to fold correctly (Corbett et al., 2000). Furthermore, PDI was found to bind calreticulin at low calcium concentrations, resulting in impaired PDI activity (Baksh et al., 1995). This binding is reversible upon increasing calcium concentrations and is coupled to an increase in PDI activity. The binding of ERp57 to calreticulin enhances ERp57 activity (Zapun et al., 1998) and is mediated by the binding of calcium to calreticulin (Corbett et al., 1999). Calcium therefore plays an essential role with regards to mediating activity of the folding enzymes and molecular chaperones provided by the ER. Without the high concentrations of calcium many chaperones fail to function, leading to protein misfolding. This is one specific way in which the ER provides a highly specialised environment to catalyse protein folding.

As well as providing a calcium rich environment, the ER also contains another protein folding aide – the tripeptide glutathione. Glutathione is present in the cytoplasm as well as the ER, although the ratios of the two redox forms of glutathione differ between the compartments. Glutathione contains a redox active cysteine residue which, in its free thiol state, classifies the reduced species (GSH). This free thiol can form a disulphide with the thiol of a cysteine within another glutathione molecule forming the oxidised species glutathione disulphide (GSSG). The cytoplasmic redox conditions are reducing (Ostergaard et al., 2004) compared to the ER and as a result disulphide formation generally does not occur here (Hwang et al., 1992). This is explained largely by the cytosolic glutathione ratio, the ratio of reduced to oxidised glutathione (GSH: GSSG), of between 10:1 and 100:1 which creates a redox potential of around -220 mV (Hwang et al., 1992). By comaparison, the glutathione ratio in the ER is between 1:1 and 3:1 creating a redox potential of around -170 mV (Hwang et al., 1992). This low ratio of GSH: GSSG is very close to the optimal ratio for oxidative protein folding determined *in vitro* to be 5:1 (Lyles

and Gilbert, 1991). Glutathione was, therefore, thought to be the source of oxidising equivalents for disulphide formation (Hwang et al., 1992). However, evidence is mounting to suggest it actually balances the oxidative activity of Ero1 and has been shown to facilitate protein folding in a novel way. It creates the necessary reducing pathway to support isomerisation (Chakravarthi and Bulleid, 2004), and maintains some of the folding catalysts in the reduced state required for their roles in their respective pathways (Jessop and Bulleid, 2004) . What is less well known is how this ratio of glutathione is maintained within the ER. The enzymes involved in glutathione synthesis are located within the cytosol and so some mechanism of transport must exist to import it into the ER. GSH uptake across microsomal membranes has been shown, however the membrane was impermeable to GSSG (Banhegyi et al., 1999). Contradictory studies have shown that radiolabelled GSSG can cross the membrane in a seemingly selective manner (Hwang et al., 1992) and so there is still a debate as to the mechanism of glutathione transport into the ER and the creation of the glutathione-based oxidising redox environment.

The ER provides a specialised environment in which secretory proteins can adopt their native conformation prior to secretion. The ER houses the folding factors such as PDI, calnexin and calreticulin and harbours a physico-chemical environment distinct from the cytosol as calcium and oxidised glutathione levels are elevated. While the glutathione transport mechanism is not well characterised, the mechanism of retention of the ER-resident enzymes has been studied. This mechanism retains the protein folding machinery in this organelle thus facilitating ER function.

1.1.3 ER-resident proteins are retained within the compartment.

As the ER forms part of the secretory system, it is a thoroughfare for each nascent protein destined either for plasma membrane incorporation or for secretion. As such, there is a net movement of proteins from the cytosol to the ER, Golgi and on to the respective destinations in an anterograde fashion. While this movement is necessary for cargo proteins, the ER-resident enzymes must be kept within the ER in order to function. An elegant mechanism of protein retrieval from the Golgi has evolved in order to facilitate ER-retention and is based on two essential components, the KDEL retrieval motif and the KDEL receptor (Erd2). The KDEL motif and receptor work together to provide retrograde movement, preventing ER-residents from travelling further along the secretory pathway. The KDEL motif is located at the C-terminus and without it bona-fide ER-resident proteins are no longer retained in the ER (Munro and Pelham, 1987). Similarly, incorporating the KDEL sequence into the C-terminus of non-ER resident proteins results in their retention (Munro and Pelham, 1987). The KDEL sequence is so called as it contains lysine-

aspartate-glutamate-leucine although there are slight variations of the sequence that still facilitate retention; for example RDEL allows the localisation of ERp44 to the ER (Anelli et al., 2003). The motif is charged and so is affected by pH which is central to the retention mechanism – the KDEL receptor binds the KDEL ligand under acidic conditions and releases it in neutral conditions (Wilson et al., 1993). The pH within the ER is thought to be approximately neutral while the Golgi is more acidic (Anderson and Pathak, 1985) thus a pH gradient is created (Wu et al., 2001). The KDEL receptor therefore binds its ligand in the relatively acidic Golgi before the complex associates with the retrograde transport machinery (Aoe et al., 1998) and is directed back towards the ER. Once the complex reaches the ER, the neutral pH causes its dissociation resulting in the release of the ligand-containing ER-resident enzyme and the release of the receptor. The receptor then moves on in an anterograde fashion to the Golgi where it can associate once more with the KDEL ligand, completing the retrieval cycle (Figure 1.1). This provides an effective mechanism for the retention of essential ER-resident enzymes.

Not all ER-resident proteins contain the KDEL sequence, however, and are retained within the ER by other mechanisms. One such process is the di-lysine and di-arginine mechanism that exists in ER integral membrane proteins. Type I integral membrane proteins, which have a luminal N-terminus, containing a C-terminal di-lysine motif are thought to be retrieved from the Golgi as they remain ER-localised with Golgi-modifications (Jackson et al., 1993, Nilsson et al., 1989). Type II integral membrane proteins, with a luminal C-terminus, are thought to be retrieved and retained within the ER by an N-terminal di-arginine motif (Schutze et al., 1994). The di-lysine and di-arginine motifs do not exist exclusively in type I and type II proteins respectively, as evidence suggests that some type I proteins may contain the di-arginine motif. Calnexin is an example of a type I protein retained by a C-terminal di-arginine motif (Rajagopalan et al., 1994). The di-lysine motif is known to interact with the coatomer complex present in COP I coated vesicles (Cosson and Letourneur, 1994) and so this provides a method to return ER resident proteins to the ER.

One further mechanism of ER-retention is thought to involve the exclusion of ER-resident proteins from transport – where protein complexes or oligomers are thought to form a molecule too large to be physically incorporated in or transported into vesicles. This was shown to be the case with N-acetylglucosaminyltransferase I (GlcNAc-TI) when it was attached to an ER retention motif. ER-retained GlcNAc-TI bound to mannosidase II and mediated the retention of the heterodimeric complex within the ER (Nilsson et al., 1996).

1.1.4 Quality control in the ER.

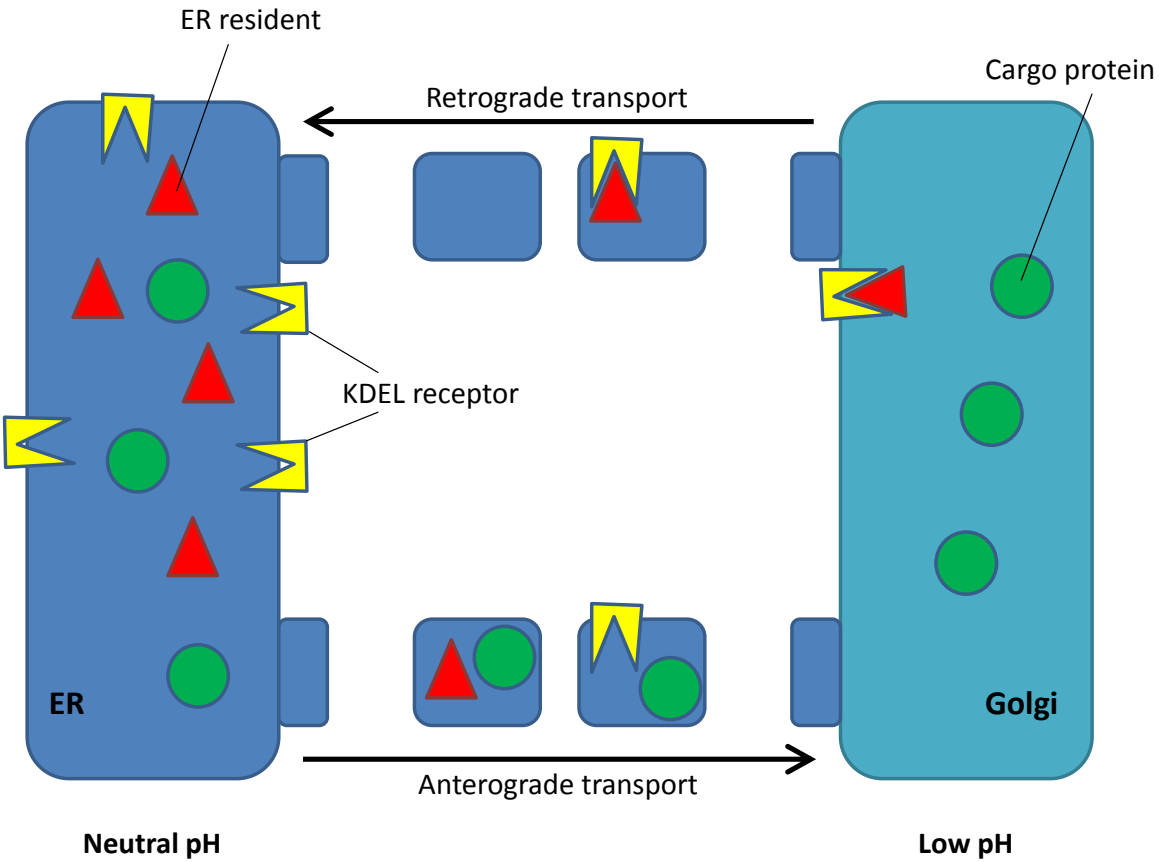

Figure 1.1 – The KDEL system retains ER residents within the ER. ER resident proteins containing the C-terminal KDEL signal are maintained within the ER via interaction with the KDEL receptor. At neutral pH the KDEL sequence and the receptor dissociate, allowing movement of ER residents alongside cargo proteins towards the Golgi in anterograde transport vesicles. The Golgi harbours a comparatively lower pH which favours re-association of the KDEL sequence with its receptor. The re-associated complex then moves back towards the ER in retrograde transport vesicles before disassociating in the neutral pH.

An ER quality control (QC) mechanism exists to ensure that nascent proteins leave the ER in their native conformation. This is a highly specialised system which ensures that non-native proteins do not escape the ER as they are non-functional, may provide a source of toxicity and are more prone to aggregation. The quality control system can differentiate between folded and unfolded proteins, and directs them for either further folding or degradation. Nascent proteins first of all bind ER chaperones, or folding factors, such as BiP. At this stage the folding factors collectively serve three purposes - they bind exposed hydrophobic patches and prevent unwanted hydrophobic interactions; they prevent the degradation of unfolded proteins; and due to their ER-retention motifs, interaction with them mediates retention in the ER thus preventing release of immature proteins (Bottomley et al., 2001).

In the case of glycoproteins, the primary sequence is first of all scanned by the ER-luminal oligosaccharyltransferase (OST) which adds an N-glycan to asparagines in the consensus sequence Asn-X-Ser/Thr. The structure of the glycan initially linked to the asparagine residue has two N-acetylglucosamines, nine mannose residues and three glucose residues. Two of the glucose residues are removed by glycanases which then allows the binding of lectins calnexin and calreticulin, while removal of the third clears the protein for release from the ER as a fully folded and mature product. UDP-glucose:glycoprotein glucosyltransferase (UGGT) acts as a folding sensor and can add back the terminal glucose residue if the protein has been released by the lectins prematurely – promoting their re-association (Solda et al., 2007). Thus, the glycan structure signifies the folding state of the protein and can recruit help if required.

Terminally misfolded proteins are subject to the process of endoplasmic reticulum-associated degradation (ERAD) (McCracken and Brodsky, 1996). It is thought that specific folding factors have a role in ERAD substrate recognition (Denic et al., 2006); without BiP ER quality control is compromised (Mimura et al., 2008). Other enzymes proposed to play a role in quality control and ERAD substrate recruitment are slow-working mannosidases, which are suggested to target terminally misfolded proteins to ERAD due to their increased time spent within the ER (Fagioli and Sitia, 2001). In addition to this, overexpression of ER mannosidase 1 enhances degradation of a misfolded antitrypsin (Hosokawa et al., 2003). A similar effect is seen with the ER degradation enhancing α-mannosidase-like protein (EDEM1) (Hosokawa et al., 2001). It is thought that EDEM1 may bind terminally misfolded proteins in place of the UGGT/calnexin/calreticulin complex to direct the substrate to ERAD (Molinari et al., 2003). Although ERAD substrate recognition is

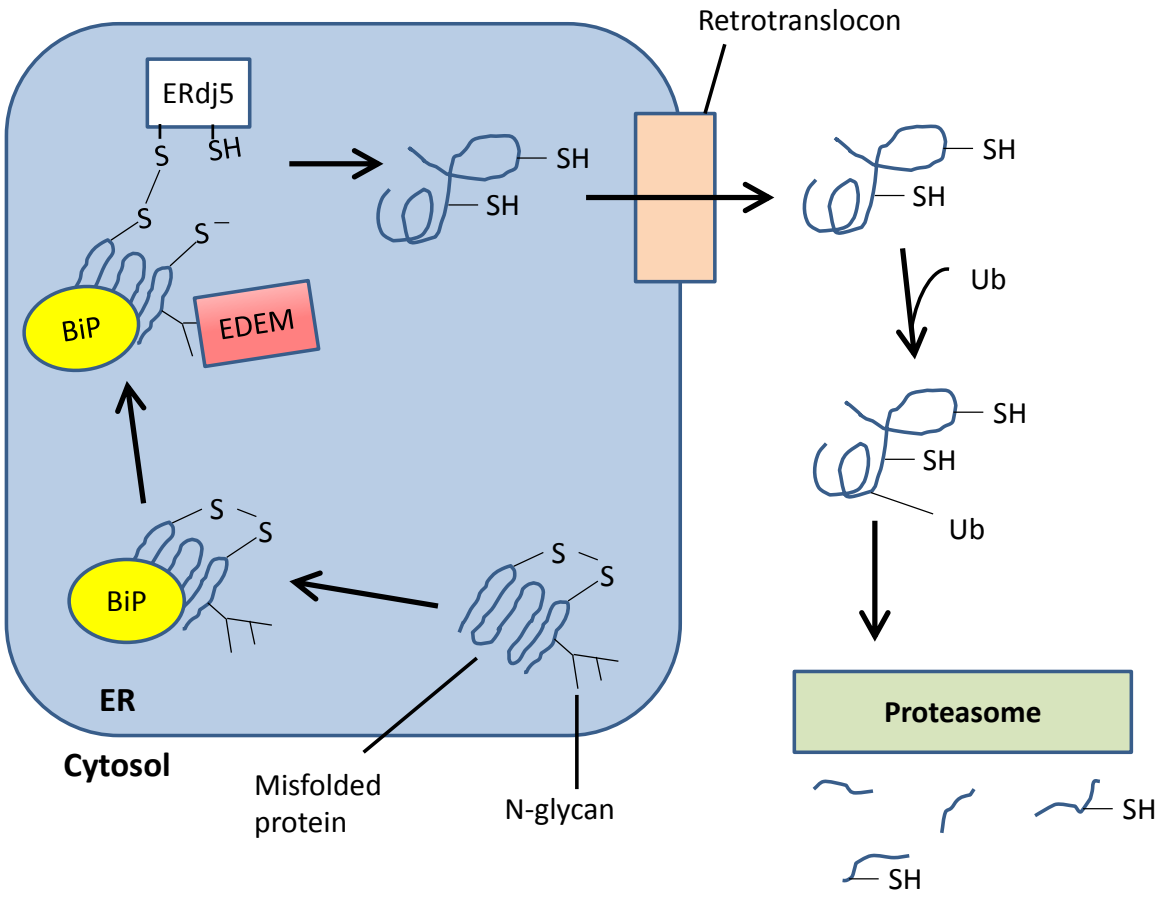

Figure 1.2 – Endoplasmic reticulum-associated degradation targets misfolded proteins for degradation. Misfolded proteins within the ER attract folding factors such as BiP to prevent aggregation. Terminally misfolded proteins interact with the ERAD targeting factors such as EDEM1 which binds and cleaves N-glycans. The cleaved glycan is thought to act as the signal which targets proteins to ERAD. ERdj5 is thought to reduce disuphides prior to retrotranslocation through the retrotranslocon to the cytosol. Once the ERAD substrate reaches the cytosol it is ubiquitinated before degradation in the proteasome.

incompletely understood, it is likely to involve a number of mechanisms due to the importance of preventing the build-up of misfolded proteins in the ER. This would provide a fail-safe recruitment mechanism where one system could intervene if another fails.

Once targeted for ERAD, substrates must be retrotranslocated into the cytosol where degradation occurs via the 26S proteasome. Recent evidence has shown that the ER localised protein ERdj5 is required to reduce targeted substrates to facilitate passage through the ER membrane (Ushioda et al., 2008). To then target the ERAD substrate to the retrotranslocon, homoCys-responsive ER-resident protein (HERP) has been implicated. HERP is thought to form a complex with BiP, derlin-1 (a potential retrotranslocon component), non-glycosylated ERAD substrates and the proteasome (Okuda-Shimizu and Hendershot, 2007). EDEM1 is thought to interact with further possible retrotranslocon components derlin-2 and derlin-3, which provides a link between the ERAD targeting enzymes and the retrotranslocon (Oda et al., 2006). Once the misfolded proteins have been identified for ERAD and unfolded, they are translocated through the retrotranslocon for ubiquitination and degradation. The composition of the retrotranslocon itself remains undefined. There are several candidates, the membrane-associated ATPase enzyme p97 is thought to extract ER membrane proteins and target them for proteasome degradation (Ye et al., 2001), while derlin-1 (Lilley and Ploegh, 2004, Ye et al., 2004) and PA700, the proteasomal regulatory complex, both promote translocation of an ERAD substrate (Wahlman et al., 2007, Ye et al., 2005). Derlin-2 is also thought to form a part of the translocon as its absence prevents retrotranslocation (Dougan et al., 2011); absence of derlin-3 prevents degradation of substrates (Oda et al., 2006). There is also evidence to suggest that the Sec61 complex may be involved in this process as it has been implicated in retrotranslocation of MHC class I (Wiertz et al., 1996) and glycopeptides (Gillece et al., 2000).

Following retrotranslocation from the ER, ERAD substrates undergo polyubiquitination prior to degradation. Ubiquitination is thought to involve an E2/E3 ubiquitin ligase enzyme complex. This complex, in mammals, is thought to include Ube2g2, an E2 ubiquitin-conjugating enzyme, and gp78, an E3 ubiquitin ligase (Chen et al., 2006). Disruption of the interaction between these two proteins results in the accumulation of substrates within the ER. Human Hrd1 has also been suggested to play the role of the E3 ligase (Kikkert et al., 2004). Taken together, this evidence is suggestive of a complex of various proteins, both integral to the ER membrane and soluble, which works to carry out the function of ERAD; that is the targeting, unfolding, retrotranslocation and ubiquitinylation of misfolded proteins prior to degradation by the proteasome (Figure 1.2).

1.1.5 The protein disulphide isomerase family.

In order to prevent the misfolding of client proteins and their degradation by ERAD, the ER contains a number of enzymes that carry out a range of functions all with the goal of promoting protein folding and introducing disulphide bonds. A subsection of these enzymes, named oxidoreductases or PDI family members, is illustrated in Figure 1.3A. There have been over 20 oxidoreductases identified so far, all with varying functions. They do all, however, have one property in common – they possess one or more thioredoxin-like motifs. These motifs are based on the structure of the small cytosolic redox-active protein thioredoxin, which contains a five-stranded β-sheet with four flanking α-helices (Holmgren et al., 1975). Thioredoxin itself is a relatively small protein of around 110 amino acids and is very highly conserved throughout archaea, prokaryotes and eukaryotes. It functions as a disulphide reductant within the cytosol as it has a redox-active CxxC motif which can exist in either the dithiol or disulphide state. Thioredoxin reductase maintains thioredoxin in the reduced state so that thioredoxin can act as a reductase and reduce interacting proteins (Holmgren and Morgan, 1976). The ER oxidoreductases contain a thioredoxin fold which is slightly smaller than the thioredoxin protein; it contains a four-stranded β-sheet with three flanking α-helices. These domains can be seen in Figure 1.3B. Other enzymes known to include this fold are redox active, including glutaredoxin, glutathione S-transferase, DsbA, and glutathione peroxidase. The ER oxidoreductases, however, are not exclusively redox active. There are members of the family which cannot participate in disulphide transfer as they do not have a CxxC motif. These enzymes are generally not well studied, however there are known roles for PDILT and ERp44. PDILT is known to be expressed only in the testes and contains two modified CxxC motifs; SKQS and SKKC (van Lith et al., 2005). PDILT interacts with substrate proteins and Ero1 via its only active site cysteine, and is essential for the correct folding of ADAM3 - a protein essential for sperm migration and binding of the zona pellucida (Tokuhiro et al., 2012). ERp44 is known to interact with Ero1α and substrate proteins to retain them in the ER (Anelli et al., 2003) via its CRFS motif cysteine. In other PDI family members the CxxC active site motif is intact and provides the characteristic redox functionality required by the ER. The PDI family members catalyse the oxidative folding of cargo protein by introducing native disulphides between proximal thiols within their primary structure via a dithiol disulphide exchange reaction. This function was first observed by experiments carried out in 1963 (Goldberger et al., 1963) which showed, *in vitro*, that ribonuclease A was oxidised and activated at an increased rate in the presence of microsomes. This finding led to the identification of PDI – an enzyme which catalysed the formation of disulphides within ribonuclease A as well as

the reduction and rearrangement of incorrect disulphides. This was the first evidence to suggest that disulphide formation within proteins was catalysed, rather than driven by the polypeptide primary sequence as suggested previously (Anfinsen et al., 1961).

Characterisation of PDI followed these experiments and a large body of evidence was collected implicating this enzyme in thiol-disulphide exchange. A 1967 study showed that PDI, upon reduction and alkylation, was inactivated (Fuchs et al., 1967). This suggested that PDI contained redox-active cysteine residues which were blocked by thiol-reactive alkylating agents. Furthermore, incubation of purified PDI with Cd^{2+} ions also caused inhibition of enzymatic activity, consistent with proteins of similar activity (Hillson and Freedman, 1980). The primary sequence of PDI was finally elucidated in 1985 and was found two contain two domains homologous to thioredoxin. These two homologous domains contain the CGHC active site motifs which give PDI its redox activity (Edman et al., 1985). PDI was subsequently shown to catalyse disulphide formation and isomerisation of a wide range of substrates *in vitro* (Bulleid and Freedman, 1988, Freedman et al., 1989).

In vivo evidence for the role of PDI in oxidative protein folding came in 1995 when a yeast knockout study revealed that the essential function of PDI is to isomerise non-native disulphides (Laboissiere et al., 1995). In this study the Δpdi1 *S. cerevisiae* mutant, first shown to be lethal by Scherens et al. (Scherens et al., 1991), was complemented with PDI cDNA constructs carrying mutations in the CGHC active site motifs to regain viability. Laboissiere et al. used a CGHS PDI mutant with impaired oxidase and reductase activity, and a SGHC mutant with impaired oxidase, reductase and isomerase activity. They found that the CGHS mutant restored viability in yeast, suggesting that the isomerase function of PDI is necessary for viability of *S. cerevisiae*. Mutations in the active sites also result in sensitivity to the reducing agent dithiothreitol (DTT) in yeast (Holst et al., 1997), suggesting that PDI is also important for disulphide formation.

Evidence for the direct involvement of PDI in oxidative protein folding was found in 1999. The yeast form of PDI was found in disulphide linked heterodimers with the ER oxidase Ero1p *in vivo*, resulting in the oxidation of PDI. PDI was then found in a mixed-disulphide complex with carboxypeptidase Y (CPY) implying that PDI either oxidises or isomerises CPY. A PDI knockout yeast mutant shows impaired CPY oxidation suggesting that PDI is important in the oxidative folding of this protein. This study concluded that there is a direct transfer of disulphide bonds from Ero1p to PDI and on to secretory proteins in the ER, for example CPY (Frand and Kaiser, 1999). In mammalian cells, Ero1α was shown to interact

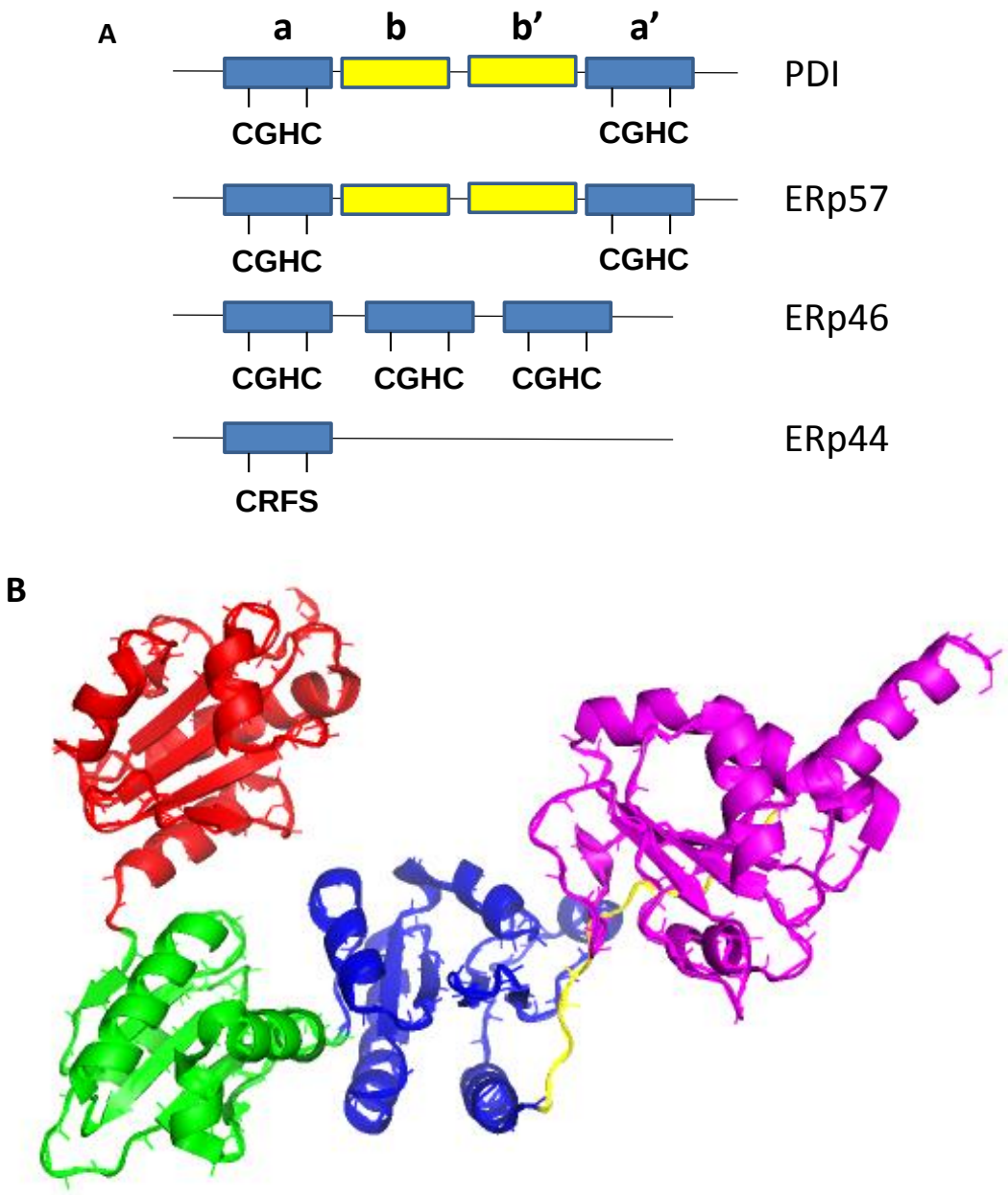

Figure 1.3 – The PDI family are based on the thioredoxin motif. A – A small subsection of the PDI family is represented schematically. Each member has at least one domain homologous to the thioredoxin fold (blue box). The domain structures of PDI, ERp57, ERp46 and ERp44 are shown as are the active site sequences of each redox active domain. B – The structure of *S. cerevisiae* PDI illustrates the overall structure of the molecule and the four domains based on the thioredoxin motif. The domains are as follows: a (red), b (green), b' (blue) and a' (purple). The x-linker region is depicted in yellow. Note the classical V-shaped structure typical of the oxidoreductases.

with PDI and formed a disulphide linked complex (Benham et al., 2000) following the identification of Ero1α (Cabibbo et al., 2000).

In addition to these oxidase and isomerase functions, PDI has since been shown to interact with and form mixed disulphides with PrxIV (Tavender et al., 2010) and VKOR (Wajih et al., 2007), while it is believed disulphides can be exchanged between PDI and Gpx7 and Gpx8 (Nguyen et al., 2011). This provides the link between *de novo* disulphide bond formation and disulphide introduction into nascent client proteins within the ER. In order to achieve this, however, the ER needs to generate a constant stream of disulphide bonds to supply PDI and ensure that the process of oxidative protein folding is not compromised. This stream originates from another subset of specialised ER-resident enzymes.

1.1.6 *De novo* disulphide formation.

The endoplasmic reticulum is a highly specialised protein-folding factory. As well as providing an environment conducive to protein folding, it must also ensure that disulphide bonds are introduced where required. It is estimated that in specialised secretory cells such as plasma cells or pancreatic β cells, around 3,000,000 disulphides are generated and introduced into immunoglobulin or insulin per minute (Scheuner and Kaufman, 2008). This figure gives some indication of the speed at which oxidative protein folding occurs and also gives an appreciation of the high fidelity to which the enzymes work. This large pool of disulphide bonds is thought to be generated by a small number of enzymes, namely quiescin sulphydryl oxidase (QSOX), and the ER-localised enzymes vitamin K epoxide reductase (VKOR), Endoplasmic reticulum oxidoreducxtase 1 (Ero1), the peroxidises peroxiredoxin IV (PrxIV), glutathione peroxidise 7 (Gpx7), glutathione peroxidise 8 (Gpx8) and also by the oxidation and reduction of ascorbate (vitamin C).

QSOX and Ero1 are thought to generate disulphide bonds via a similar mechanism, as both enzymes are flavoproteins; flavin adenine dinucleotide (FAD) is bound and essential for function (Hoober et al., 1996, Tu et al., 2000). FAD acts as an electron acceptor and facilitates the flow of electrons required to produce disulphide bonds within the associated enzymes. This mechanism relies principally on two sulphydryl groups of conserved cysteine residues, which exist as –SH groups in their reduced, electron rich form. In order to generate a disulphide bond, the electrons from these two sulphydryl groups are passed on to the FAD molecule and as a result become oxidised thus forming a covalent link between the two sulphur atoms. This is the newly generated disulphide bond. Other mechanisms of disulphide bond generation include VKOR, an ER localised enzyme (Schulman et al., 2010) which catalyses the reduction of vitamin K to vitamin K

hydroquinone (Jin et al., 2007). This results in the oxidation of the VKOR CxxC active site and the generation of a disulphide bond. Ascorbate is an indirect source of disulphide bonds, being oxidised to dehydroascorbate. Dehydroascorbate can be reduced by PDI (Saaranen et al., 2010), a key member of the oxidative protein folding machinery, resulting in the oxidation of PDI and the formation of a new disulphide bond.

The other major method of disulphide bond generation comes from the recycling of hydrogen peroxide – a reactive oxygen species (ROS) which can be broken down into water by enzymes with a peroxidase function, of which there are three known to exist within the ER. The glutathione peroxidases (Gpx7 and Gpx8) enzymes and peroxiredoxin IV (PrxIV) all react with hydrogen peroxide to form cysteine sulphenic acid groups which are extremely reactive. These groups can react with proximal cysteine sulphydryl groups to form a disulphide bond between the sulphur atoms, coupled to the release of a water molecule.

1.2 Ero1 structure and regulation.

The Ero1 family of proteins provide a means of generating disulphide bonds within the ER and are well conserved amongst eukaryotes. In humans two forms of Ero1 exist, each exhibiting different mechanisms of regulation and tissue specific expression. Ero1α, the most widely expressed isoform, exists in most cells and tissues whereas Ero1β is expressed only in certain cells and tissues such as the pancreatic islets of Langerhans (Dias-Gunasekara et al., 2005). Ero1α is upregulated by the Hypoxia-inducible factor (HIF-1α) in times of low oxygen (May et al., 2005), whereas Ero1β expression is stimulated by an ER stress response - the unfolded protein response (UPR) (Pagani et al., 2000). Comparatively little is known about the Ero1β structure and regulatory mechanisms and so the main focus and comparison will be made between Ero1α and the yeast Ero1p, both of which have been much more widely studied. Ero1p was first identified in 1998 in two separate studies (Frand and Kaiser, 1998, Pollard et al., 1998) and has since been the focus of further work due to its requirement for viability in *Saccharomyces cerevisiae*.

1.2.1 The unique structure of Ero1p.

The properties of yeast Ero1p have been intensely studied in the last few years. It is a 65kDa glycosylated (Frand and Kaiser, 1998), flavin-adenine dinucleotide (FAD) binding protein (Tu and Weissman, 2002) that is localised to the luminal face of the ER membrane via a 127 amino acid C-terminal tail (Pagani et al., 2001). Interestingly, this tail sequence is absent in the human isoforms, Ero1α and Ero1β. A thermosensitive yeast *ero1-1* mutant gave insight into the functions of the C-terminal region of Ero1p. The *ero1-1* strain is non-

viable at temperatures over 36°C but is rescued by both Ero1α and a truncated Ero1p missing the 127 amino acid C-terminal domain (Cabibbo et al., 2000). The C-terminal domain, therefore, is not essential for viability but is necessary for Ero1p localisation to the ER membrane. Furthermore, the tail region is required to rescue an Ero1p deletion strain (Pagani et al., 2001). Interestingly, Ero1p is a globular protein which is rich in α-helical structure with short connecting loops between helices, and an additional lengthy loop with no secondary structure (Gross et al., 2004). While the C-terminus is important for Ero1p localisation, there are important structural, catalytic and regulatory features found elsewhere within the molecule.

10 cysteines within Ero1p are known to form intramolecular disulphide bonds (Figure 1.4A), including four which form the catalytically active disulphides; Cys352-Cys355 and Cys100-Cys105. Cys352 and Cys355 are known as the active site cysteines, whereas the Cys100-Cys105 pairing is known as the shuttle cysteines (Sevier and Kaiser, 2008). The active site cysteines are positioned adjacent to the FAD cofactor, and transfer electrons from the shuttle cysteines to FAD (Tu et al., 2000, Tu and Weissman, 2002). The electrons are then passed on to molecular oxygen, producing hydrogen peroxide – a reactive oxygen species and potential source of cellular stress (Gross et al., 2006). This is thought to be one reason for the tight regulation of Ero1. The shuttle cysteines are so called as they pass electrons from protein disulphide isomerase (PDI), the partner of Ero1 in the disulphide bond formation pathway, to the active site cysteines (Figure 1.5A). This is done via intramolecular dithiol-disulphide exchange (Sevier and Kaiser, 2006). With PDI in an oxidised state, it can then act upon its substrate proteins by oxidising cysteine pairs thus donating its disulphide bonds (Figure 1.5B). The shuttle cysteines are positioned on a long, flexible loop which allows movement of the cysteines between the active site cysteines and PDI. The loop lacks secondary structure, which is thought to increase the affinity of PDI for the shuttle-containing loop as PDI substrates tend to be in unfolded conformations (Sevier and Kaiser, 2008). The cysteine residues of Ero1p also have another role to play in addition to disulphide bond transfer; they provide a crucial method of regulation of Ero1p activity.

1.2.2 **Regulation of Ero1p.**

A further significant role of the cysteines in Ero1p is their formation of two regulatory disulphides, Cys150-Cys295 and Cys90-Cys349. These disulphides are thought to sense the ER oxidation state and modulate Ero1p activity accordingly. The positioning of the

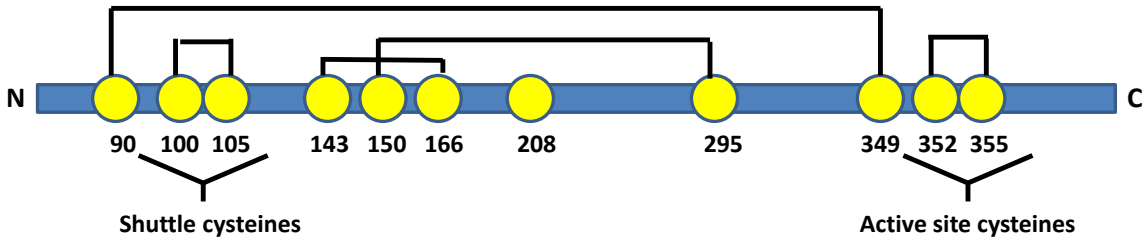

Figure 1.4 – Ero1p intramolecular disulphide connectivity. Schematic diagram of the Ero1p primary structure with cysteines numbered and in yellow. Native disulphides are shown connected by black lines, active site and shuttle cysteines are labelled.

regulatory disulphides is crucial; they control the flexibility of the shuttle cysteine loop, directly influencing its ability to pass electrons from PDI to the active site. The Cys143-Cys166 disulphide is thought to be structurally important as an Ero1p-c-C143A-C166A double mutant has a lower activity compared to the wild type in activity assays (Sevier et al., 2007). This is thought to result from a loss of structure rather than regulation of activity. A further interesting property of Ero1p is that the initial activation lag phase in Ero1p-c activity is shortened significantly in the case of the C150A-C295A mutant (Gross et al., 2006). The C90A-C349A mutant also showed a moderate reduction in the lag phase, which was confirmed to be due to the reduction of these disulphides before Ero1p is activated suggesting that these disulphides are inhibitory. Sevier et al show that Ero1p can be completely deregulated by introducing the C150A-C295A mutant into yeast, as this mutation destabilises the Cys90-Cys349 disulphide and creates a constitutively active form of the enzyme (Sevier et al., 2007). This disulphide bond system forms an effective regulatory mechanism; when the ER environment is reducing the regulatory disulphides will be broken and Ero1p will be activated. It can then work to raise the oxidation potential of the ER. However, in oxidising conditions, the regulatory disulphides will re-form and Ero1p will become inactivated.

A more recent study shed further light on the regulation of Ero1p, specifically the molecular steps required to reduce and activate the enzyme. This study built upon the previous knowledge on the electrophoretic mobility of the various redox forms of Ero1p. Heldman et al. used thiol alkylating agents, either N-ethyl maleimide (NEM) or 4-acetamido-4’-maleimidylstilbene-2,2’-disulfonic acid (AMS), to trap the redox form of Ero1p at various stages of reaction with substrate. This approach confirmed that the C150A/C295A mutant Ero1p reached its fully reduced, active form more quickly when compared to the wild type enzyme (Heldman et al., 2010) which would explain why the mutant has a reduced lag phase. This approach also showed that upon completion of substrate oxidation Ero1p returned to its oxidised form, with the C150A/C295A mutant again reaching this form faster than the wild type. Together, these findings suggest that the breaking of the C150-C295 disulphide is one of the early events in the activation as well as being one of the initial events of the re-oxidation of Ero1p. Mass spectrometry investigations, however, showed that the C143-C166 disulphide is broken first of all during reduction of Ero1p, with the C150-C295 disulphide only being broken later in the process (Heldman et al., 2010). Interestingly, these results were observed using the non-physiological substrate thioredoxin and were different to those observed when using PDIp as a substrate. With PDIp as a substrate, Ero1p never reaches the reduced state that it does

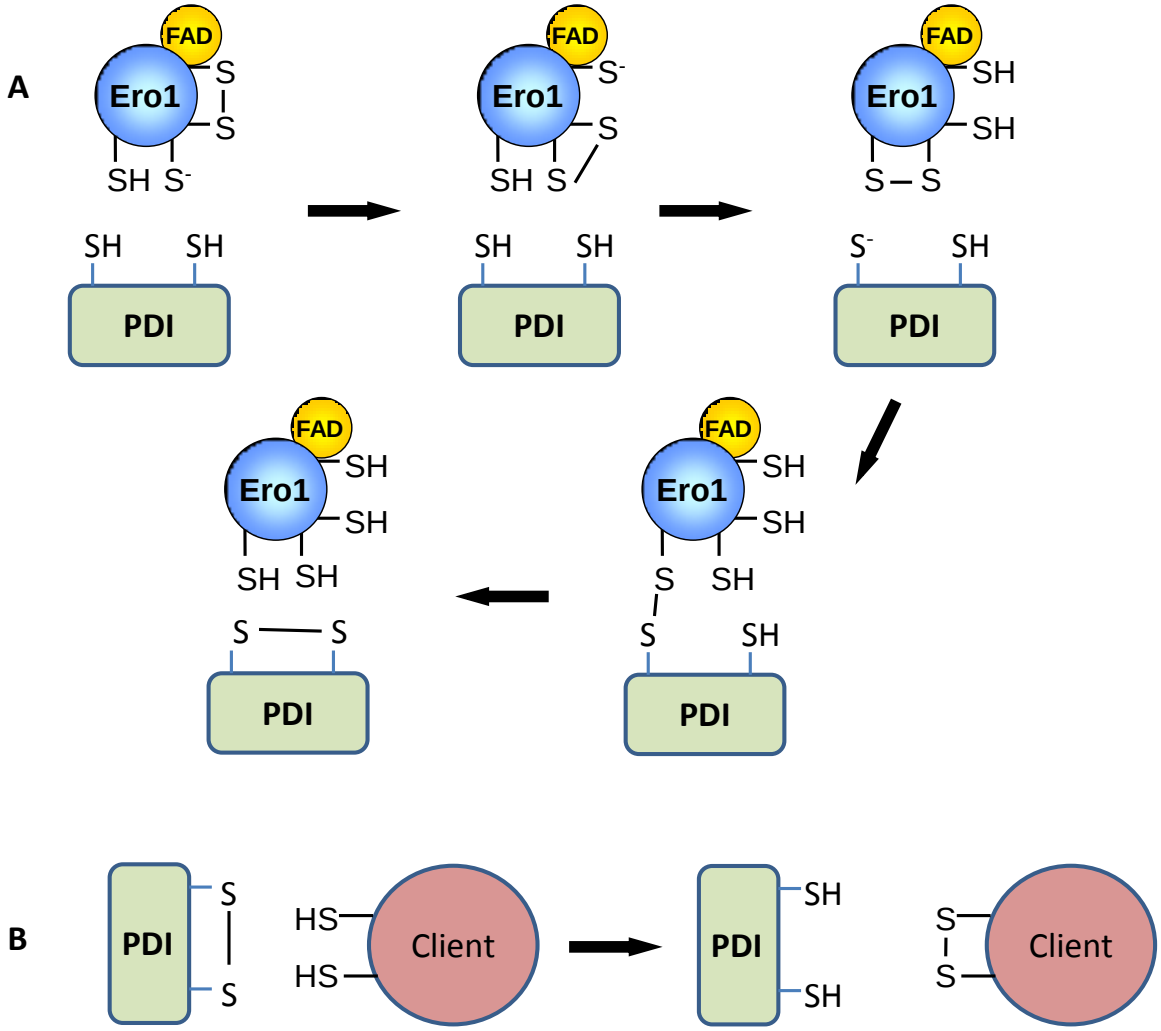

Figure 1.5 – Disulphide bond transfer from Ero1 to PDI occurs via dithiol-disulphide exchange prior to client oxidation by PDI. A - The Ero1 active site disulphide, adjacent to the FAD cofactor is passed on to the Ero1 shuttle cysteines in a dithiol-disulphide exchange where the active site disulphide is attacked by the thiolate anion of a shuttle cysteine. This creates a disulphide linking the two active sites. This disulphide is attacked by the second shuttle cysteine to form the shuttle disulphide. A thiolate anion from PDI then attacks the shuttle disulphide, forming a mixed disulphide between the two enzymes. This is resolved within the PDI molecule by the second active site cysteine resulting in the oxidation of the PDI active site and reduction of the Ero1 shuttle disulphide. B – Oxidised PDI introduces disulphides into client proteins within the ER via a similar dithiol-disulphide exchange mechanism resulting in the oxidation of the client and the reduction of the PDI active site.

with thioredoxin. The reason for this observation is as yet unknown and may have implications for many studies which have investigated the activation and inactivation of Ero1p using thioredoxin.

1.2.3 Discovery of Ero1α and its function.

While there are similarities between the structure and regulatory mechanisms of the human and yeast forms of Ero1, there are many more distinguishing features. Following the discovery of Ero1p in 1998, (Frand and Kaiser, 1998, Pollard et al., 1998) the search for the human homologue resulted in the discovery of Ero1α (Cabibbo et al., 2000). A BLAST search using the yeast ERO1 nucleotide sequence found a human homologue with 49% similarity and 37% identity to the yeast Ero1p. Further bioinformatical analysis of this gene suggested an N-terminal ER-signal sequence with a cleavage site between residues 23 and 24 as well as two N-glycosylation sites, both suggestive of an ER protein. Furthermore, the sequence was predicted to contain a CxxCxxC motif – important for Ero1p activity (Frand and Kaiser, 1998, Pollard et al., 1998). Follow up experiments confirmed a myc-tagged Ero1α gene product co-localised with ER proteins and that Ero1α is sensitive to EndoF and EndoH treatment, suggestive of a glycosylated ER protein (Cabibbo et al., 2000). *In vitro* translation assays confirmed microsome localisation and glycosylation of Ero1α. Solubility assays suggested that Ero1α is associated to the membrane either directly or through interactions with an integral membrane protein, similar to Ero1p. Ero1α is able to rescue viability of the yeast *ero1-1* mutant strain and alleviated DTT sensitivity (Cabibbo et al., 2000); proof that Ero1α has a similar function to Ero1p. Mutation of the second and third cysteines in the CxxCxxC motif diminished the ability of the enzyme to complement the *ero1-1* strain suggesting that these residues are crucial to the functioning of Ero1α. Cabibbo et al. also explored the function of Ero1α with respect to oxidative protein folding. Ero1p or Ero1α are required for CPY to reach its mature form in yeast. Taken together, this evidence suggests that Ero1α is an ER protein, possibly associated with the ER membrane, it is glycosylated, can functionally complement Ero1p in yeast, contains an essential CxxC motif and is important in the oxidative folding and maturation of substrates within the ER *in vivo*.

In addition to this work by Cabibbo et al., a further study was published in 2000 by Benham et al. on the function of Ero1α. The study shed insight on the oxidative folding state of the enzyme in the ER and the involvement of the CxxCxxC motif in this. Benham et al. set out to determine the extent of disulphide bond formation within Ero1α as it contains 15 cysteine residues within its primary structure. *In vitro* translation assays in semi-permeabilised (SP) cells (treated with the detergent digitonin and washed to remove

the cytosol and leave an intact ER system) produced Ero1α which was taken up by a functional ER system. The group found that Ero1α was glycosylated and that the majority of the enzyme was bound to the membrane, in agreement with Cabibbo et al. Under reducing SDS-PAGE conditions Ero1α was found to exist in two forms – either glycosylated or non-glycosylated. Under non-reducing SDS-PAGE Ero1α formed two distinct bands of increased mobility, termed OX1 and OX2, indicating the formation of disulphide bonds within the molecule. The glycosylation state of these Ero1α forms was confirmed by using lectin binding ConA-beads which pulled down the OX2, OX1 and reduced forms of Ero1α. These bands all presented as a single reduced and glycosylated form after treatment with DTT and were all sensitive to glycosidase treatment. This experiment also showed that Ero1α was present in a complex with molecular weight of 120kDa which was subsequently shown to be an Ero1α-PDI disulphide linked complex. This was the first evidence to suggest Ero1α-PDI interactions.

To investigate the involvement of the CxxCxxC motif in the structure and function of the enzyme, Benham et al. created cysteine to alanine mutants of the three cysteines (C391A, C394A, and C397A). These were again translated in the presence of SP cells and their folding states analysed via reducing and non-reducing SDS-PAGE. The results led Benham et al. to conclude that Cys391 and Cys397 contribute to the oxidative folding of Ero1α but that Cys394 does not. Benham et al. then confirmed that the OX2 form is the native and most stable form found in cells. Investigation of the CxxCxxC mutants showed that the C391A and C394A mutants were either unstable and degraded or secreted. C391A showed a decreased ability to interact with PDI and ran as a diffuse smear after SDS-PAGE; it was unable to form the OX2 state suggesting this residue may play a role in the formation of the most oxidised state of Ero1α. C394A achieved the OX1 and OX2 forms and maintained its interaction with PDI, suggesting that PDI prefers to interact with correctly folded Ero1α. C397A was eventually able to reach the OX2 state, unlike during the *in vitro* translations, and interacted with PDI in both its OX1and OX2 states. Taken together, this data suggests that each of the cysteine residues investigated did not play a direct role in the interaction with PDI but that they are crucial for the folding and stability of the protein. As the Ero1α-PDI interaction is strongest with wild type Ero1α and with non-reduced and folded forms of Ero1, the data from this study suggests that PDI does not act as a chaperone.

Further information can be drawn from data provided by both Benham et al. and Cabibbo et al. The C394A and C397A Ero1α mutants cannot complement the *ero1-1* yeast mutant strain, whereas C391A can. Interestingly, Benham et al. showed that the C394A and

C397A mutants can interact with PDI which would suggest that interaction with PDI is not sufficient for the functioning of Ero1α and that the C394 and C397 residues play an important role in Ero1α function. This is consistent with the now-established mechanism of Ero1α function, thus providing the first real insight into the way in which this complicated and fascinating enzyme functions. It also raised a number of questions that would be subsequently studied and prompted further investigation to find out exactly how Ero1α works, the function of the cysteine residues, the significance and the features of the reduced, OX1 and OX2 forms and the role of Ero1α within the ER.

1.2.4 Ero1α drives disulphide formation in substrates via oxidation of PDI.

With the capability of Ero1α to complement the yeast *ero1-1* mutant, it was hypothesised that this enzyme could act in a similar manner to yeast Ero1p, mediating disulphide bond formation within the ER. Following on from the discovery that Ero1p transfers electrons from an active site disulphide to its FAD cofactor (Tu et al., 2000, Tu and Weissman, 2002), investigations began on Ero1α to elucidate the potential *de nov*o disulphide generation mechanism in the human ER. Confirmation of disulphide generation came from a 2001 study by Mezghrani et al. by monitoring the oxidative folding of immunoglobulin in cells overexpressing Ero1α and Ero1β (Mezghrani et al., 2001). This group carried out a pulse chase experiment and analysed the folding states of immunoglobulin by SDS-PAGE. They found that overexpression of Ero1α and Ero1β led to the oxidation of the murine J chain (JcM) at an increased rate as seen by the formation of oxidised monomers, dimers and higher molecular weight complexes. The group confirmed that the Ero1s had no direct oxidative effect on the JcM as no JcM-Ero1 complexes were visible. A PDI-JcM complex was detected however, suggesting that the JcM oxidation is PDI-mediated. PDI-JcM mixed disulphides decreased with time, coupled to the increase in oxidised JcM, again suggesting that PDI is the oxidant required for disulphide formation in the JcM.

Mezghrani et al. then confirmed that PDI and Ero1 could form mixed disulphides, seen in previous studies (Benham et al., 2000). In Ero1α overexpressing cell lines, PDI was found in high-molecular weight complexes as well as in a fast-migrating monomer species. This was not the case in control cells or cells expressing the C391A, C394A or C397A Ero1α mutant as the majority of PDI was found in the reduced monomeric state. Furthermore, after brief treatment with DTT during a pulse labelling period, the more oxidised form of monomeric PDI formed quickly in Ero1α overexpressing cells but not in control cells as seen from the chase samples. This suggests that Ero1α is driving PDI oxidation *in vivo*. To investigate the ability of the CxxCxxC motif mutants to drive disulphide formation in the JcM, JcM folding was monitored in cells via SDS-PAGE and was impaired in the C394A

and C397A mutants. The C391A mutant accelerated folding when compared to control cells but this acceleration was less than in wild type Ero1α expressing cells. The Mezghrani et al. study therefore showed for the first time that Ero1α could drive disulphide bond generation for ER-targeted substrates by oxidising PDI. This was a pivotal finding in itself, however the finding that mutating cysteines C394A and C397A disrupted Ero1α activity, in addition to the Benham et al. study. This again raised questions of the specific function of these critical residues, and how the Ero1α-PDI interaction is mediated.

1.2.5 The Ero1α cysteines create two active sites and a regulatory mechanism at the molecular level.

With the discovery of the disulphide bond generating and PDI-oxidising abilities of Ero1α, attentions then turned to determining the precise mechanisms by which these abilities are mediated. These issues were investigated by a study in 2004 by Bertoli et al. who generated a number of Ero1α cysteine mutants and tested their capability to carry out four functions: to complement the *ero1-1* yeast mutant; to accelerate oxidative protein folding in cells; to form mixed disulphides with known interaction partners PDI and ERp44; and to form the characteristic redox isoforms seen previously (Benham et al., 2000). A Δ86-95 mutant showed impaired activity in a folding assay as well as being unable to complement the *ero1-1* mutant. This suggested an important role for the region of the enzyme containing cysteine 94.

Bertoli et al. found that cells expressing C85S, C94S and C99A Ero1α mutants all displayed impaired JcM folding compared to the wild type and suffered from reduced growth during complementation assays. C394A and C397A mutants did not grow at all, thus suggesting that cysteines 85, 94 and 99 are important for functionality and that cysteines 394 and 397 are indispensible. This is similar to the properties of Ero1p (Frand and Kaiser, 2000). Cysteine 94, 166, 208 and 241 mutants all displayed impaired binding of PDI, and considering that only the C94S mutant is inactive in activity assays then this would imply that the Ero1α-PDI interaction may not exclusively transfer oxidising equivalents to PDI. Interestingly, these four mutants bound ERp44 as well as the wild type enzyme suggesting a different mechanism of interaction which has since determined to be a multivalent interaction between Ero1α cysteines and ERp44 (Anelli et al., 2003).

To determine the redox isoforms formed by the cysteine mutants, reducing and non-reducing SDS-PAGE was performed to separate the reduced, OX1 and OX2 forms. The results suggested that cysteines 85 and 391 are required for OX2 formation. The JcM folding activity of two double mutants were tested and concluded that the two primary

residues of the CxxCxxC motifs in Ero1α, C85 and C391, are important for function as their absence results in a less active Ero1α. Taken together with the data showing that cysteines 94, 394 and 397 are essential to complement the *ero1-1* mutant, and that cysteines 94, 99, 394 and 397 are important or essential for binding of PDI and oxidative folding of the JcM, this suggests that cysteines 85 and 391 coordinate the cooperation of the two CxxC motifs to allow the functioning of Ero1α possibly by forming a disulphide. This study therefore provided the first evidence that Ero1α contains two active sites and proposed that electron transfer occurs from PDI, through these Ero1α active sites and on to an upstream electron acceptor; resulting in a net transfer of disulphides in the opposite direction. This mechanism is similar to that found in Ero1p (Sevier and Kaiser, 2006).

While this evidence provided a function for the CxxCxxC motif cysteines, there remained ambiguity over the role of the remaining Ero1α cysteines. These were dispensible for functioning of Ero1α but did influence the folding state of the enzyme (Bertoli et al., 2004). Insight into the specific functions of these cysteines then came from two studies in 2008 which showed that these residues are essential for regulation of Ero1α activity, following on from studies in Ero1p (Sevier et al., 2007). Baker et al. approached the investigation using a purified recombinant Ero1α and several mutants in order to characterise activity towards substrates and the influence of the cysteines on this activity. Biophysical studies confirmed that Ero1α contains a number of intramolecular disulphides.

Ero1α activity towards the non-physiological substrate thioredoxin was characterised using a gel-based assay to distinguish between the reduced and oxidised forms of thioredoxin and Ero1α. Analysis of the redox states revealed that reduction of Ero1α coincides with activity, suggesting that reduction of disulphides within the molecule may allow its activation. There was a distinct lag between the completion of thioredoxin oxidation and the re-oxidation of Ero1α – something witnessed previously in Ero1p (Sevier et al., 2007). This, therefore, implies that Ero1p and Ero1α have similar regulatory mechanisms in place and provides further evidence that Ero1α has the ability to generate disulphides and oxidise substrate proteins.

Baker et al. also investigated Ero1α-mediated oxidation of PDI by measuring oxygen concentration in solution as an indication of Ero1α activity. This approach had been used previously to determine Ero1p activity (Sevier et al., 2007) and works on the principle that oxygen is depleted as disulphide bonds are formed. This assay revealed that PDI oxidation is more efficient in the presence of reduced glutathione than in its absence, and that Ero1α activity turned over three disulphides per minute per molecule. This is comparable to activity witnessed with Ero1p (Sevier et al., 2007). Baker et al. also showed that PDI is

able to reduce the regulatory disulphides within Ero1α using a gel shift assay. Interestingly, the partially reduced form of Ero1α remained visible for much longer in the presence of PDI and GSH than with PDI alone. It was hypothesised that GSH maintained PDI in a reduced state enabling PDI to reduce the Ero1α regulatory disulphides – hinting that glutathione could play an indirect role in regulating the Ero1α redox state.

In order to identify the regulatory disulphides within Ero1α, Baker et al. created a number of cysteine mutants and analysed any resultant changes in SDS-PAGE mobility or redox state. It was concluded that the absence of cysteines 85, 94, 131 or 104 all prevented the formation of disulphide bonds which contribute to the fully oxidised form of Ero1α. From this assay, Baker et al. were able to deduce that a disulphide exists between C94 and C131. Interestingly, a C85/131A double mutant ran with further decreased mobility compared to the C85A and C131A single mutants – indicating that perhaps two disulphides could not be formed and this has a cumulative effect on the mobility of this mutant.

To investigate the effects of the absence of these disulphides on Ero1α activity, the abilities of the Ero1α mutants to oxidise thioredoxin and PDI were tested. Using thioredoxin as a substrate, C99A and C94/99A mutants showed complete inactivity while the C94A mutant showed weak activity. This complements previous data which suggested that these residues constitute an active site. Using PDI as a substrate, Baker et al. discovered that the C131A Ero1α mutant showed increased activity towards PDI and lacked the initial lag phase that is seen with the wild type enzyme. The C85/131A double mutant showed an even greater activity towards PDI. This data suggests that the proposed C94-C131 and C85-C391 disulphides are regulatory in nature and that reduction of these disulphides results in a cumulative increase in activity towards PDI. The possibility of a C99-C104 disulphide was investigated as the C104A mutant displays a slight decrease in SDS-PAGE mobility. A C104/131A double mutant was produced and found to have a further increased activity towards PDI when compared to the C85/131A double mutant. This suggests that two regulatory disulphides play a critical role in Ero1α regulation – C94-C131 and C99-C104 and that their reduction results in an activated enzyme. The Baker et al. study therefore shed light on the function of the cysteine residues that are not involved in the active sites. They provided evidence that Ero1α activity is strictly governed by a set of regulatory disulphides that inhibit activity when oxidised and permit activity upon their reduction.

This regulatory mechanism was confirmed by a parallel study in 2008 by Appenzeller-Herzog et al. This group tackled the question of regulatory disulphide formation from a different angle and used a mass spectrometry approach. This approach, combined with the Baker et al. study, provided complementary evidence that Ero1α activity is controlled by

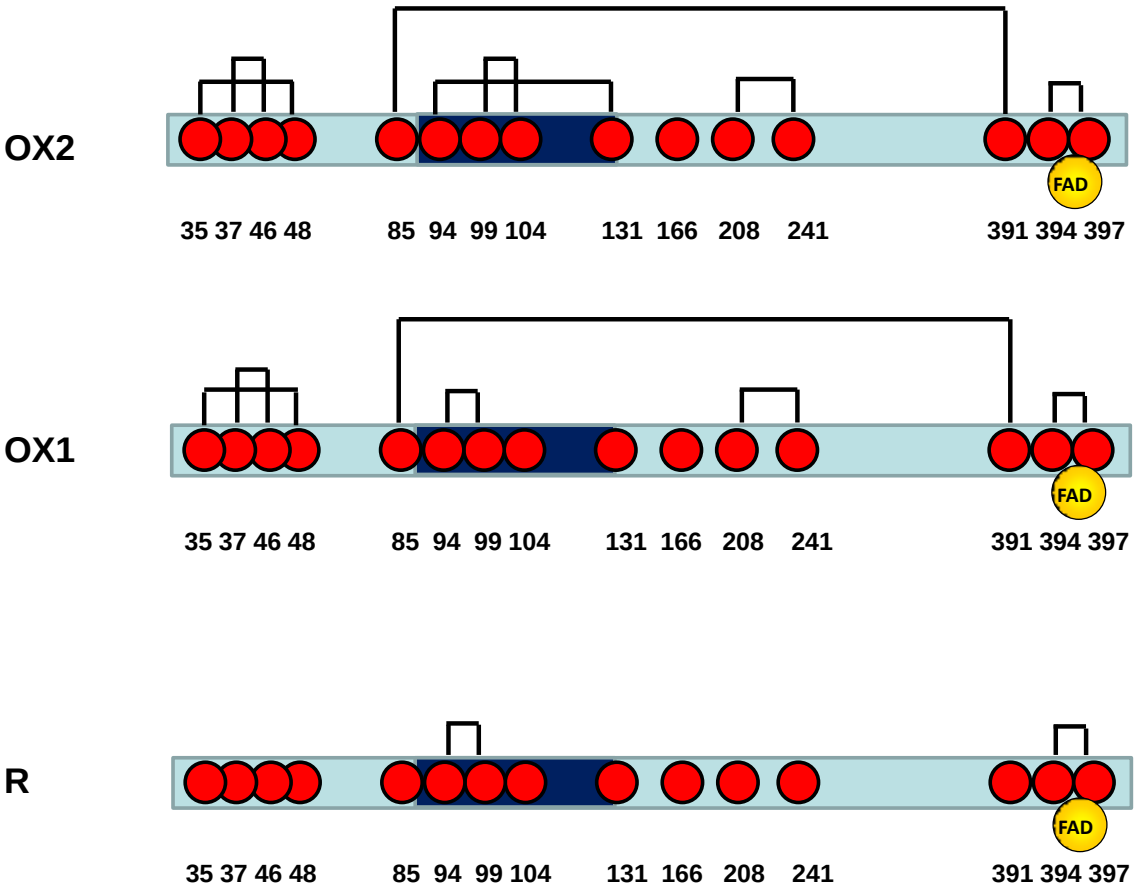

Figure 1.6 – Disulphide bonding pattern within Ero1α. The primary sequence of Ero1α (light blue) contains 15 cysteine residues (red). The inner active site cysteines 391, 394 and 397 are positioned adjacent to the bound FAD cofactor (yellow). The shuttle cysteines, 94 and 99, are positioned on a flexible loop region (dark blue). In the Ox1 form, all of the intramolecular disulphides are formed. These disulphides exist between cysteines 35-48, 37-46, 85-391, 94-131, 99-104, 208-241 and 394-397. In the Ox1 form, the disulphide between cysteines 94-131 is broken allowing formation of the shuttle cysteine active site disulphide (cysteines 94 and 99). In the R form, all of the disulphides are broken although the two active site disulphides, between cysteines 94-99 and 394-397, can still form.

intramolecular disulphide bonds. Both studies were able to map disulphide connectivity and each provided unique insights which contributed greatly to the wider understanding of Ero1α activity and regulation. Appenzeller-Herzog et al. overexpressed and purified Ero1α from cells and used it for mass spectrometry analysis. Analysis of the mass spectrometry data revealed that disulphide bonds were present between cys85 and one of cys391/394/397, and cys94-cys131. Further analysis via SDS-PAGE led to the conclusion that disulphides exist between cys85-cys391 and cys94-cys131, both of which define the OX2 form of Ero1α. Three further disulphides were detected; two between the N-terminal cluster of four cysteines, and one between cys208 and cys241. Armed with this information on the intramolecular disulphides, Appenzeller-Herzog et al. moved on to investigate how these influence Ero1α interactions with PDI.

PDI had been shown to interact with cysteine 94 in the Ero1α 'shuttle' active site. An inter-molecular disulphide between a PDI active site cysteine and Ero1α forms due to the nucleophilic attack on the Ero1α cys94-99 active site disulphide. The new data proposed by Appenzeller-Herzog et al. and Baker et al. suggest that there may be competition for this reaction from Ero1α cysteine 131 which would form a regulatory disulphide. To investigate this possibility, Appenzeller-Herzog et al. devised an assay which would determine whether the availability of PDI had an effect on the redox state of Ero1α. Using shRNA to knock down expression of PDI resulted in an increase in OX2 formation compared to OX1. Furthermore, Ero1α formed more OX1 relative to the OX2 form when PDI was overexpressed. Taken together this data suggests that lowering levels of PDI increased formation of the cys94-131 disulphide, or conversely, increasing PDI availability prevents formation of the cys94-131 disulphide. PDI therefore competes with Ero1α cysteine 131 for the nucleophilic attack of the Ero1α active site. This provides an insight into the regulatory mechanism – when PDI exists in a reduced state it will reduce the cys94-131 disulphide and activate Ero1α, thus generating disulphide bonds. With PDI in an oxidised state, for example during hyperoxidising conditions, it will no longer reduce this regulatory disulphide and Ero1α will remain oxidised and inactive.

The evidence provided in these studies from Bertoli et al., Baker et al. and Appenzeller-Herzog et al. suggests that the Ero1α molecule contains a network of conserved cysteine residues which are involved in an intricate and elegant mechanism of catalytic activity and regulation (Figure 1.6). Two separate CxxC motifs are proposed to work together and transfer electrons from PDI and onto an Ero1α-bound FAD cofactor. Adjacent to each active site are cysteine residues which are thought to bring into close proximity these active sites. Furthermore, two regulatory cysteines provide a means of modulating activity

by preventing the ‘shuttle’ disulphide from forming by occupying the active site cysteines in non-catalytic disulphides. Cysteine 94 is thought to be attacked by electron rich PDI but can also be attacked by cysteine 131 thus forming a regulatory disulphide and the OX2 conformation. Cysteine 99 can form a regulatory disulphide with cysteine 104, providing an extra degree of regulation. Without this regulatory mechanism Ero1α could potentially generate disulphide bonds in a futile manner which has the potential to upset the delicate redox balance within the ER, and consequently preventing oxidative protein folding and isomerisation, essential for the health of the cell.

1.2.6 Ero1α crystal structure.

The crystal structure of Ero1α was solved in 2010 by Inaba et al. which provided insight into the structure-function relationship and validated previous work carried out on the enzyme. The crystal structures of two mutants were determined – the hyperactive C104/131A mutant and the C99/104A mutant (Inaba et al., 2010). These allowed homogenous populations of Ero1α to form by ensuring that only the C94-99 and C94-131 disulphides could form, respectively, in addition to the surrounding structural disulphides. In the case of the hyperactive mutant, disulphides were subsequently identified between residues 35-48, 37-46, 85-391, 208-241 and 394-397, thus confirming previous work on disulphide connectivity (Appenzeller-Herzog et al., 2008, Baker et al., 2008). Ero1α has a globular structure which is rich in α-helical content (Figure 1.7), similar to Ero1p. The N-terminal sequence, absent in the Ero1p study (Gross et al., 2004), creates an anti-parallel β-hairpin structure stabilised by two disulphides, C35-48 and C37-46. The function of this structure remains unknown as it is dispensable; Ero1α activity is unaffected without it.

Another difference between Ero1p and Ero1α is the elongation of the loop regions between α-helices. This discrepancy may help accommodate the additional regulatory disulphide that Ero1α possesses as both the regulatory cysteine residues, C104 and C131, are positioned within an extended loop lacking structure. Inaba et al. also propose that this may be to facilitate electron shuttling between PDI and the Ero1α FAD active site. One interesting feature of the Ero1α structure is that the catalytic core region is nearly identical to that of Ero1p and consists of four closely packed helices adjacent to the bound FAD cofactor. The sulphur atom of cysteine 397 is positioned 3.3Å from the C4a atom of the flavin cofactor thus facilitating electron transport between the two. FAD binds to Ero1α via interactions with conserved residues tryptophan 200 and histidine 255 which secure the isoalloxazine ring and adenine moiety. The oxygen group of arginine 287 is proposed to interact with the pyrophosphate group thus further stabilising the FAD cofactor. These residues are conserved across flavoenzymes indicating their importance (Fass, 2008).

One further interesting observation made by Inaba et al. concerns the apparent lack of a channel through which molecular oxygen can pass to come into the proximity of the flavin group. However, an extended loop region containing residues 183-194 is suggested to cover the isoalloxazine ring and could potentially move during interactions with PDI to facilitate access for oxygen. While the structure of the hyperactive Ero1α produced some interesting observations regarding activity and FAD binding, the structure of the inactive C99/104A mutant revealed more details concerning regulation and the governing disulphides. This structure showed no gross conformational changes compared to the hyperactive form suggesting that formation of the regulatory disulphides does not alter the overall structure of the molecule. There was, however, one major difference between the two structures – the loop containing residues 89-132 is structured in the inactive mutant due to the formation of the C94-131 regulatory disulphide, compared to the same unstructured region in the hyperactive mutant. Taken together, this study therefore builds upon knowledge drawn from 10 years of study on Ero1α.

1.2.7 Correct regulation of Ero1p and Ero1α activity is essential for homeostasis in the ER.

The ER environment is delicately balanced to ensure that nascent proteins undergo oxidative protein folding, but can also undergo disulphide isomerisation to correct non-native disulphide formation. The balance therefore must prevent the ER from becoming either hyper- or hypo-oxidising; a hyperoxidising environment will prevent isomerisation while a hypo-oxidising environment will impair disulphide formation. While glutathione is the major redox buffer in the ER, it is not always sufficient to prevent the upset of the redox balance and as a result there are mechanisms to combat this. The unfolded protein response (UPR) is one such mechanism that can help alleviate stress or can induce cell death if necessary (Haynes et al., 2004). This highlights the fact that it is imperative to maintain the correct ER oxidative balance. Hyper- and hypo-oxidising states are therefore an established source of cellular stress and have been studied in detail to determine the mechanism whereby these conditions come to exist. As a major contributor to oxidative protein folding, Ero1α is central to this balance. It can generate disulphide bonds as well as hydrogen peroxide as a by-product of its activity. Therefore Ero1α, without the appropriate regulation, can lead to the hyperoxidation of the ER. This source of ER stress has been investigated by a number of groups.

In 1999, Cuozzo & Kaiser showed that Ero1p was a major source of oxidised glutathione as overexpression of Ero1p perturbed the glutathione balance (Cuozzo and Kaiser, 1999). Harding et al. then suggested that the oxidase activity of Ero1 could contribute to

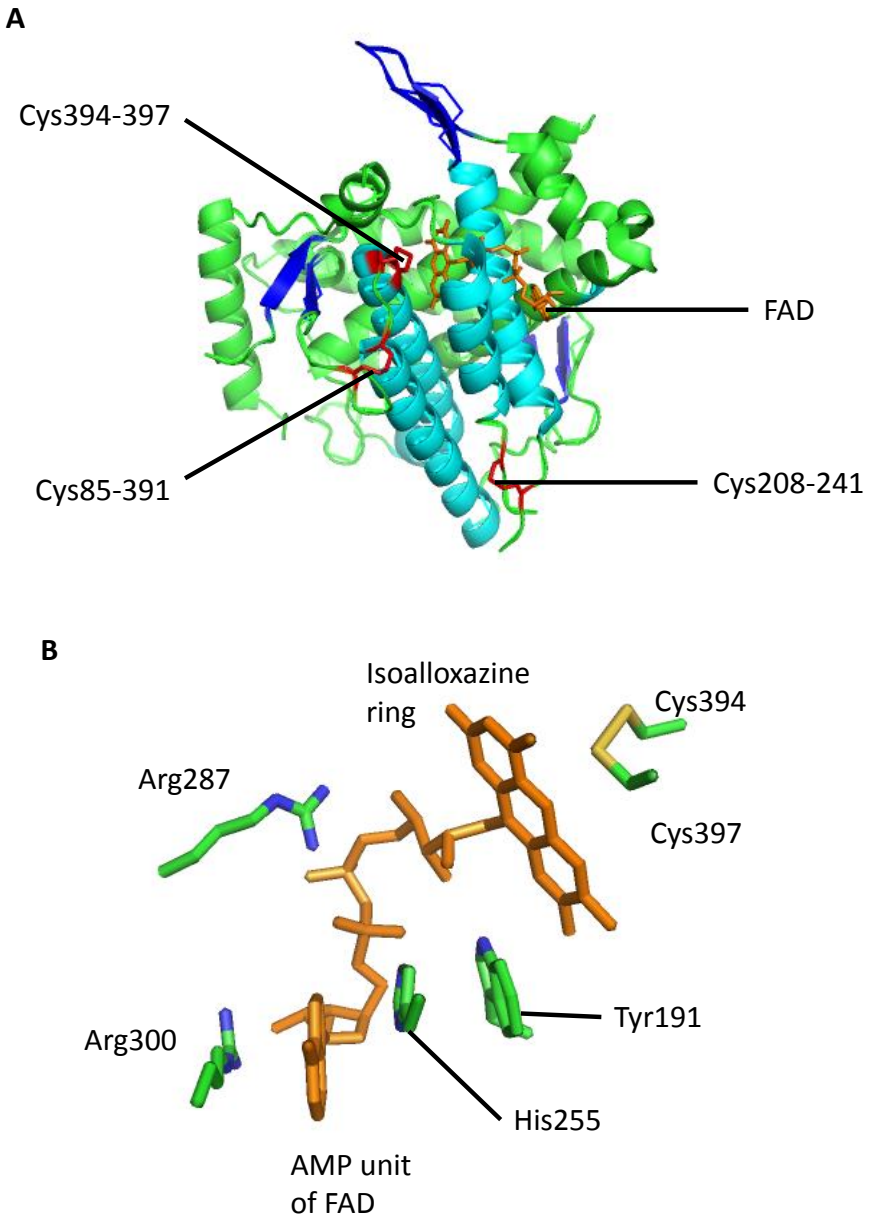

Figure 1.7 – Overall molecular structure of Ero1α and the FAD binding region. A Ribbon diagram showinh the structure of Ero1α showing FAD as orange sticks, the conserved four-alpha helical core in cyan, β-sheet structures in blue, visible cysteine residues disulphide bonded and in red and the remaining structure in green. The loop region containing the shuttle disulphide and cysteines 104 and 131 is not shown due to poor electron density. The structure highlights the conserved alpha helical core which is crucial to the binding of FAD and for catalytic activity. B – Close up view of the FAD binding site within Ero1α. Sidechain atoms of labelled residues are represented as sticks with carbon atoms in green, nitrogen in blue, oxygen in red and sulphur in yellow. Tyr191, His255, Arg287 and Arg300 all contribute to the stabilisation of FAD (orange) allowing the adjacent positioning of Cys394 and Cys397. Adapted from Inaba et. al. (2010).

oxidative stress by showing that induced ER stress resulted in an accumulation of reactive oxygen species, but that this could be negated by the silencing of Ero1 by RNAi (Harding et al., 2003). These studies provided indirect evidence that Ero1 was a source of ROS and ER stress, however direct evidence of Ero1p involvement in ER stress and ROS came from a 2007 study which characterised deregulated mutants and highlighted the necessity for regulation of activity.

Having determined that mutating regulatory cysteines to alanines resulted in an increased activity of Ero1p *in vitro*, and that reduction of Ero1p was coupled to activity, Sevier et al. investigated the implications of this on cell growth. A C150/295A mutant defective in regulatory disulphide formation was overexpressed and was shown to be detrimental to growth in yeast. Mutants unable to form the C90-C349 or C134-C166 disulphides grew as well as a control strain, suggesting that deregulation of Ero1p by preventing the C150-C295 disulphide from forming causes cell stress. This effect was negated in the C150/295A-C100/105A mutant, unable to form the regulatory disulphide or the shuttle disulphide, suggesting the decreased viability was linked to catalytic activity. Cells deficient in UPR induction were more susceptible to defective growth, implicating ER stress in this observation and indicating that the stress response provided a compensatory mechanism. Sevier et al. also showed via SDS-PAGE analysis that the C150/295A mutant existed in the reduced form and that it exhibited increased activity *in vivo*; its overexpression was counteracted by the addition of the reducing agent DTT at concentrations previously shown to be toxic to cells. Furthermore, the GSH: GSSG ratio was disturbed by overexpression of this mutant as GSSG was generated in significant quantities. The evidence presented in this study therefore suggests that adequate regulation of Ero1p is essential for cell viability as its hyperactivity is detrimental to cell viability.

Hyperactivity associated with mammalian Ero1α was investigated in 2008 by the parallel studies of Baker et al. and Appenzeller-Herzog et al., as both groups witnessed increased Ero1α activity in mutants. Baker et al. showed *in vitro* that preventing the C99-104 and C94-131 disulphides from forming resulted in a hyperactivity towards PDI, oxidising it more completely and at an increased rate when compared to the wild type enzyme (Baker et al., 2008). Appenzeller-Herzog et al. determined that hyperactive Ero1α can upset ER redox homeostasis *in vivo*. While overexpression of Ero1α did not alter the redox states of the ER oxidoreductases ERp57 or TMX3, overexpression of C131A Ero1α caused an increase in the relative oxidation of the two enzymes. In addition, depleting glutathione levels increased the level of oxidation of ERp57 and TMX3 suggesting that the effects of C131A Ero1α overexpression are masked by compensation from the redox buffer.

Overexpression of Ero1α C131A also caused an increase in oxidised glutathione, while no difference was witnessed with wild type Ero1α overexpression. The results presented by these studies therefore provide *in vitro* and *in vivo* evidence that deregulation or incomplete regulation by the Ero1α regulatory disulphides can affect the ER redox balance. The absence of the C94-131 disulphide in Ero1α results in an increase in oxidation of ER oxidoreductases and an increase in the ratio of oxidised to reduced glutathione – a shift towards a hyperoxidising environment.

More recent work on a deregulated Ero1α mutant has shed yet more light on the resulting ER redox conditions, using a C104/131A double mutant which cannot form either of the regulatory disulphides that occupy the shuttle cysteine active site (Hansen et al., 2012). This study by Hansen et al. compared the effect of wild type and C104/131A Ero1α overexpression on the redox state of ERp57. They found that the double mutant produced a pronounced increase in ERp57 oxidation compared to the wild type, and more so than the effect of the C131A mutant Ero1α (Appenzeller-Herzog et al., 2008). They also investigated the effect of the expression of Ero1α or a deregulated mutant on the ERp57 redox state in the presence of N-acetylcysteine (NAC). NAC is a reducing agent and glutathione precursor and therefore leads to increased production of GSH and a shift towards a more reducing environment. Treatment with NAC partially prevented the oxidative shift in ERp57 indicating that this effect is likely a result of the perturbed redox environment. NAC treatment also prevented the increase in BiP and HERP expression levels, upregulated during times of ER stress and part of the UPR, which was observed with overexpression of C104/131A Ero1α. To follow up further the compensatory effect of the glutathione redox buffer on C104/131A Ero1α overexpression, cells were treated with the glutathione synthesis inbibitor buthionine sulphoximine (BSO). In agreement with previous work with the C131A Ero1α mutant (Appenzeller-Herzog et al., 2008), decreasing the glutathione buffer available to the cells resulted in an aggravated phenotype when overexpressing the C104/131A mutant as ERp57 shifted further towards the oxidised form. An additional experiment using metabolic activity as a measure of cell viability revealed that cells overexpressing the double mutant had decreased viability when grown in the presence of BSO. Taken together, the data from the Hansen et al. study suggests that deregulated Ero1α can disturb the redox balance of the ER by causing a shift towards a more oxidising environment. This shift affects the ER oxidoreductase ERp57 as well as the glutathione ratio. Furthermore, this data reveals that without the glutathione redox buffer

the cells are much less viable and suggests therefore that the correct regulation of Ero1α activity is imperative for the health of the ER and the cell.

As yet there have been no reported incidences of Ero1α interaction with ERp57, while reaction with GSH can be very slow. It is therefore thought that oxidation of these molecules is mediated by Ero1α interaction with PDI as PDI can oxidise GSH. Oxidation of ERp57 is also proposed to be glutathione mediated. In addition to the disulphide-mediated oxidation of GSH, the glutathione balance is likely to be pushed further in the oxidising direction by the production of hydrogen peroxide by Ero1α. GSH is a known peroxide scavenger which can generate GSSG, while the peroxidase function of peroxiredoxin IV can also lead to the oxidation of ER oxidoreductases (Tavender et al., 2010). Deregulation of Ero1α therefore has the potential to cause hyperoxidation of the ER in a variety of ways.

1.2.8 Excessive hydrogen peroxide production is detrimental to ER function.

Hydrogen peroxide production by a deregulated Ero1α has the potential to upset the redox balance within the ER. The above studies allow the conclusion that creating a more oxidising environment can be detrimental to the health of the cells. A study conducted in 2012 aimed to investigate the physiological implications of excessive hydrogen peroxide production in the liver of mice and generated some interesting results. This Margittai et al. study created a hydrogen peroxide-producing system by administering gulonolactone which is metabolised in the ER lumen with the concomitant production of hydrogen peroxide. Administration of gulonolactone resulted in a swelling of the liver and increase in liver weight, while ER cisternae were also found to be dilated (Margittai et al., 2012). These effects could be reversed by the coadministration of DTT. Margittai et al. found that increased hydrogen peroxide production increased the oxidation of NADPH and NADH, the glutathione content within the ER and protein thiol content as ERp72, ERp46 and ERp5 all showed a shift towards the oxidised species. Furthermore, ER stress was induced as witnessed by the phosphorylation of the transcription factor eIF2α, a target of the UPR. The study also produced results to suggest that eliminating hydrogen peroxide can also have a detrimental effect on protein folding as evidenced by impaired immunoglobulin folding and secretion in cells expressing ER-localised catalase. In conclusion, this data suggests that the delicate balance of the ER must be maintained in order to facilitate oxidative protein folding. Hypo-oxidising conditions prevent effective oxidative protein folding while hyperoxidising conditions also prevent this process and can result in the induction of the UPR, raising the chances of cell death.

1.3 Sulphenylation: a significant redox-based post-translational modification.

Sulphenylation is becoming an increasingly relevant and studied method of post-translational modification. The investigation into the yeast Gpx3 and Yap1 system showed that this modification is crucial for the functioning of the Yap1 transcription factor (Paulsen and Carroll, 2009). It is also known that sulphenylation of catalytic cysteine residues can be detrimental to their function such as in the bacterial protein OhrR (Eiamphungporn et al., 2009) and so a protective mechanism exists within the bacterial periplasm to keep single cysteine residues in a reduced state (Depuydt et al., 2009). Recent results have therefore painted a very diverse picture concerning the function of cysteine oxidation; however it is clear that sulphenylation can have a critical impact upon the activity of enzymes and thus many cellular processes.

1.3.1 Thiol sulphenylation is a potential method of reversibly modulating enzymatic activity.

Sulphenylation of thiols occurs when the thiolate ion of a cysteine residue side chain ($-S^-$) is reversibly oxidised by a ROS, such as a peroxide or superoxide, to form a sulphenic acid group (-SOH). Sulphenic acid is a highly reactive species and will react with proximal thiol-containing molecules such as proteins or glutathione, or with additional oxidants to form the hyperoxidised species - sulphinic ($-SO_2H$) or sulphonic ($-SO_3H$) acid. Recent evidence has shown that sulphenic acid groups can be protected from hyperoxidation by the local environment and may therefore provide a means of reversible activity modulation. This is thought to occur in peroxiredoxin IV where structuring of the local environment after sulphenylation of the peroxidatic cysteine prevents hyperoxidation and thus allows the protein to retain its activity (Cao et al., 2011). Another study investigating protein tyrosine phosphatase 1B showed that the active site cysteine undergoes sulphenylation which is stabilised by the formation of a sulphenyl amide, protecting it from further oxidation (van Montfort et al., 2003). Hyperoxidation was thought to be an irreversible modification however there is evidence to suggest that the sulfiredoxin family of enzymes can rescue proteins with this modification (Jeong et al., 2006) again suggesting a role for cysteine oxidation in reversible modulation. The van Montfort et al. and Cao et al. studies adopted a crystallographic approach to implicate cysteine sulphenic acid in the activity of protein tyrosine phosphatase 1B and peroxiredoxin IV respectively. However, a growing number of studies are adopting a chemical approach to identify cysteine sulphenic acid in enzyme activity.

1.3.2 Detecting sulphenic acid in proteins using chemical probes.

The development of chemical probes to selectively react with cysteine sulphenic acid has provided a powerful means by which this modification can be investigated. A 1974 study by Benitez et al. first showed that sulphenic acid could react specifically and irreversibly with the chemical probe 5,5-dimethyl-1,3-cyclohexadione (dimedone). Dimedone was used to show that sulphenic acid formed in glyceraldehyde-3-phosphate dehydrogenase and that activity was subsequently abolished (Benitez and Allison, 1974). Dimedone is a cell permeable cyclic diketone which reacts with the electrophilic sulphur atom within cysteine sulphenic acid in a condensation reaction, covalently linking the chemical probe to the protein. This chemical probe was utilised in a 2009 study by Seo & Carroll where a means to visualise the dimedone-protein adduct was developed. A specific antibody was described which could bind the adduct and allow Western blotting and immunofluorescence techniques to provide a widely applicable method for sulphenic acid detection *in vitro* and *in vivo* (Seo and Carroll, 2009).

In addition to the dimedone system, Carroll's group developed a new probe, based on dimedone, in an attempt to improve the identification, enrichment and visualisation of labelled proteins (Reddie et al., 2008). Dimedone was used as a scaffold and modified to include an azide group attached to the 1,3-cyclohexadione via an amide link – allowing the addition of phosphine groups, for example pBiotin. The advantage of linking the chemical probe to pBiotin allows exploitation of the extremely specific and stable binding of biotin to avidin or streptavidin. Streptavidin can be coupled to agarose beads or conjugated to antibodies for purification or Western blotting techniques, respectively. These properties were subsequently confirmed using the newly created DAz-1 molecule and thus provide an additional method to detect sulphenic acid in proteins (Reddie et al., 2008).

A 2009 study by Paulsen & Carroll utilised these chemical probes to investigate the role of cysteine sulphenic acid in the Yap1 transcription factor system in yeast, which is central to the oxidative stress response. The Yap1 system is essential for survival under conditions of oxidative stress and is known to upregulate over 100 genes including thioredoxin and glutathione biosynthesis genes. Yap1translocation to the nucleus under oxidative stress has been shown to be dependent on conserved cysteine residues (Kuge et al., 1997). Further work subsequently implicated disulphide formation in the regulation of the enzyme; a nuclear export signal is masked in the active, disulphide bonded state thus retaining the transcription factor in the nucleus (Wood et al., 2004). Gpx3, a glutathione peroxidase, was shown to have a role in Yap1 activation and implicated an essential Gpx3 cysteine in this activation. Furthermore, a cysteine to alanine mutation at residue 303 in Yap1 stabilised a Gpx3-Yap1 disulphide-linked complex, suggesting disulphide transfer to Yap1 (Delaunay

et al., 2002). Therefore the proposed mechanism of Yap1 activation is mediated by the peroxide-induced oxidation of Gpx3 which generates a disulphide bond. This disulphide is transferred to cysteine residues 303-598 of Yap1, masking the nuclear export signal and allowing the transcription factor activity of Yap1 to upregulate oxidative stress protection genes.

The Paulsen & Carroll study confirmed that Yap1 accumulated in the cytosol in untreated cells and that peroxide treatment prevented nuclear export. However, peroxide treatment coupled with dimedone prevented Yap1 translocation from the nucleus, suggesting that sulphenic acid formation is essential for Yap1 accumulation in the nucleus (Paulsen and Carroll, 2009). To prove that this effect was as a result of Gpx3 sulphenylation and modification by dimedone, DAz-1 was used as an alternative sulphenic acid-reactive probe. Treatment with peroxide and DAz-1 again blocked Yap1 translocation from the nucleus. Immunoprecipitation of Gpx3 and subsequent ligation of p-Biotin then allowed detection of the DAz-1 labelling by a HRP Western blot. This confirmed that Gpx3 selectively reacted with DAz-1 in the presence of hydrogen peroxide and thus DAz-1 traps Gpx3 in the sulphenylated state *in vivo*. This was also confirmed *in vitro* using recombinant protein. Paulsen & Carroll then provided evidence suggesting that dimedone could prevent formation of the Gpx3-Yap1 complex, confirming the hypothesis that dimedone modification of the sulphenylated Gpx3 cysteine would prevent mixed disulphide formation between the two enzymes. This study therefore provides clear evidence that oxidation of cysteine residues can play a critical role in the yeast oxidative stress response. It also shows that chemical probes can be used to detect sulphenic acid formation *in vitro* and *in vivo*, and provides a means of disrupting the system to determine the function of sulphenylation.

1.3.3 The DsbG sulphenylation protection mechanism in gram negative bacteria.

The Dsb system in bacteria provides an oxidative protein folding pathway within the periplasmic space. To balance the oxidative pathway, a reductive pathway exists and is mediated by the proteins DsbB and the periplasmic isomerases DsbC and DsbG. In addition to maintaining the isomerase machinery in a reduced state, the reductive pathway is now known to be important for other purposes. For example, the discovery of a periplasmic peroxiredoxin enzyme and its reduction by the DsbB-like protein ScsB in *Caulobacter crescentus* prevents inactivation of the due to hyperoxidation (Cho et al., 2012). This has implications in the scavenging of peroxides and the balancing of oxidative power in the periplasm. A novel PDI-like protein within the periplasm of the same organism, ScsC, and its ScsB-dependent reduction again demonstrates that this reductive

pathway is important for protein folding and is a widely adopted mechanism for electron transport (Cho et al., 2012). However, one particularly interesting and crucial function of the reductive pathway is the protective mechanism mediated by DsbG. While DsbG shares a certain level of identity and similarity with DsbC, one crucial difference between the two is the composition of the binding domains – DsbG is thought to bind larger, more fully-folded proteins.

As yet, no substrates have been found to be affected by the absence of DsbG in terms of folding; however a mutant of DsbG in which has the resolving cysteine of its active site mutated to alanine (CxxA) interacts with a host of substrates in a disulphide-dependent manner (Depuydt et al., 2009). This was shown in a 2009 study by Depuydt et al. which isolated and determined YbiS as an interacting factor; a transpeptidase involved in the crucial process of peptidoglycan synthesis. This protein contains a single cysteine residue which is essential for functioning (Mainardi et al., 2007). Depuydt et al. showed that, after reacting purified YbiS with the thiol-reactive 2-nitro-5-thiobenzoate (DTNB) to form YbiS-TNB, DsbG was able to reduce the YbiS cysteine. By spectrophotometrically following the reaction between these two reagents, the reduction of the YbiS cysteine residue is coupled to the release of the TNB moiety – which absorbs light at 412nm. The Depuydt et al. study showed that this reaction produced an increase in absorbance at 412nm thus indicating the reduction of the YbiS cysteine. An *in vivo* disulphide-dependent interaction was confirmed between YbiS and DsbG when a dsbG null mutant was complemented with a DsbG containing the CxxA mutation in the active site. This mutant cannot resolve the mixed disulphide formed between the two molecules therefore the reaction intermediate is stabilised; the resultant complex was confirmed by Western blotting. Crucially, the equivalent experiments performed with DsbC showed no interaction, providing *in vivo* evidence for the distinctive substrate specificity of DsbG.

Further *in vivo* studies by Depuydt et al. suggest that the cysteine thiol in YbiS is susceptible to oxidation or sulphenylation. This was shown by looking at the oxidation state of YbiS using a number of *E. coli* strains: *dsbC*, *DsbG*, *dsbCdsbG* and wild type. YbiS was found to be more oxidised in the *dsbG* null mutant compared to the *dsbC* null mutant, suggesting that it is preferentially reduced by DsbG. However, more oxidised YbiS was found in the *dsbCdsbG* mutant suggesting that DsbC may contribute slightly to the reduction of the thiol. Next, the study tested the YbiS oxidation state in a *dsbB* mutant which, as expected, resulted in an increased oxidation of the YbiS free thiol due to the absence of a reductive pathway. This oxidation was shown to be due to sulphenylation; incubating YbiS with hydrogen peroxide increased the cysteine sulphenic acid content.

This effect was confirmed both *in vitro* and *in vivo*. Further *in vivo* work subsequently showed that protein sulphenic acid content was elevated in *dsbC* and *dsbG* mutants, and was most prevalent in the *dsbCdsbG* double mutant. The conclusion from this study is that DsbG, with its increased affinity for folded proteins, is likely to reduce oxidised single cysteine residues and protect from sulphenylation and inactivation. DsbC is proposed to act as a backup for DsbG in this function so that proteins within the periplasm are protected from this unwanted modification.

1.3.4 The peroxiredoxin family; protecting from and harnessing the oxidative power of hydrogen peroxide.

While gram-negative bacteria possess the DsbG sulphenylation protection system, another conserved group of enzymes are widely adopted by prokaryotes and eukaryotes to prevent unwanted peroxide-mediated oxidation. The peroxiredoxin (Prx) group of enzymes, of which there are six in mammals (PrxI-VI), are all antioxidant enzymes with a high reactivity towards hydrogen peroxide. They have specific expression patterns: PrxI exists in the cytosol and nucleus (Immenschuh et al., 2003), PrxII in the nucleus, PrxIII in the mitochondria (Matsushima et al., 2006), PrxIV in the ER and potentially secreted (Tavender et al., 2008), PrxV in peroxisomes and PrxVI in the cytosol (Figure 1.8). The peroxiredoxins can be split into two main groups – the typical and the atypical 2-Cys Prxs. The typical 2-Cys peroxiredoxins are the most extensively studied group of peroxiredoxins with their general structures and catalytic mechanisms well established. PrxIV is a member of the typical 2-Cys family and is known to be directed to the ER by an N-terminal signal sequence and retained by an as yet unknown mechanism as it lacks the KDEL ER-retention motif (Tavender et al., 2008).

The peroxiredoxins are characterised by a conserved redox active cysteine, termed the ‘peroxidatic’ cysteine. The sulphydryl group of the residue attacks peroxides resulting in the formation of a cysteine sulphenic acid (-SOH) (Choi et al., 1998). The 2-Cys Prxs also have a C-terminal ‘resolving’ cysteine, which will then attack the sulphenic acid to form a disulphide with the concomitant release of water. PrxIV specifically exists as a homodecamer with the peroxidatic cysteine (C124) attacked by the resolving cysteine (C245) of another enzyme thus linking the two molecules together via a disulphide bond. This interaction arranges the dimer in such a way that the remaining free peroxidatic and resolving cysteines come into close proximity. Upon oxidation by further peroxide a disulphide can form between these residues resulting in the linking of the dimer by two disulphides rather than one (Figure 1.9). The remaining solvent accessible cysteine (C51) can then disulphide bond with adjacent C51 residues to build the homodecamer. The

reaction of Prx with peroxide is thought to be facilitated by the local environment of the peroxidatic cysteine. Thiols have a pKa of around 8, however the peroxidatic cysteine thiol is thought to have a pKa of around 5-6 (Nelson et al., 2008) allowing for a rate constant of around 10^7 M^{-1} s^{-1} (Peskin et al., 2007). A conserved hydrogen bonding network present in the active site is also thought to activate peroxide to increase reactivity with the thiolate anion (Hall et al., 2011), resulting in the high rate constant.

This high rate constant ensures that the peroxiredoxins are efficient peroxide scavengers and are sensitive to peroxide levels within the cell. However, they are susceptible to hyperoxidation by high concentrations of hydrogen peroxide (Wagner et al., 2002, Tavender and Bulleid, 2010). A sulphenic acid group can be oxidised further to create the hyperoxidised sulphinic ($-SO_2H$) or sulphonic ($-SO_3H$) acids. This effectively inactivates the enzyme as the hyperoxidised peroxidatic cysteine side chain cannot be resolved by the resolving cysteine and so cannot form the intramolecular disulphide bond. In the inactive form peroxiredoxin is thought to allow the accumulation of higher concentrations of hydrogen peroxide in order to propagate a signal, leading to cell cycle arrest for example (Phalen et al., 2006). They have also been suggested to provide a chaperone function when peroxidase activity is abolished (Lee et al., 2007). Hydrogen peroxide scavenging, chaperoning and signal propogation are therefore three functions carried out by the peroxiredoxins.

One function particular to PrxIV was discovered recently relating to the specific localisation of PrxIV in the ER and its proximity to the oxidative protein folding machinery. The presence of the sulphydryl oxidase Ero1α within the ER leads to the production of hydrogen peroxide within the compartment. This hydrogen peroxide is now known to be not just mopped up by PrxIV but actually utilised in order to harness its oxidising power. Under steady state conditions oxidative stress is not induced within the ER, however when the UPR is induced Ero1β is upregulated, providing greater oxidising power (Harding et al., 2003). This in turn generates higher concentrations of reactive oxygen species and oxidative stress (Marciniak et al., 2004) which is exacerbated in a PrxIV knockdown cell line (Tavender and Bulleid, 2010). This suggests that PrxIV is the main peroxidase involved in the breakdown of Ero1α generated hydrogen peroxide. It is now known that the disulphide bonds generated by PrxIV can be passed on to PDI in a dithiol-disulphide exchange mechanism (Tavender et al., 2010, Zito et al., 2010) which, when coupled to the direct oxidation of PDI by Ero1α, results in the formation of two disulphides within PDI. The implications of this are that oxidative protein folding is more efficient and can be driven independently of the Ero1α-PDI mechanism and this

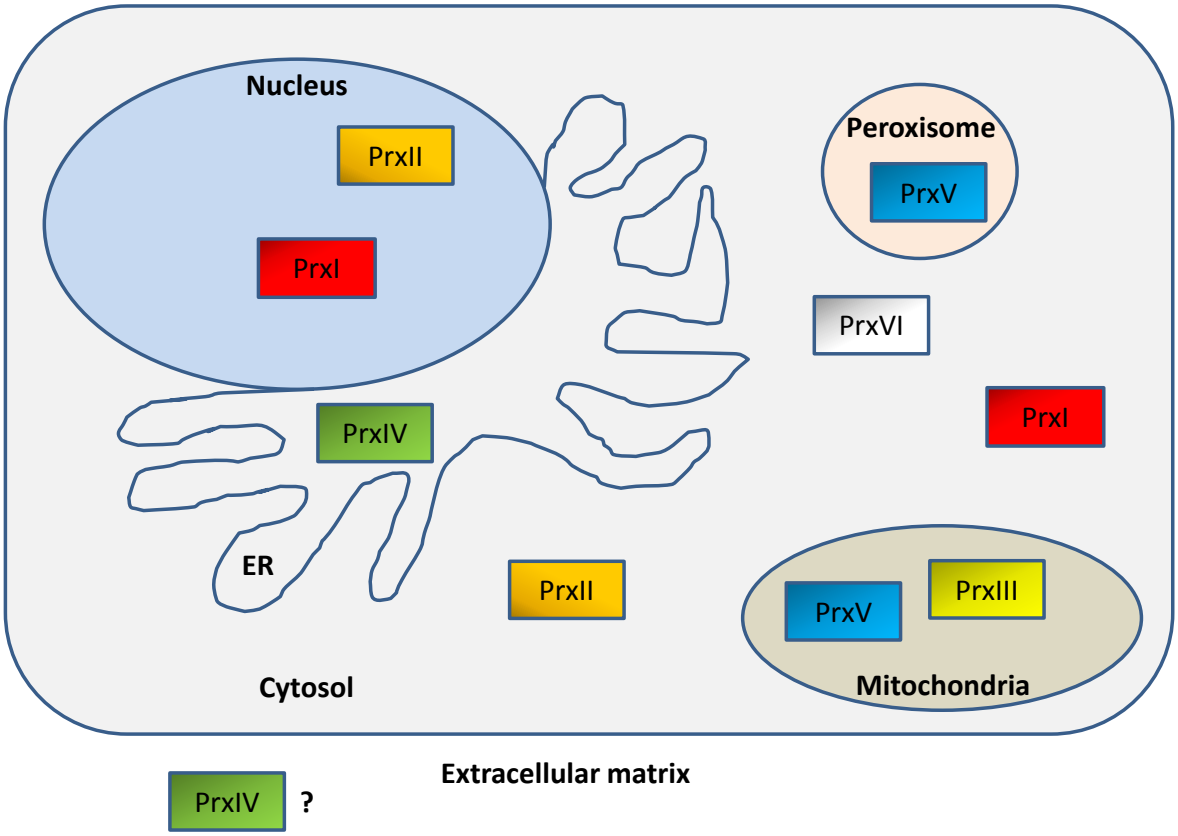

Figure 1.8 – Cellular and extracellular localisation of the peroxiredoxin peroxide scavangers. PrxI and PrxII are found in the nucleus, while PrxI, II and VI are found in the cytosol. PrxIII and V are localised to the mitochondria; PrxIV is found within the ER and is potentially secreted; PrxV is found in peroxisomes.

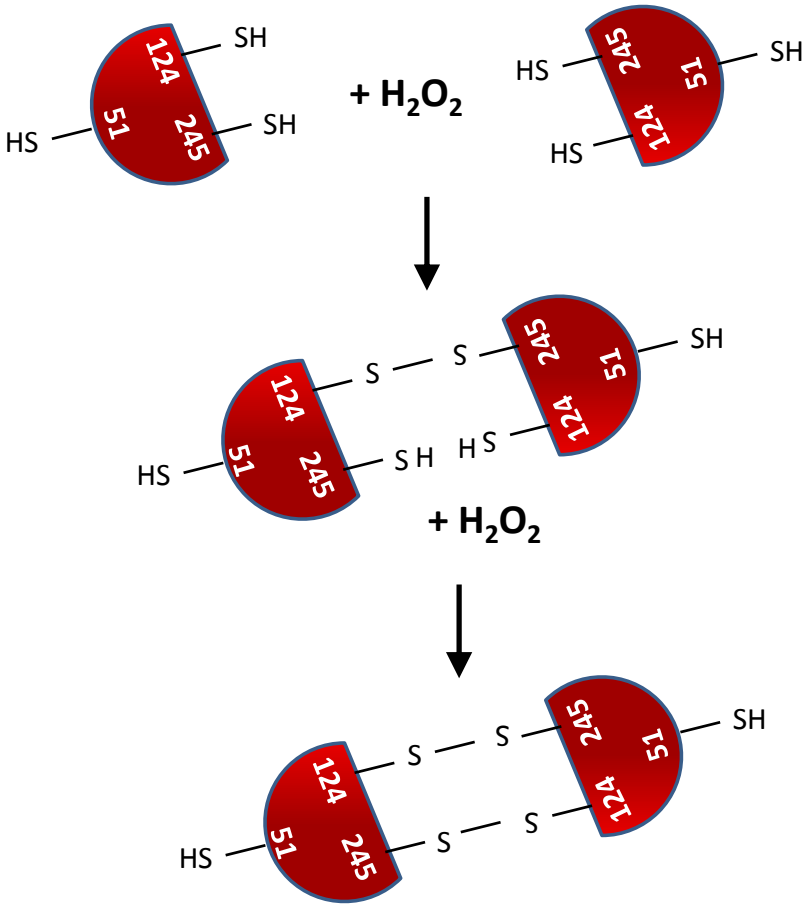

Figure 1.9 – Peroxiredoxin IV reacts with hydrogen peroxide which creates disulphide linked homodimers. Hydrogen peroxide reacts with cysteine 124, the 'peroxidatic' cysteine, of one molecule of PrxIV resulting in the sulphenylation of cysteine 124. The 'resolving' cysteine, cysteine 245, of a second PrxIV molecule reacts with the cysteine sulphenic acid, releasing water and linking the two molecules via a disulphide. A second hydrogen peroxide molecule can then react with the second peroxidatic cysteine before resolution of the sulphenic acid by the second resolving cysteine. This links the dimer via a second disulphide.

observation has been confirmed *in vivo* (Zito et al., 2010).

1.4 Aims of this study.

The mechanism of reduction of the Ero1α regulatory disulphides has been well characterised. What is unclear is how these regulatory disulphides are re-formed. This is of significant interest as Ero1α hyperactivity, or deregulated activity, can have dire consequences for oxidative protein folding, the ER and the cell. Correct regulation of Ero1α activity is imperative to prevent hyperoxidation of the ER and the misfolding of client proteins. The Kim et al. study in 2012 highlighted the ability of Ero1p to regulate its own activity via autonomous oxidation, while PDI was also identified as a major source of disulphides for this purpose. Many studies have shown previously, however, that there are subtle differences between the Ero1p and Ero1α isoforms. This study aimed to investigate the regulation of Ero1α activity at the molecular level.

Three hypotheses were proposed which could all feature in the mechanism of Ero1α re-oxidation and inactivation, and could be tested experimentally. These were:

- That Ero1α regulatory disulphide formation may be driven by hydrogen peroxide; creating a feedback loop that would ensure Ero1α activity would be regulated when hyperactivity generated excessive quantities of hydrogen peroxide.
- That the flexible nature of the loop accommodating the Ero1α shuttle disulphide may provide a means of distributing disulphides within the Ero1α molecule itself, from the active site adjacent to the FAD cofactor to the regulatory cysteine residues. Autonomous Ero1α oxidation may also be feasible.
- That PDI family members and ER residents may provide a means of oxidising Ero1α regulatory disulphides due to the propensity of PDIs to oxidise reduced substrates. This would also provide a feedback loop which would shut down Ero1α activity when the pool of oxidoreductases becomes overly oxidised, or when the ER glutathione balance is shifted towards a more oxidising ratio and prevents the reduction of the PDIs.

Furthermore, the role of glutathione within the ER has been debated for a number of years. To further investigate the role of glutathione on the ER redox balance, this study aimed to:

- Investigate role of glutathione in redox homeostasis in the ER
- Investigate the impact of Ero1α on redox homeostasis in the ER in the absence of cytosolic glutathione
- Compare the redox states of ER oxidoreductases in SP cells and microsomes

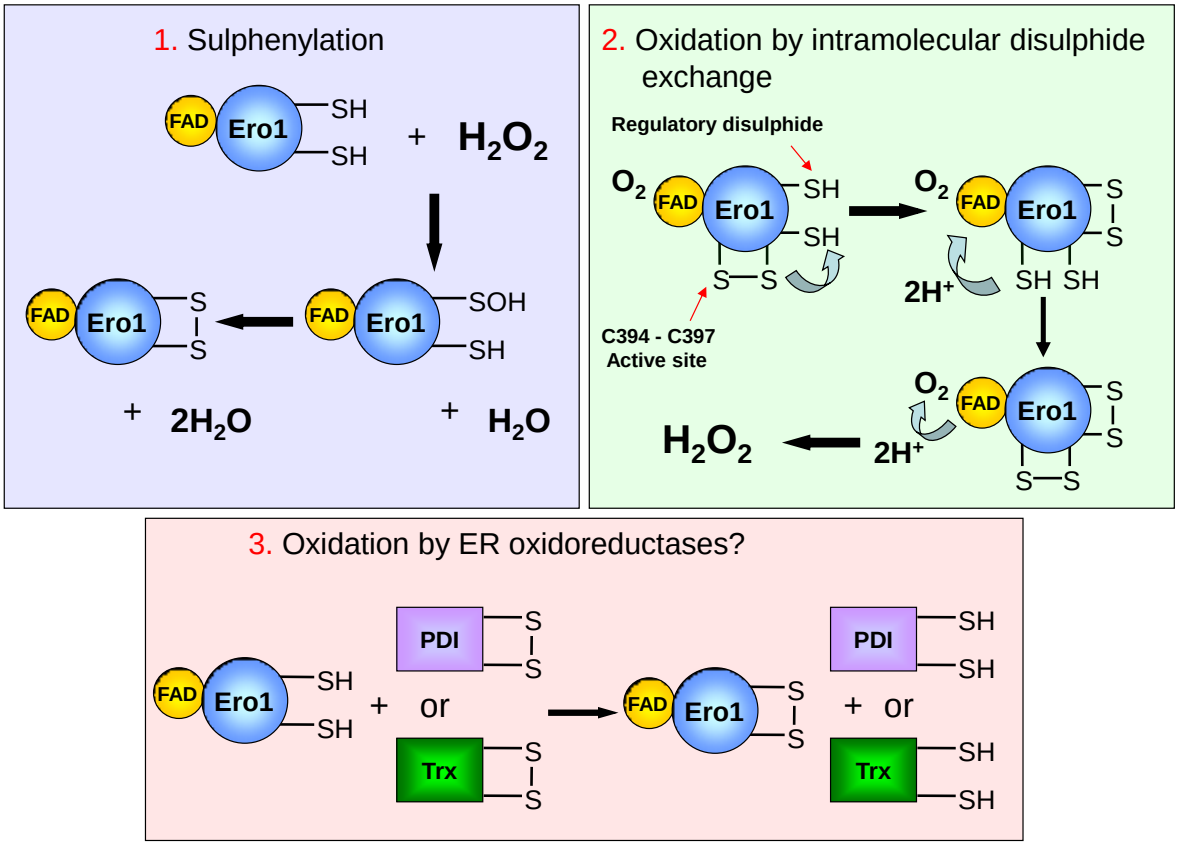

Figure 1.10 – Oxidation and inactivation of Ero1α may result from Sulphenylation, intramolecular disulphide exchange or by oxidation by ER oxidoreductases. Schematic diagram to depict the potential mechanisms of oxidation of Ero1α. 1 – Sulphenylation may drive oxidation of the regulatory disulphides. 2 – The disulphides generated by Ero1α may be distributed within the molecule to the regulatory cysteine residues. 3 – ER oxidoreductases, such as PDI, or the non-physiological substrate Trx, may provide a means of regulating Ero1α activity.

Chapter 2.0
Materials and Methods

2.1 Strains and plasmids.

2.1.1 Bacterial strains.

Escherichia coli XL1 blue cells (Invitrogen) were used for the replication of plasmid vectors. These cells are endonulease and recombinase deficient so inserts are more stable. For expression and purification of recombinant proteins, *E. coli* Origami B (DE3) pLysS cells were used (Novagen). These cells lack thioredoxin reductase and glutathione reductase; preventing reduction of thioredoxin and glutathione thus greatly enhancing disulphide bond formation within the cytoplasm.

2.1.2 Plasmids used during this study.

The human Ero1α expression vector was previously prepared as described (Baker et al., 2008). A pET23a vector construct was used to express a His-tagged version of PDI. A pET28a vector was used to express a His-tagged version of *E. coli* thioredoxin. A pVD85 construct expressing His-tagged PDI binding mutant (I272A, D346A, D348A) wasobtained from Lloyd Ruddock (University of Oulu).

2.2 Growth of bacteria, culture media and general growth conditions.

Unless stated, bacterial growth was carried out in Luria-Bertani (LB) medium (Tryptone 10 g/l, yeast extract 5 g/l and NaCl 10 g/l in dH_2O, pH 7). For LB-agar plates, 15 g/l agar was added to LB before autoclaving. All media was autoclaved immediately following preparation.

Overnight cultures were grown in 5ml LB for 15 hr at 37 °C, shaking at 200 rpm. Inoculation was carried out using frozen glycerol stocks or a single colony grown on LB-agar plates. Larger overnight cultures were grown in 50 ml volumes to be used in Midi-prep plasmid purifications.

Antibiotics were prepared by dissolving antibiotics in dH_2O (ampicillin, kanamycin or tetracycline) or ethanol (chloramphenicol) before filter sterilising. Ampicillin was used at a final concentration of 100 μg/ml, chloramphenicol at 30 μg/ml, and kanamycin and tetracycline at 10 μg/ml.

For LB-agar plates containing antibiotic, LB-agar was heated until liquid before cooling to 42 °C before the addition of the appropriate antibiotic.

For short term storage, growth on LB-agar plates was stored at 4 °C for up to two weeks. For longer periods of storage, overnight cultures were grown and mixed with sterile glycerol (50% v/v) at a ratio of 4:1 of culture: 50% glycerol. The mix was then stored at -80 °C.

2.3 Transformations and extraction of plasmid DNA.

2.3.1 Transformations.

Approx. 1ng DNA was added to 50 µl of competent cells (gifted by Dr. Jana Rudolf, University of Glasgow) and left on ice for 30 min after gently mixing. Cells were then heat shocked for 90 s at 42 °C before LB was added. Cells were incubated at 37 °C for 45 min, shaking at 200 rpm, before plating onto an LB-agar plate containing the appropriate antibiotics. Plates were left to dry then incubated at 37 °C overnight.

2.3.2 DNA purification.

DNA or shRNA was purified using a Qiagen Plasmid Midi Kit under the instructions recommended by the manufacturer. The final purified DNA was resuspended in dH_2O. DNA was also purified by alkaline lysis. Using the alkaline lysis method, bacterial culture was spun at 14,000 x g before resuspending the pellet in chilled GTE solution (25 mM Tris-HCl, pH 8.0 containing 50 mM glucose, 10 mM EDTA; autoclaved). This was incubated for 2 min before adding NaOH/SDS solution (0.2 M NaOH and 1% (w/v) SDS) and inverting to mix. This was incubated on ice for 5 min then potassium acetate solution (5 M potassium acetate, pH 4.8) was added and mixed well. This mix was centrifuged at 14,000 x g for 5 min then supernatant was moved to a fresh tube.

Phenol:chloroform:isoamyl alcohol was added before centrifuging for 2 min at 14,000 x g. The resulting upper phase was moved to a new tube and choloform:isoamyl alcohol was added then mixed and centrifuged at 14,000 x g for 2 min. The upper phase was again moved to a fresh tube with 95% ethanol, mixed and centrifuged at 14,000 x g for 5 min. Supernatant was discarded and pellet was washed with 70% ethanol. The pellet was spun again, 95% ethanol removed and left to dry. The resulting dry pellet was resuspended in dH_2O and used appropriately or frozen at -20 ºC.

2.4 Recombinant protein expression and purification.

2.4.1 Ero1α expression and purification.

The Ero1α expression vector was transformed into Origami B (DE3) pLysS *E. coli* cells. A glycerol stock was used to inoculate 5 ml LB containing 100 µg/ml ampicillin, 30 µg/ml chloramphenicol, 10 µg/ml tetracycline and 10 µg/ml kanamycin. This culture was

incubated at 37 ºC overnight, shaking at 200 rpm. The 5 ml culture was used to inoculate 500 ml LB containing the same antibiotics at the same concentrations, which was left to grow until the A_{600} reached between 0.5 and 1. At this point an additional 100 ml LB was added along with 0.4% glucose, 0.2 mM IPTG, 10 µM FAD and 20 µg/ml ampicillin. The culture was moved to a 16 ºC incubator where expression of Ero1α was induced for 24 hr.

Cells were then pelleted by centrifugation at 8832 x g for 15 min before resuspending in 20 ml ice-cold lysis buffer (50 mM Tris-HCl buffer, pH 7.5 containing 1 mg/ml chicken egg white lysozyme, 20 µg/ml DNase I, 2.5 µg/ml RNase A, two complete EDTA free protease cocktail inhibitor tablets, 1 mM EDTA and 0.1% v/v Triton X-100) per litre of culture. Cells were lysed by freeze-thawing in liquid nitrogen and a 37 ºC water bath then incubated at room temperature with gentle agitation for 10 min. Samples were centrifuged at 13,248 x g for 30 min and the supernatant was incubated with 1 ml glutathione sepharose beads (pre-equilibrated in 50 mM Tris-HCl buffer, pH 7.5, GE Healthcare). This was left for between 1 and 4 hr at 4 ºC with gentle agitation before washing with 50 ml 50 mM Tris-HCl buffer, pH 7.5. Beads were then resuspended in 2.5 ml of 50 mM Tris-HCl buffer, pH 8 containing 2.5 mM $CaCl_2$ and 100 units of thrombin. This was left at 4 ºC overnight with agitation. Supernatant was passed through a Nickel-affinity column (GE Healthcare, His-trap FF 1ml) pre-equilibrated with 50 mM Tris-HCl buffer, pH 7.5 containing 5 mM imidazole. The column was then washed with wash buffer containing 50 mM imidazole. Elution was carried out by gradually increasing the imidazole concentration up to 500 mM.

The fractions containing Ero1α were then pooled and desalted in a PD10 column before buffer exchanged into 50 mM Tris-HCl buffer, pH 7.5 containing 1 mM EDTA and concentrated in a 10,000 Da Mw cut-off Vivaspin (GE Healthcare). Concentrations were determined via spectrophotometer using the bound FAD absorption coefficient of 12.9 mM^{-1} cm^{-1}at 280 nm.

2.4.2 PDI wild type and binding mutant expression and purification.

PDI wild type or binding mutant expression vectors were transformed into Origami B (DE3) pLysS *E. coli* cells. A single colony was used to inoculate a 5 ml overnight culture of LB containing 100 µg/ml ampicillin. This was then used to inoculate 500 ml YT media (10 g/l tryptone, 5 g/l yeast extract, 25 mM Na_2HPO_4, 25 mM KH_2PO_4, 50 mM NH_4Cl, 5 mM Na_2SO_4, 2 mM $MgSO_4$, 2 mM $CaCl_2$, 0.5% glycerol, 2.5 mM glucose and 0.2% lactose in dH_2O. This culture was grown for 30 hr at 30 °C before harvesting at 8832 x g for 15 min at 4 °C. Cells were lysed in 50 mM Tris-HCl buffer, pH 8 containing 300 mM

NaCl, 1 mg/ml chicken egg white lysozyme, 20 μg/ml DNase I, 2.5 μg/ml RNase A, two complete EDTA-free protease inhibitor cocktail tablets, 1 mM EDTA and 0.1% v/v Triton X-100. This was left at room temperature for 20 min then freeze/thawed three times. Samples were centrifuged at 13248 x g for 30 min and the supernatant was filtered through 0.22 μm filter then passed through a Nickel-affinity column (His-trap FF 1ml, GE Healthcare) pre-equilibrated with Buffer A (50 mM Tris-HCl buffer, pH 8 containing 300 mM NaCl). Bound material was eluted over a linear concentration gradient from 0 – 500 mM imidazole in Buffer A. Eluted material was concentrated and passed down a gel filtration column (Superdex 200 10/300 GL, GE Healthcare) pre-equilibrated in 50 mM Tris-HCl buffer, pH 7.5 containing 300 mM NaCl and 10% v/v glycerol. PDI-containing fractions, as determined by SDS-PAGE and Western blot, were either subject to further chromatography or pooled, concentrated, aliquoted and stored at -80 °C until needed. Protein concentration was determined as with Ero1α, using an absorption coefficient of 45.8 mM^{-1} cm^{-1}.

2.4.3 Purification of thioredoxin.

Purification of thioredoxin was carried out as for PDI but supplementing growth media with 10 μg/ml kanamycin in place of ampicillin. Protein concentration was calculated spectrophotometrically at 280 nm using an absorption coefficient of 14.1 mM^{-1} cm^{-1}.

2.4.4 Size-exclusion chromatography.

Size exclusion chromatography was carried out using a Superdex 200 10/300 GL column (GE Healthcare). Samples were clarified by centrifugation at 13248 x g for 10 min and concentrated to 0.5 ml in a Vivaspin column (10,000 Da cut-off). Samples were loaded onto the column in a buffer of 50mM Tris-HCl, pH 7.5 containing 300mM NaCl and elution was carried out in the above buffer. 500 μl fractions were collected and analysed by SDS-PAGE where necessary. The elution volumes of proteins of interest were compared to that of known standards in order to calculate the molecular weights.

2.4.5 Ion-exchange chromatography.

Ion exchange chromatography was carried out using a HiTrap Q FF column (GE Healthcare). Samples were buffer exchanged to remove NaCl in a Vivaspin column (10,000 Da cut-off), clarified by centrifugation at 13248 x g for 10 min and loaded onto the column. After loading, the column was washed with 5 column volumes of buffer (50 mM Tris-HCl, pH 7.5). To elute proteins, a linear gradient elution was applied in the above buffer containing 0 – 1 M NaCl over 5 column volumes. 250 μl fractions were collected and samples from each analysed by SDS-PAGE.

2.5 SDS-PAGE, Western blotting and gel staining.

Samples for sodium dodecyl-sulphate polyacrylamide gel electrophoresis (SDS-PAGE) analysis were resuspended in SDS sample buffer (25 mM Tris-HCl buffer, pH 6.8 containing 2% w/v SDS, 2% v/v glycerol and 0.004% w/v bromophenol blue). Reduced samples contained 20 mM DTT or 10 mM TCEP. Gels were then Coomassie stained, silver stained or transferred onto a nitrocellulose membrane for Western blotting. For Western blots, membranes were blocked in 3% milk in TBST (Tris-buffered saline, 10 mM Tris-HCl buffer, pH 7.5 containing 150 mM NaCl supplemented with 0.1% v/v Tween-20) for 1 hr. Primary antibodies were used at 1:10,000 (α-GAPDH; Abcam), 1:2,000 (α-Ero1α, Cell Signalling Technologies; α-ERp46, Prof. Ellgaard, Univ. Copenhagen; and α-$PrxSO_{2/3}$, Abcam), 1:1,000 (α-PDI, Prof. Freedman, Univ. Warwick; α-ERp57, Abcam; and α-PrxIV, Lab Frontier) or 1:500 (α-dimedone, Prof. Carroll, Scripps Institute) in TBST for 1 hr or overnight. Secondary antibodies (Thermo Scientific) were used at 1:2,500 for 1 hr, and blots were visualised using an Odyssey Imaging System (LI-COR Biosciences). α-mouse secondary antibody was used to bind α-GAPDH, α-PrxIV and α-$PrxSO_{2/3}$ primary antibodies. α-rabbit secondary antibody was used to bind α-PDI, α-ERp46, α-ERp57 and α-dimedone primary antibodies. α-goat secondary antibody was used to bind α-Ero1α primary antibody.

SDS-PAGE gels were cast and run using Pharmacia Biotech mini VE Complete apparatus. The resolving gel with appropriate acrylamide content was poured using 30% ProtoGel (w/v) acrylamide (National Diagnostics), resolving buffer (1.5 M Tris-HCl, pH 8.8), 10% (w/v) ammonium persulphate in dH_2O (APS), 10% SDS in dH_2O and 25 µl N, N, N', N'-Tetramethylethylenediamine (TEMED) (Sigma). Once poured and before setting, the resolving gel was overlaid with 0.5 ml isopropanol. The isopropanol was removed once the gel was set. The resolving gel was poured using resolving buffer (0.5 M Tris-HCl, pH 6.8) in place of stacking buffer.

Molecular weight markers used were either 10 µl 6H (Sigma) or 3 µl Prestained marker (New England Biolabs).

Following electrophoresis, proteins were visualised by gently shaking in Coomassie blue staining solution (45% v/v methanol, 9% v/v glacial acetic acid, 0.1% w/v Sigma Brilliant Blue G-250) for a minimum of 1 hr. Excess stain was removed by washing with dH_2O overnight.

For silver staining, gels were fixed for a minimum of 2 hr in Fixer (50% methanol, 12% acetic acid, 0.05% formalin) and washed three times in 35% ethanol (20 min each). Gels

were sensitised in 0.02% sodium thiosulfate for 2 min before three 5 min washes in water. Gels were stained in 0.2% silver nitrate and 0.076% formalin for 20 min before two 1 min washes in water. Developer (6% sodium carbonate, 0.05% formalin and 0.0004% sodium thiosulfate) was added until bands were visible. Staining was stopped in 50% methanol; 12% acetic acid. Gels were gently agitated throughout the silver staining protocol.

2.6 *In vitro* assays.

2.6.1 Ero1α – Thioredoxin assays.

Thioredoxin was reduced with 10 mM DTT for 10 min at 4 °C and desalted on a PD10 column (GE Healthcare). 2 μM Ero1α was incubated with 100 μM reduced thioredoxin. Assays were performed over 1200 s with samples taken at specific time points and the reactions were stopped in SDS sample buffer containing either 50 mM N-ethylmaleimide (NEM) or 20 mM 4-acetamido-4′-maleimidylstilbene-2,2′-disulfonic acid (AMS) to freeze the redox states. Samples were then analysed via 8% SDS-PAGE to visualise Ero1α redox state or 15% SDS-PAGE to visualise the Trx redox state. For anaerobic assays, all reagents and buffers were kept in an anaerobic chamber overnight to eliminate oxygen. Buffers were purged with nitrogen prior to incubation in anaerobic chamber. Reactions were carried out in 50 mM Tris buffer, pH 7.5 containing 1 mM EDTA. 200 μM free FAD or 50 mM dimedone were included in the reaction buffer as indicated.

2.6.2 Oxygen electrode assays.

Changes in oxygen concentration in solution were measured using a Clarke-type oxygraph instrument (Hansatech Instruments Ltd). Assays were carried out in 50 mM Tris-HCl buffer, pH 7.5 containing 300 mM NaCl; in a total volume of 500 μl. Ero1α was included at a concentration of 2 μM with DTT (10 or 20 mM). Measurement of the oxygen concentration was continued for 900 s or until the oxygen in the chamber had been completely consumed.

For Ero1α-PDI oxidation assays using the oxygen electrode, reactions were carried out using 1μM Ero1α and 10μM PDI under the above conditions. Increasing concentrations of GSH (350μM, 1mM, 2mM or 10mM) were included to maintain PDI recycling.

2.6.3 Ero1α re-oxidation assays.

The redox state of Ero1α was determined using an SDS-PAGE based approach. For the oxygen titration assay, Ero1α was reduced with 10 mM DTT for 1 min before applying to a Micro Bio-Spin 6 Chromatography Column (Bio-Rad) which was pre-equilibrated in anaerobic buffer (50 mM Tris-HCl, pH 7.5 containing 1 mM EDTA) to remove DTT.

Aerobic buffer (50 mM Tris-HCl, pH 7.5 containing 1 mM EDTA and approximately 250 μM O_2) was added to the reaction to increase the O_2 concentration from 0 μM to 50 μM or 225 μM. Samples were taken at time points 0, 10, 30, 60 and 300 s and immediately alkylated in SDS sample buffer containing 25mM NEM. Samples were analysed by 8% SDS-PAGE and silver stained.

For the ER oxidoreductase assays, Ero1α was reduced and DTT was removed as described above. Purified ER oxidoreductases were oxidised by incubation with 20 mM GSSG for 15 min before applying to Micro Bio-Spin columns to remove GSSG. 2 μM Ero1α was incubated with 10 μM oxidoreductase in anaerobic buffer. Samples were taken at time points 0, 10, 30, 60 and 300 s and immediately alkylated in SDS sample buffer containing 25 mM NEM. Samples were analysed by 8% SDS-PAGE and silver stained or Western blotted as required.

For the hydrogen peroxide assays, Ero1α was reduced and DTT removed as above. 10 or 100 μM hydrogen peroxide was added to 2 μM Ero1α then samples were taken at 0, 10, 30, 60 and 300 s. Samples were immediately alkylated in SDS sample buffer containing 25 mM NEM. Samples were analysed by 8% SDS-PAGE and silver staining.

2.6.4 Dimedone labelling.

To label recombinant, purified PrxIV with dimedone in order to identify sulphenic acid formation, 10 μM PrxIV was incubated with 5 mM dimedone and 60 μM hydrogen peroxide in 50 mM Tris-HCl buffer containing 300 mM NaCl. The reaction was titrated to pH 7.5 using sodium hydroxide prior to protein addition. After 10 min, reactions were quenched and dimedone removed by precipitation of protein in 500 μl 10% trichloroacetic acid (TCA). Samples were left on ice for 30 min before centrifucation at 16,000 x g. Precipitated protein was washed three times with 1 ml ice-cold acetone and resuspended in SDS sample buffer and analysed by SDS-PAGE under reducing conditions (50 mM DTT).

Labelling of C245A PrxIV was carried out as above but using 0, 5 or 50 μM hydrogen peroxide during the incubation. Labelling of Ero1α was carried out in the presence of 0, 10, 20 or 60 μM hydrogen peroxide. Samples were then analysed as above. All samples were Western blotted, probing with the α-dimedone antibody.

Trapping Ero1α in its active, reduced form with dimedone during the Ero1α-Trx assay was carried out as in Chapter 2.6.1 but included 50 mM dimedone in the reaction mixture. The solution was titrated to pH 7.5 using sodium hydroxide.

2.7 *In vivo* assays.

2.7.1 Semi-permeabilised cell preparation.

HT1080 cells were grown to confluence in a T75 flask. Cells were washed with 10 ml PBS then trypsinized in 2 ml Trypsin solution (0.05% Trypsin – EDTA; Gibco) for 3 min at 37 °C. Detached cells were resuspended in 8 ml KHM buffer (20 mM HEPES buffer, pH 7.2 containing 110 mM KOAc and 2 mM MgOAc). Soybean trypsin inhibitor was added to a concentration of 100 μg/ml and the cell suspension moved to a 15 ml Falcon tube. Cells were pelleted at 250 x g for 5 min and resuspended in 6 ml ice cold KHM buffer. Digitonin was added to a final concentration of 40 μg/ml and the cells were incubated on ice for 5 min. A further 6 ml KHM buffer was added and mixed before pelleting cells at 250 x g for 5 min. Cells were resuspended in 14 ml HEPES buffer (90 mM HEPES buffer, pH 7.2 containing 50 mM KOAc) and incubated on ice for 10 min before pelleting at 250 x g for 5 min. Cells were resuspended in 1 ml KHM buffer and a 10 μl aliquot was taken in order to count cells and confirm their permeability using Trypan blue (0.4% in dH_2O). Cells were transferred to a 1.5 ml Eppendorf, pelleted and resuspended in 100 μl KHM buffer.

2.7.2 DTT-recovery.

HT1080 cells were grown in 6cm dishes in Dulbecco's Modified Eagle Medium (DMEM, Invitrogen) containing 10% FCS, 0.1 mg streptomycin and 100 units per ml penicillin (Sigma) and 2 mM glutamine. Cells were treated with 2 ml DMEM containing 10 mM DTT for 5 min before washing the cells in 4 ml fresh DMEM for up to 60 min. Cells were incubated in PBS containing 20 mM NEM for 10 min to freeze the redox status of ER proteins. PBS containing NEM was then removed and cells were lysed in 100 μl ice cold lysis buffer (50 mM Tris-HCl buffer, pH 8 containing 1% Triton X-100, 150 mM NaCl and 5 mM EDTA) and detached using a cell scraper. Lysates were incubated on ice for 20 min before spinning at 16,000 x g for 10 min. The supernatant was transferred to a fresh tube and 20 μl of this was added to 5 μl 5x SDS PAGE sample buffer. Samples were analysed by 8% SDS-PAGE. The oxidised control sample was created by treating cells with 2 ml DMEM containing 1 mM DPS for 5 min before washing cells in PBS containing NEM and processing as above.

2.7.3 shRNA knockdown assays.

HT1080 cells were grown to 80% confluence in 15 cm dishes.12 μg of DNA constructs encoding shRNA against either PDI or ERp46 (or 10μg of each for the PDI-ERp46 double transfection) was mixed with 0.5 ml serum-free DMEM for 10 min at room temperature. 360 μM polyethylenimine (PEI) was added and mixed by gently pipetting and left at room temperature for 20 min. 0.5 ml of this mixture was added drop by drop to 20 ml of

complete DMEM in each 15 cm dish. After gentle mixing, cells were returned to the 37 °C incubator for 6 hr. Media was aspirated and replaced with 20 ml complete DMEM. Selection media (1 μg/ml puromycin in complete DMEM) was added 16 hr post-transfection and replenished 48 hr post transfection. Cells were used to complete DTT-recovery assay, above, after 5 days.

2.7.4 Determining the redox state of PDI and ERp57.

Cells, SP cells or microsomes were treated with 10 mM DTT, 1 mM DPS or left untreated for 10 min on ice in KHM buffer. The redox states of the enzymes were frozen by adding 20 mM NEM. Cells were centrifuged at 300 x g for 5 min before lysing in 10% TCA. Precipitated proteins were pelleted by centrifugation at 16,000 x g for 10 min and washed three times in ice-cold acetone. Samples were resuspended in SDS sample buffer. 10 mM TCEP was added and incubated at room temperature for 10 min before incubating with 20 mM AMS. Samples were then analysed via 8% SDS-PAGE and Western blotted.

2.7.5 Quantifying the glutathione content in cells and SP cells.

Cells or SP cells were lysed in 400 μl 1% 5-sulfosalicyclic acid on ice for 1 hr. Precipitated proteins were removed by centrifugation at 16,000 x g for 10 min. 10 μl of supernatant was added to 150 mM sodium phosphate buffer, pH 7.5 containing 0.2 mM NADPH, 0.6 mM Ellman's reagent and 1 unit of glutathione reductase in a total volume of 500 μl. The rate of change of absorption at 405 nm was monitored at 30 ºC and compared to that of glutathione standards to quantify glutathione content in cell or SP samples.

Ero1α knockdown cells were created previously: HT1080 cells expressing roGFP-iL-KDEL were transfected with and Ero1α shRNA construct. These cells were grown under selection and single colonies were tested for expression of Ero1α by Western blot (van Lith et al., 2011).

Chapter 3.0
Characterisation of Ero1α and its chemically-mediated re-oxidation

3.1 Introduction.

3.1.1 Hydrogen peroxide production.

Hydrogen peroxide is a reactive oxygen species (ROS) which is produced by a number of enzymes throughout the cell: (i) in the ER as a result of oxidative protein folding; (ii) in the mitochondria from electron transport chain enzymes; (iii) in the peroxisome to fight foreign bodies;(iv) throughout the cytosol and plasma membrane as a byproduct of enzymatic activity. These enzymes are generally involved in electron transfer and are bound to electron transfer-facilitating cofactors such as FAD or transition metals. Within the ER, Ero1α is known to produce one molecule of hydrogen peroxide per disulphide bond created (Gross et al., 2006). QSOX, an enzyme which traverses the ER prior to secretion is also known to generate hydrogen peroxide (Hoober et al., 1996). These two enzymes are linked to an FAD cofactor which, upon reduction, leads to hydrogen peroxide production. Within mitochondria, a number of proteins can generate hydrogen peroxide as a byproduct of activity. Respiratory complexes I and III are major producers of ROS as a result of their role in oxidative phosphorylation (Ksenzenko et al., 1983, Kussmaul and Hirst, 2006, Sun and Trumpower, 2003). Amine oxidases, involved in amino acid metabolism, also produce hydrogen peroxide as a byproduct (Cona et al., 2003), while superoxide dismutase (SOD) is another source.

While many enzymes produce hydrogen peroxide and its precursors as byproducts of activity, there are a number of sources where peroxide is generated for a specific function. In peroxisomes there are a number of hydrogen peroxide producers including D-amino acid oxidase, Acyl CoA oxidase, and Xanthine oxidase. These enzymes produce hydrogen peroxide in order to combat foreign bodies; powerful oxidants damage the foreign bodies and eliminate potential threats. The hydrogen peroxide produced by the amine oxidases are proposed to contribute to defence and cell wall synthesis in plants (Cona et al., 2003). The NADPH oxidase (NOX) family of enzymes are thought to contribute significant quantities of hydrogen peroxide to the phagocyte-mediated killing of bacteria (Geiszt et al., 2003, Moore and MacKenzie, 2009).

There are a variety of hydrogen peroxide sources within the cell, therefore, which provide potential sources of ROS which may result in the unwanted or debilitating oxidation of a host of molecules.

3.1.2 PrxIV reduces hydrogen peroxide; increasing the oxidative power of the ER.

A number of peroxidase enzymes located within the ER possess the ability to eliminate excessive concentrations of hydrogen peroxide. PrxIV is able to protect cells from DTT or tunicamycin-induced ER stress (Tavender and Bulleid, 2010). Upon DTT treatment, Ero1α generates an increased concentration of hydrogen peroxide as the oxidative balance within the ER is restored. PrxIV is sensitive to increased hydrogen peroxide levels, implicating this enzyme in the elimination of Ero1α-generated hydrogen peroxide.

Several members of the PDI family, such as ERp46, PDI and P5, are able to reduce the peroxidatic disulphide within PrxIV. Reduction of the peroxidatic disulphide is enhanced when PDI family members are reduced by glutathione, indicating that the recycling of the PDIs leads to increased recycling of PrxIV. In cells, overexpression or shRNA knockdown of P5, ERp46 and PDI leads to increased or decreased PrxIV recycling, respectively (Tavender et al., 2010). A PrxIV-PDI mixed disulphide has been isolated, confirming disulphide transfer between the two molecules (Zito et al., 2010). PrxIV is thought to provide an alternative source of disulphides in Ero1α deficient cells, as it can drive oxidative folding of RNase and supports collagen folding (Zito et al., 2010). PrxIV, therefore, has a cytoprotective role and its absence increases cellular sensitivity to oxidative stress. PrxIV also complements the disulphide generating ability of Ero1α and provides a novel mechanism of driving oxidative protein folding coupled to the elimination of hydrogen peroxide. The ER therefore generates two disulphides per molecule of hydrogen peroxide formed.

3.1.3 The autonomous oxidation of Ero1p.

Ero1p is capable of autonomous oxidation – where one molecule of Ero1p can oxidise another. Three Ero1p mutants, a C-terminal and N-terminal truncated form named Ero1pc, a shuttle-disulphide deficient mutant termed C100A-C105A, and a mutant unable to form the active site disulphide termed C355A-Ero1pc, were created and used in a number of assays to investigate their re-oxidation (Kim et al., 2012). The C100A-C105A Ero1p mutant is re-oxidised at a slower rate than the fully active Ero1pc. C355A-Ero1pc remained in the reduced form indicating that this mutant is incapable of autonomous oxidation. The ability of a maltose binding protein-Ero1pc fusion (MBP-Ero1pc) to oxidise C355A-Ero1pc was measured and shown to be able to oxidise both itself and the inactive mutant – indicative of intramolecular disulphide exchange between the two molecules. Further investigation using a MBP-ero1-C100A-C105A mutant, catalytically active but lacking a shuttle disulphide, proved that this mutant is incapable of disulphide transfer and prevented oxidation of both proteins when incubated with C355A-Ero1pc. Ero1p re-

oxidation and inactivation can, therefore, occur by autonomous oxidation and is mediated by the shuttle disulphide (Kim et al., 2012).

3.1.4 The Ero1α shuttle disulphide.

The shuttle disulphide (C100-105 in Ero1p) plays a crucial role in the autonomous oxidation and inactivation of Ero1p (Kim et al., 2012). The shuttle disulphide within Ero1α (C94-99) may carry out a similar function. The Ero1α shuttle cysteine-containing loop is predicted to be extremely flexible and was unable to be mapped during crystallographic studies due to poor electron density (Inaba et al., 2010). Furthermore, the Ero1α loop regions are longer and more flexible than their Ero1p equivalents. This may therefore provide Ero1α with a means of distributing disulphide bonds inter- or intra-molecularly. The flexible loop, between residues Asp90 and Cys131, may facilitate disulphide transfer between the shuttle disulphide and the two adjacent regulatory disulphides, thus inactivating Ero1α.

3.2 Ero1α expression, purification and characterisation.

In order to investigate the oxidation and inactivation of Ero1α, an *in vitro* approach was adopted as this facilitated control of several important variables that would have been difficult to control *in vivo*. With three possible mechanisms of Ero1α oxidation and inactivation (discussed in Chapter 1.4), it was important to assess the ability of each individually. Work was undertaken to express and purify recombinant Ero1α lacking the 23 N-terminal residues thought to constitute the ER signal sequence which is cleaved *in vivo*.

3.2.1 Ero1α expression and purification.

Expression of GST and His-tagged Ero1α was carried out in Origami B (DE3) pLysS cells. Samples were taken before and after induction of Ero1α expression and analysed by SDS-PAGE (Figure 3.1A). A band corresponding to a protein of approximately 80 kDa was less intense in the pre-induction sample (lane 2) than in the post-induction sample (lane 3). After lysis, glutathione-sepharose beads were used to purify the GST-His-Ero1α fusion protein. Unbound material from the supernatant was sampled and shows the disappearance of the 80 kDa band (lane 4). The beads were washed with buffer which also shows that the 80 kDa band was absent (lane 5). A sample of bound material showed the reappearance of the 80 kDa band (lane 6). The GST moiety was cleaved with thrombin to leave GST bound to the beads, releasing His-tagged Ero1α into the supernatant. His-tagged Ero1α ran with a mobility corresponding to a molecular weight of approximately 50 kDa (lane 7). Elution of remaining bound material showed an intense band running at approximately 25 kDa with

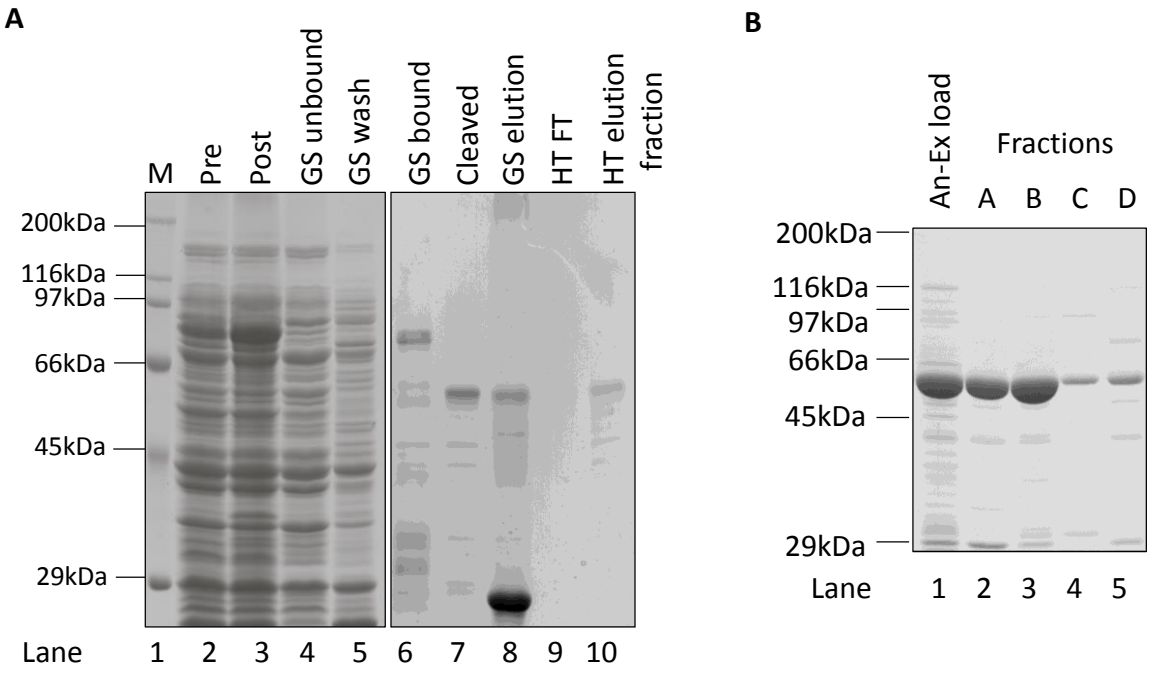

Figure 3.1 – Recombinant Ero1α expression and three-step purification. A - Ero1α was expressed in *E. coli* DE3 pLysS Origami cells with samples taken before (lane 2) and after (lane 3) induction with IPTG. Lysate was incubated with glutathione sepharose (GS) beads, unbound material was sampled and run in lane 4. Beads were washed with buffer (lane 5). Material bound to the beads (lane 6) was cleaved with thrombin and the supernatant collected (lane 7). Elution of material with reduced glutathione shows some Ero1α remained bound (lane 8). This material was loaded onto a HisTrap (HT) column; flowthrough (lane 9) and a protein-containing fraction (lane 10) shows an intense band around 50 kDa and some smaller, less intense bands. B – After concentration of the pooled HisTrap fractions containing Ero1α (lane 1), anion exchange was used to remove contaminants and degradation products. Lanes 2 – 5 represent the eluted Ero1α. Samples were run under reducing conditions and Coomassie stained.

a small amount of material running at approximately 50 kDa (lane 8). Further purification by nickel-affinity chromatography was carried out. Diluted unbound flowthrough from the column (lane 9) contained no Ero1α while the eluted and pooled material contained the 55 kDa band (lane 10).

The nickel affinity eluate was concentrated before applying to an anion exchange column to clean up the product (Figure 3.1B). The concentrated sample was analysed by SDS-PAGE (lane 1) as were the eluted fractions (lanes 2-5) which revealed a cleaner product (lanes 3 and 4) which were pooled, aliquoted and kept at -80 °C until required.

3.2.2 Further characterisation of purified Ero1α.

Equipped with recombinant Ero1α, the next step was to determine its concentration. This was carried out as described previously (Baker et al., 2008). Spectrophotometric analysis revealed that Ero1α displays the characteristic spectra of an FAD-bound protein as absorption peaks at 454 nm and 280 nm (Figure 3.2A). This analysis reveals the concentration of Ero1α was 9.1 μM, while the concentration of FAD present was 7 μM. The ratio of FAD: Ero1α was 7: 9, therefore approximately 78% of Ero1α was natively folded and bound by FAD.

To determine whether Ero1α had been successfully folded and adopted its oxidised redox state after expression and purification, a simple SDS-PAGE based assay was used as described previously (Baker et al., 2008). There was a large mobility shift between reduced and non-reduced samples; non-reduced Ero1α ran with a molecular weight of approximately 50 kDa compared to the reduced form which ran at approximately 60 kDa (Figure 3.2B).

The oligomeric state of Ero1α was analysed by size-exlusion gel filtration chromatography (Figure 3.2C), as reported previously (Baker et al., 2008, Dias-Gunasekara et al., 2005). Several absorption peaks were observed at 280 nm, while two absorption peaks were observed at 454 nm, corresponding to elution volumes of approximately 10.6 ml and 14.45 ml. These peaks correspond to molecular weights of approximately 41 kDa and 87 kDa, comparing the volume of elution to a calibration curve (Appendix 1).

3.2.3 Measuring Ero1α activity with an oxygen electrode.

Having shown that the purified Ero1α had bound FAD, was largely monomeric and had intramolecular disulphide bonds, enzymatic activity was characterised. To confirm that Ero1α was active towards select substrates, an oxygen electrode based assay was used as previously desctibed for Ero1p (Gross et al., 2006). This assay works on the principle that

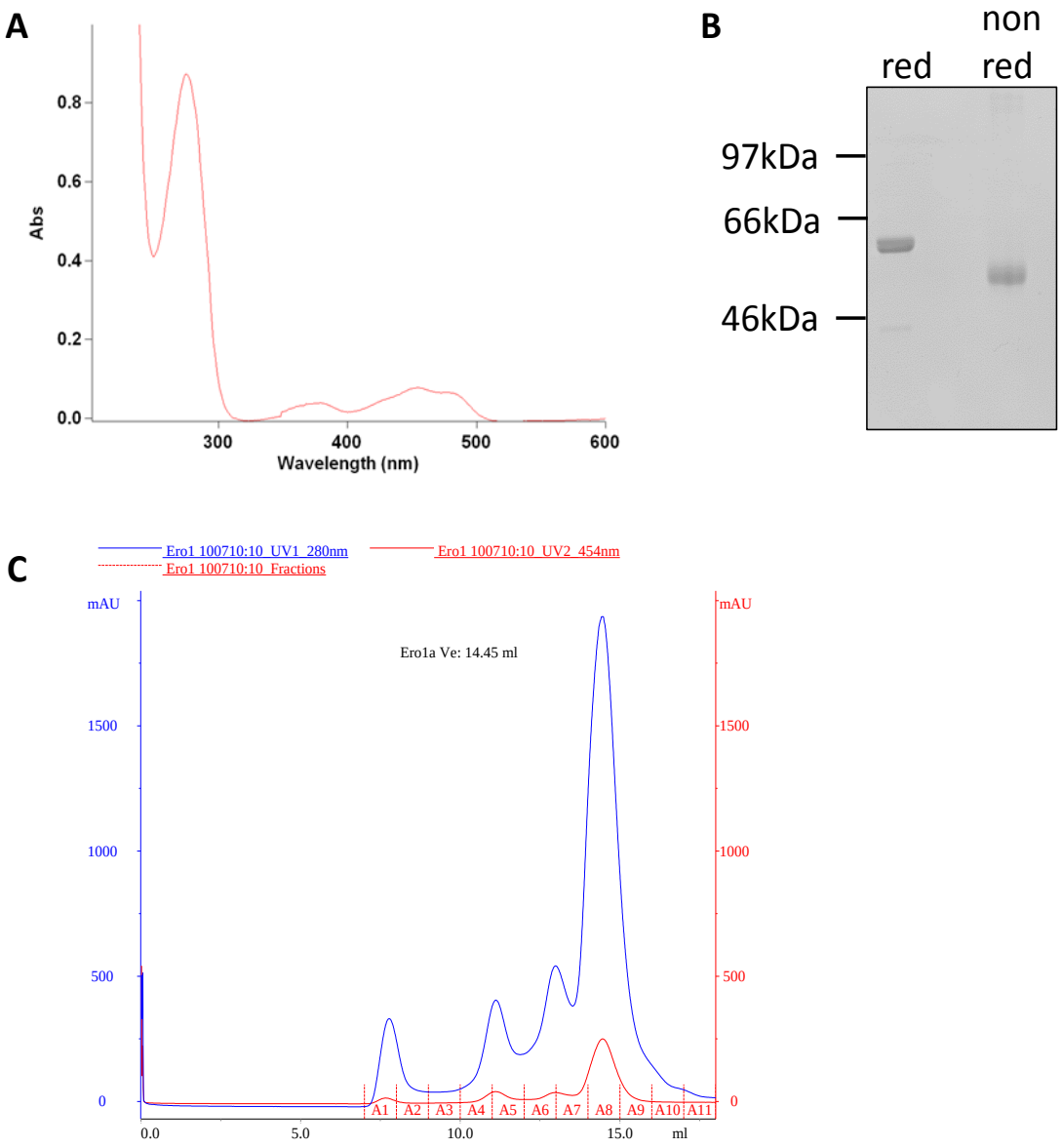

Figure 3.2 – Further characterisation of Ero1α. A – The absorbance of purified recombinant Ero1α was measured between 260 and 600 nm. B – Ero1α was analysed by SDS-PAGE in the presence or absence of DTT. The gel was Coomassie stained to visualise. C – Ero1α was analysed by size exclusion gel filtration chromatography. The absorbance of eluted material was measured at 280 nm as a measure of protein content (blue trace), while the absorbance at 454 nm was monitored as a measure of FAD content.

oxygen acts as the terminal electron acceptor in the Ero1α activity cycle; electrons are passed from Ero1α to FAD and on to molecular oxygen with the resulting disulphide formation within the enzyme and the production of hydrogen peroxide. Therefore, enzymatic activity is coupled to oxygen depletion. DTT was used as a substrate as it is a strong reducing agent and is readily oxidised. It was oxidised by Ero1α as detected by a decrease in oxygen concentration (Figure 3.3A), however in the absence of Ero1α limited oxygen was consumed. Likewise, Ero1α incubated in the absence of DTT produced a limited depletion of oxygen without a reductant present. This confirmed that the purified Ero1α was redox active towards DTT. Further investigation revealed that oxygen consumption increased with increasing concentrations of DTT (Figure 3.3A). The reaction was limited by the availability of oxygen at DTT concentrations of 10 mM and 20 mM.

Ero1α activity towards its physiological substrate PDI was tested using the oxygen electrode assay (Figure 3.3B). When Ero1α (1 μM) was incubated alone it consumed approximately 15 μM oxygen over 900 s. When Ero1α (1 μM) was incubated with reduced PDI (10 μM), consumption of 20 μM oxygen was observed. Including 350 μM GSH with Ero1 and PDI resulted in the consumption of 20 μM oxygen. This was somewhat unexpected because 350 μM GSH is theoretically sufficient to reduce 175 μM of disulphides within PDI and thus consume 175 μM oxygen (if two molecules of GSH are required to reduce a disulphide, per molecule of oxygen). Including 1 mM GSH resulted in a larger concentration of oxygen consumption; 50 μM oxygen was consumed under these conditions. Including 2 mM GSH in the chamber resulted in the consumption of approximately 90 μM oxygen. The inclusion of 10 mM GSH allowed complete consumption of the oxygen, approximately 220 μM, within 200 s. Interestingly, Ero1α displayed the characteristic lag- phase under these conditions, as seen by the slow initial consumption of oxygen in the presence of DTT (10 mM and 20 mM), and with GSH (1 mM, 2 mM and 10 mM). Ero1α was active towards DTT and PDI thus was used to further investigate its activity using thioredoxin.

3.2.4 Ero1α oxidises recombinant thioredoxin.

Ero1α is able to oxidise thioredoxin (Trx) in *vitro* and displays characteristic redox patterns during a time course assay; an initially oxidised Ero1α is quickly reduced by thioredoxin before its subsequent re-oxidation at later time points (Baker et al., 2008). The equivalent assay was performed on Ero1p, obtaining similar results (Heldman et al., 2010, Sevier et al., 2007). To confirm that purified Ero1α could oxidise thioredoxin, displayed the lag-phase and displayed the intermediate redox forms, an SDS-PAGE based assay was performed.

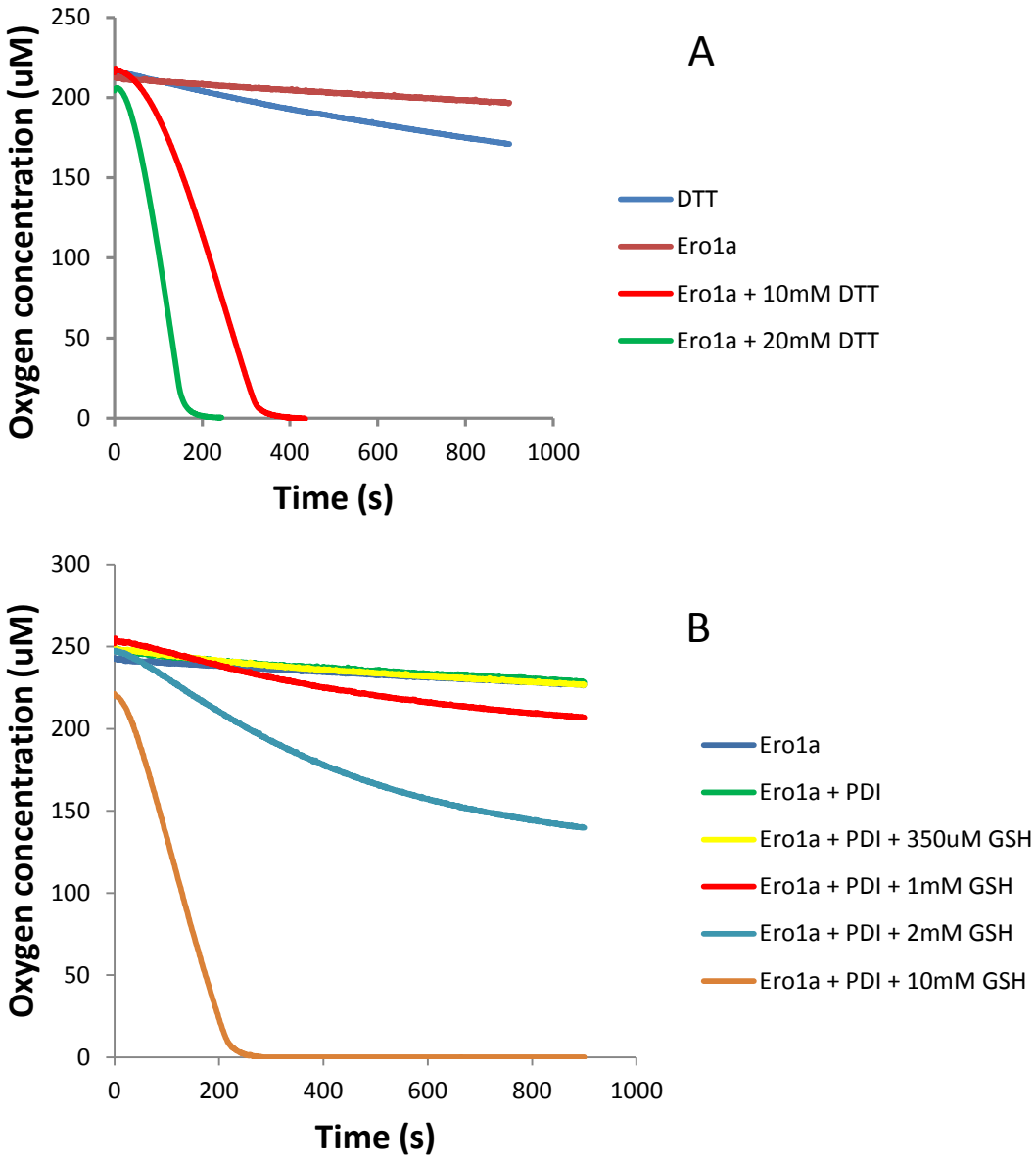

Figure 3.3 – Measuring oxygen consumption to characterise Ero1α activity. A – Using DTT as a substrate. 1 µM Ero1α alone (red line) and 20 mM DTT alone (blue line) were incubated in the oxygen electrode chamber as controls to show that oxygen consumption by these two molecules in isolation is minimal. Upon the addition of 10 mM (green line) or 20 mM (purple line) DTT to 1 µM Ero1α, oxygen is consumed as Ero1α oxidises DTT. B – Ero1α activity towards PDI was measured in the presence and absence of GSH. Assays with Ero1α only (dark blue), Ero1α with 10 µM PDI (green), and Ero1α with PDI and 350 µM GSH (yellow) show minimal oxygen consumption. Including 1 mM (red), 2 mM (light blue) and 10 mM GSH (brown) increases oxygen consumption. Assays were carried out in 50 mM Tris buffer, pH 7.5 containing EDTA and were monitored for 900 s or until the oxygen was completely consumed.

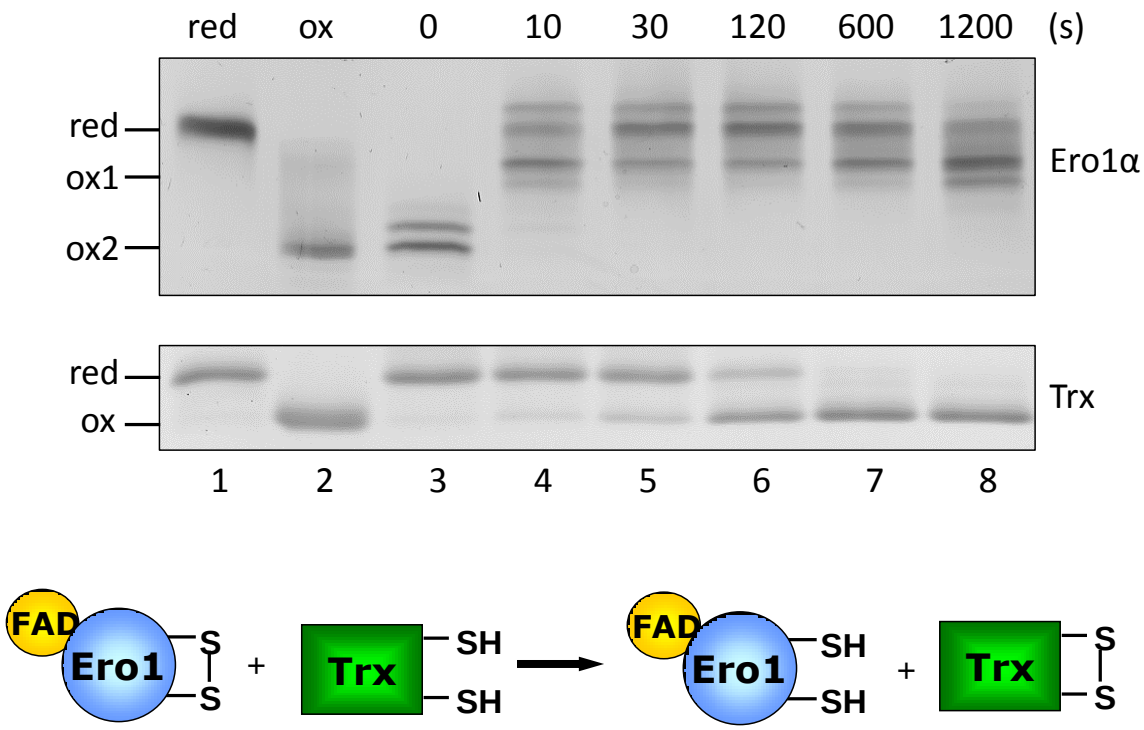

Figure 3.4 – Ero1α oxidises thioredoxin and displays the characteristic redox pattern. 2 µM Ero1α was incubated with 100 µM Trx and the redox states of both enzymes were frozen using AMS (except the oxidised control) at the given time points. Samples were analysed via SDS-PAGE and stained to visualise the proteins. Reduced and oxidised controls are included for comparison. The assay is depicted schematically; an initially oxidised Ero1α is incubated in the presence of reduced Trx and, upon its reduction, oxidises Trx.

Purified Ero1α (2 μM) was incubated with purified and reduced Trx (100 μM), with samples taken at various time points (0, 10, 30, 60, 120, 600 and 1200 s) and alkylated with 4-acetamido-4'-maleimidylstilbene-2,2'-disulfonic acid (AMS) (Fig 3.4). AMS acts to freeze the redox state of free thiol groups and adds a mass of 510 Da per thiol modified, resulting in a decreased mobility of the modified protein during electrophoresis. Reduced proteins therefore run with slower mobility during SDS-PAGE compared to oxidised proteins due to their increased mass as well as the increase in hydrodynamic radius due to disulphide reduction.

DTT-reduced and alkylated Ero1α (lane 1, upper panel) ran much more slowly through the gel than non-reduced and non-alkylated Ero1α (lane 2). Ero1α existed initially in the fully oxidised conformation which migrated quickly through the gel (lane 3) and likely corresponded to the OX2 conformation. Ero1α mobility rapidly decreased within 10 s, indicating the reduction of one or more disulphides and likely corresponded to the OX1 form. By 30-120 s the fully reduced form was clearly seen, indicated by the further decrease in mobility. Ero1α then slowly shifted back towards, although did not form, the OX2 species, indicating incomplete re-oxidation of Ero1α at the later time points.

The Trx redox state showed that it was initially fully reduced with very little oxidation witnessed before 30 s, but was fully oxidised between120-600 s; coinciding with the appearance of the fully reduced form of Ero1α.

3.3 Using sulphenic acid-reactive molecular probes.

Dimedone has been used previously in a number of studies and reacts specifically with cysteine sulphenic acid form. Dimedone was therefore used to determine whether a sulphenic acid intermediate is formed within Ero1α, which would indicate that re-oxidation and inactivation of Ero1α is mediated by sulphenylation. Dimedone reactivity and specificity towards sulphenic acid was initially characterised using peroxiredoxin IV as a model system, as sulphenic acid is known to drive PrxIV oxidation.

3.3.1 Peroxiredoxin IV is sulphenylated and reacts with dimedone.

To confirm that dimedone was selectively reactive with sulphenic acid, PrxIV (previously purified by Dr. Timothy Tavender, University of Glasgow) was treated with dimedone (5 mM) in the presence or absence of hydrogen peroxide (60 μM). Samples were analysed via SDS-PAGE and Western blot using an α-dimedone antibody (Prof. K. Carroll, Scripps Research Institute, Florida). The results confirmed that PrxIV is sulphenylated and reacted with dimedone both in the presence and absence of hydrogen peroxide (Figure 3.5A). In the absence of hydrogen peroxide, sulphenylation may occur due to the high affinity of

the peroxidatic cysteine for hydrogen peroxide which may be present in buffers in trace amounts. To prevent dimedone reactivity with the peroxidatic cysteine, and any solvent accessible cysteines within PrxIV, a PrxIV triple mutant (TM) was used. This mutant (a gift from Dr. Timothy Tavender) has all three solvent accessible cysteines mutated to alanines and has only one remaining cysteine buried within the hydrophobic core of the molecule. Dimedone reactivity with the PrxIV TM was undetectable, both in the presence and absence of hydrogen peroxide. In treating PrxIV TM with SDS, the sole cysteine is exposed as the molecule is denatured and is therefore solvent accessible. In the presence of hydrogen peroxide this cysteine reacts with dimedone, however in its absence no signal is visible. Taken together, this data suggested that the dimedone reaction is cysteine specific and is related to oxidation of the thiol sidechains by hydrogen peroxide.

To show that dimedone reacts specifically with sulphenic acid rather than sulphinic or sulphonic acid groups, another PrxIV mutant was used. The PrxIV C245A mutant is a cysteine to alanine mutant at position 245 and so does not have a resolving cysteine. Any sulphenic acid formed by reaction of hydrogen peroxide with the peroxidatic cysteine will not be resolved thus the sulphenic acid will either react with dimedone or be further oxidised. C245A PrxIV was treated with dimedone (5 mM) and with increasing concentrations of hydrogen peroxide (0 to 50 µM). Samples were then analysed by SDS-PAGE and Western blot, probing with the α-dimedone antibody. The results showed that in the absence of hydrogen peroxide, dimedone had not reacted (upper left panel). In the presence of hydrogen peroxide (5 µM) the C245A PrxIV mutant was modified with dimedone indicating the formation of sulphenic acid under these conditions. Increasing the concentration of hydrogen peroxide to 50 µM resulted in decreased dimedone modification. Using an antibody that recognises the hyperoxidised form of peroxiredoxin (α-Prx $SO_{2/3}$) it was possible to see that decreased dimedone reactivity in the presence of 50 µM hydrogen peroxide was due to the increased formation of hyperoxidised cysteine residues. Thus dimedone seemed to be reacting specifically with cysteine sulphenic acid. The absence of any band in the samples without dimedone also confirmed that this signal was specific to dimedone reactivity (upper right panel).

3.3.2 Ero1α – dimedone reactivity.

Having shown that dimedone reacts specifically with cysteine sulphenic acid, it was used to investigate the potential formation of sulphenic acid within Ero1α. Ero1α was treated with hydrogen peroxide (0-60 µM) and dimedone (5 mM) in an attempt to trap sulphenic acid (Figure 3.6A). Samples were analysed by SDS-PAGE and Western blotted using the α-dimedone antibody. In the absence of hydrogen peroxide, Ero1α reacted with

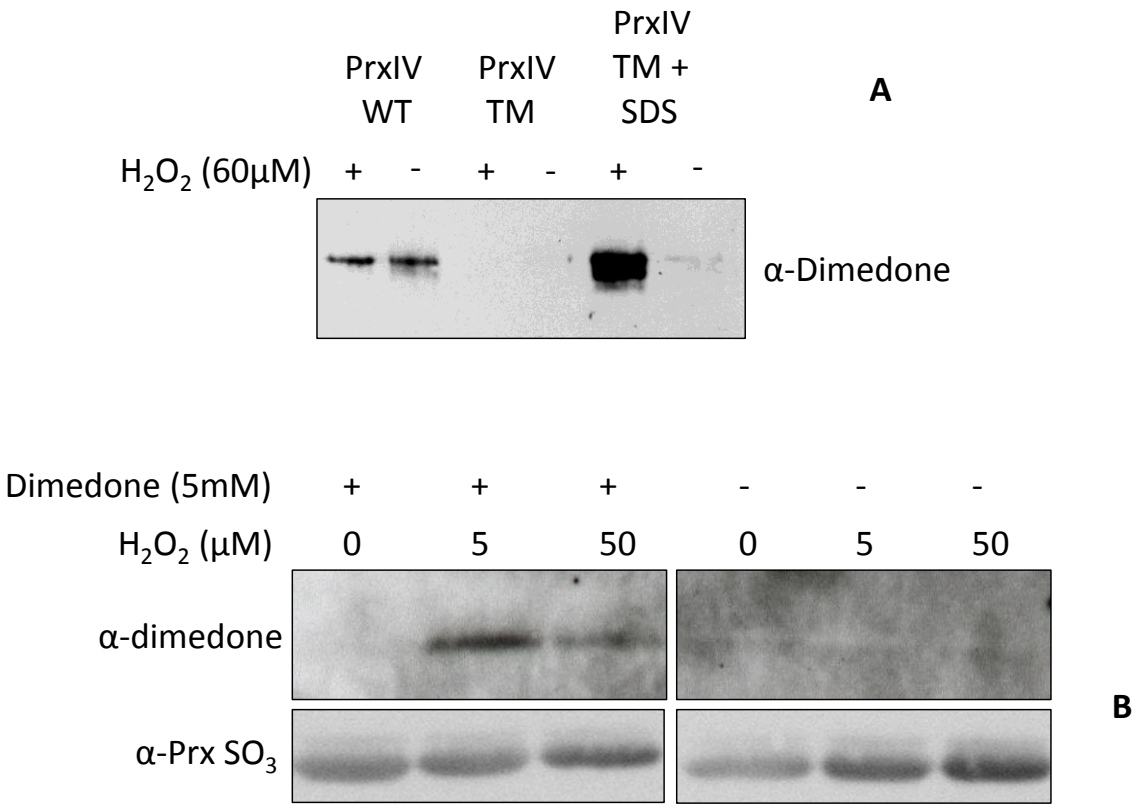

Figure 3.5 – Dimedone reacts specifically with cysteine sulphenic acid. A – Purified PrxIV was treated with 5 mM dimedone in the presence and absence of hydrogen peroxide (60 µM). The same treatment was carried out on the PrxIV TM and the PrxIV TM in the presence of SDS. Samples were analysed by SDS-PAGE and Western blot, probing with the α-dimedone antibody. B – C245A PrxIV was treated with or without dimedone in the presence of increasing concentrations of hydrogen peroxide. The reaction was quenched by acidification in 10% TCA and samples were analysed via SDS-PAGE and Western blot, probing with α-dimedone or α-Prx SO_3.

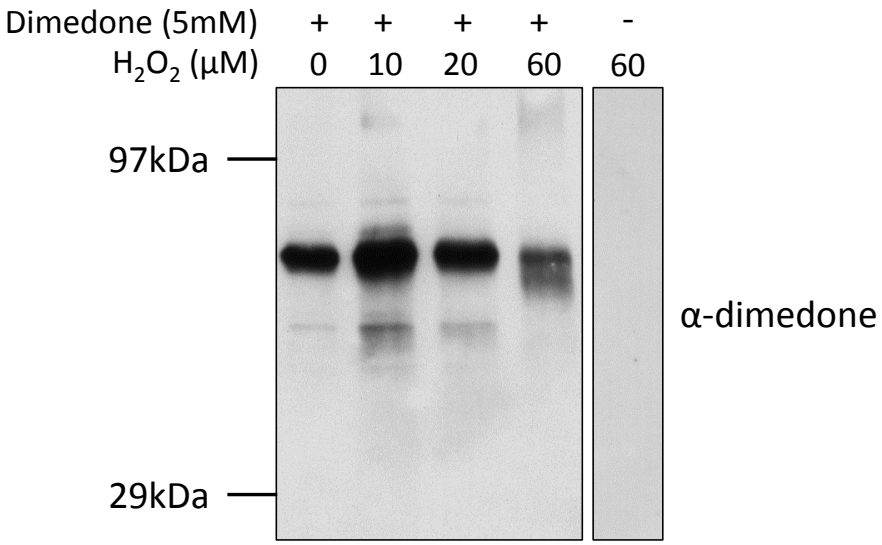

Figure 3.6 – Ero1α reacts with dimedone. Ero1α was incubated with 5 mM dimedone in the presence of increasing concentrations of hydrogen peroxide for 10 min. The reaction was quenched by acidification in 10% TCA and samples were analysed via SDS-PAGE before Western blotting with the α-dimedone antibody.

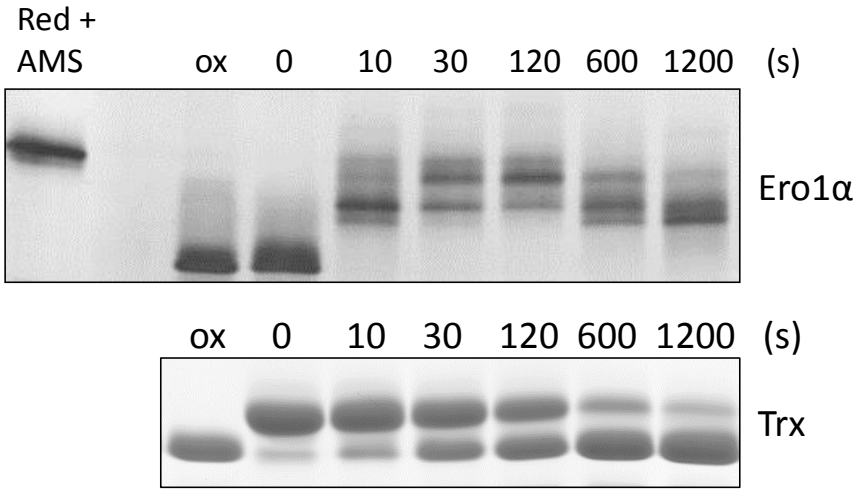

Figure 3.7 – Dimedone does not trap Ero1α in an active state. 2 μM Ero1α was incubated with 100 μM Trx in the presence of 50 mM dimedone and the redox state of both enzymes were monitored over 1200 s. Samples were alkylated with AMS at the stated time points, analysed by SDS-PAGE and stained to visualise. Reduced and non-reduced (ox) samples are included for comparison.

dimedone as it was recognised by the α-dimedone antibody. Concentrations of 10 and 20 μM hydrogen peroxide caused similar levels of sulphenylation in Ero1α, however at 60 μM hydrogen peroxide the level of Ero1α recognised decreased. In the absence of dimedone there was no visible signal, again confirming that the signal was dimedone specific and that Ero1α was sulphenylated.

3.3.3 Ero1α is not trapped in an active form by dimedone.

To investigate the possibility of Ero1α re-oxidation and inactivation being induced by sulphenylation, the above Ero1α-Trx assay (Chapter 3.2.4) was repeated in the presence of dimedone (Figure 3.7). Sulphenic acid should rapidly react with dimedone and pin Ero1α in the reduced state rather than induce disulphide formation. This reduced state could then be visualised on a gel due to its decreased mobility. 50 mM dimedone was used in this assay rather than the 5 mM above to ensure that sulphenic acid formation would be quickly trapped to prevent disulphide formation. Ero1α was not trapped in this state as re-oxidation was seen as an increase in mobility at the later time points (600-1200 s). Thioredoxin was oxidised completely by Ero1α, confirming that enzymatic activity had not been disturbed in the presence of dimedone. Furthermore, Ero1α showed the typical redox pattern witnessed previously (Figure 3.4) and in previous studies and, therefore, was not trapped in the reduced state by dimedone.

3.4 Hydrogen peroxide induced oxidation of Ero1α.

While dimedone was used to determine if sulphenic acid groups were formed within Ero1α, the ability of hydrogen peroxide to cause the direct oxidation of Ero1α was investigated using an SDS-PAGE based assay. Reduced Ero1α was incubated with hydrogen peroxide (0, 10 or 100 μM) under anaerobic conditions to prevent *de novo* disulphide generation by Ero1α. The sole source of disulphides, therefore, was sulphenylation of cysteine thiols. The redox state of Ero1α was monitored over the course of 300 s and samples were alkylated with N-ethylmaleimide (NEM) to freeze the redox state before SDS-PAGE analysis (Figure 3.8, upper panel).

Under anaerobic conditions Ero1α existed in the Ox1 forrm for the duration of the assay. The inclusion of 10 μM hydrogen peroxide in the assay resulted in a band of increased mobility appearing after 10 s, and the disappearance of the reduced band. This showed that 10 μM hydrogen peroxide caused a degree of Ero1α re-oxidation. In the presence of 100 μM hydrogen peroxide, Ero1α was almost completely oxidised within 30 s as indicated by the disappearance of the reduced forms and the formation of the species with increased mobility. Densitometry analysis was performed using the ImageJ software

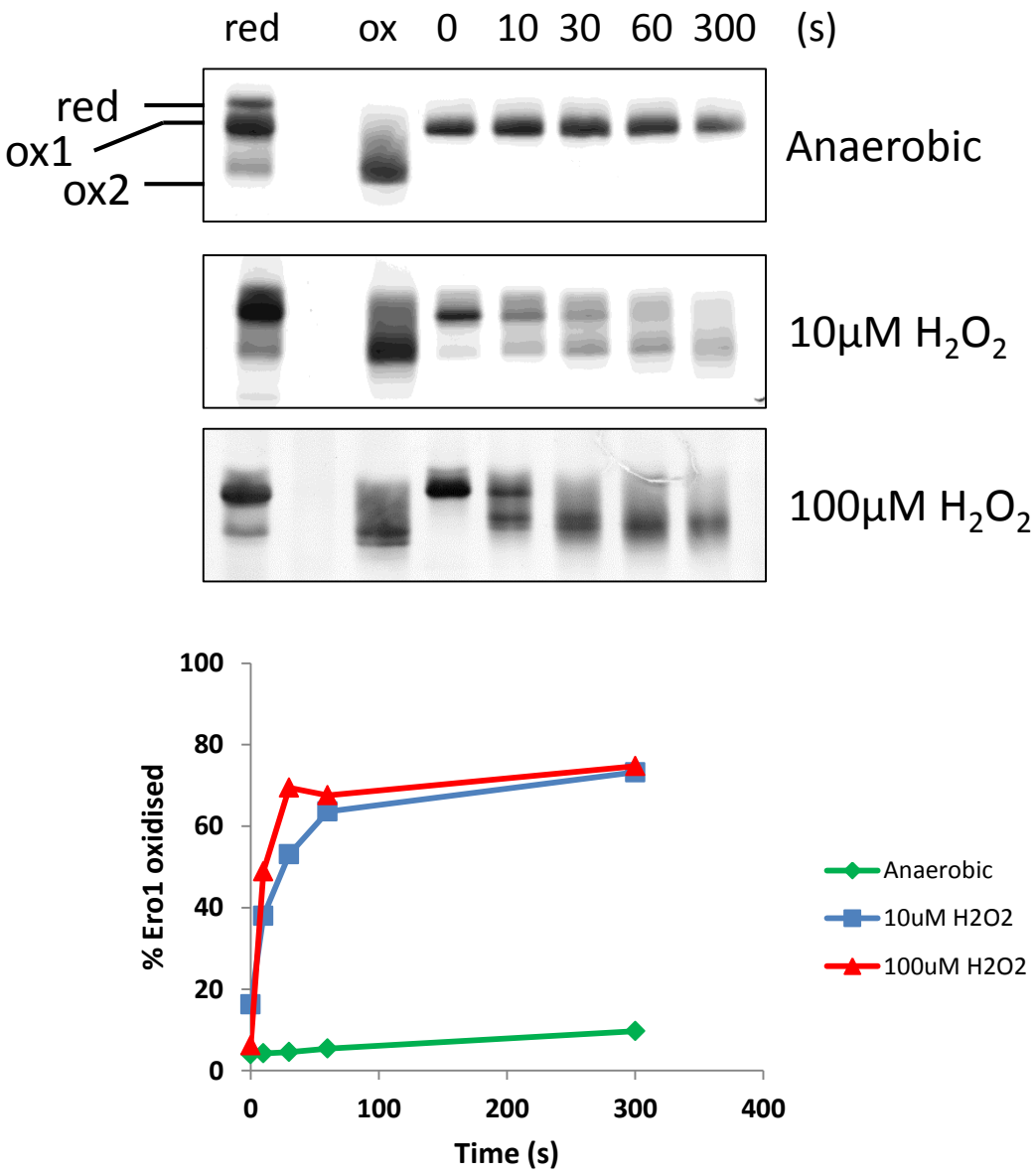

Figure 3.8 – Hydrogen peroxide oxidises Ero1α. Ero1α was reduced with DTT before passing through a Spin Column with a molecular weight cut-off of 6 kDa to remove the reducing agent. The reduced Ero1α was incubated with increasing concentrations of hydrogen peroxide. Samples were taken at the given time points and the redox state was frozen with NEM.The whole assay was performed under anaerobic conditions. Samples were analysed via SDS-PAGE and silver stained to visualise Ero1α. The assay was repeated three times independently and densitometry analysis was performed to quantify the re-oxidation of Ero1α. Representative values of Ero1α oxidation for each treatment are plotted against time.

(Schneider et al., 2012), with the proportion of oxidised Ero1α shown as a percentage of total Ero1α (Figure 3.8, lower panel). Hydrogen peroxide was able to directly oxidise approximately 70% of total Ero1α after 300 s. The assay was repeated a total of three times independently, with representative results shown.

3.5 Ero1α inter- or intra-molecular disulphide exchange.

One hypothesis for the mechanism of re-oxidation and inactivation of Ero1α is the inter- or intra-molecular disulphide exchange mechanism, where disulphides could be generated by and distributed within Ero1α, or between molecules, in order to regulate activity. This would be possible if a lack of reduced PDI was available and would prevent hyperoxidation of the ER. *De novo* disulphide formation at the C394-C397 active site provides a source of disulphides which could be distributed internally to the structural and regulatory disulphides via the shuttle disulphide positioned on the flexible loop region. By inhibiting the generation of disulphides under anaerobic conditions, the controlled addition of electron acceptors could re-start disulphide formation meaning the sole source of disulphides for the regulatory cysteines would be Ero1α itself.

3.5.1 Ero1α cannot utilise exogenous FAD.

Exogenous FAD has been shown to act *in vitro* as a terminal electron acceptor for yeast Ero1p in the absence of oxygen (Gross et al., 2006, Tu and Weissman, 2002). Ero1α has been reported to be unable to do this (Wang et al., 2009). To clarify this issue, Ero1α (2 μM) was incubated with Trx under aerobic or anaerobic conditions, with samples removed at the given time points and alkylated immediately in AMS. Under aerobic conditions (Figure 3.9A) Ero1α was able to fully oxidise Trx. During the assay, Ero1α was reduced quickly by Trx, indicated by the decrease in mobility, before returning to its more oxidised forms at the later time points. Under anaerobic conditions (Figure 3.9B), Ero1α oxidised approximately 54% of the total Trx (quantified using ImageJ) and remained in a reduced state, seen from 10-1200 s. The assay was repeated in the presence of 200 μM free FAD. Under these conditions, Ero1α remained in a reduced state and Trx oxidation was approximately 45% of total Trx (Figure 3.9C). In the absence of Ero1α, Trx was stable in its reduced form (Figure 3.9D). Ero1α was unable to utilise exogenous FAD as a terminal electron acceptor.

3.5.2 Oxygen cannot fully re-oxidise Ero1α.

With tissue oxygen concentrations around 3-6% it is possible that oxygen facilitates internal disulphide exchange within Ero1α itself. This potential mechanism of Ero1α re-oxidation and inactivation was investigated using molecular oxygen as a terminal electron

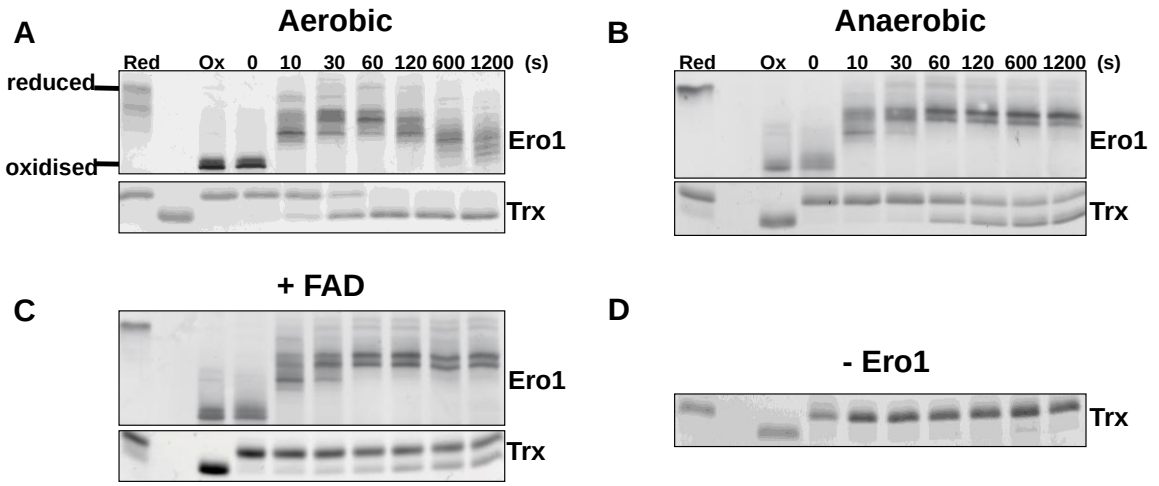

Figure 3.9 – Exogenous FAD cannot act as a terminal electron acceptor for Ero1α. Ero1α was incubated under aerobic (A) or anaerobic (B) conditions with reduced thioredoxin. At each time point, the reaction was stopped by alkylation with AMS before analysis via SDS-PAGE. Ero1α gels were silver stained, thioredoxin gels were Coomassie stained. C – Ero1α was incubated with thioredoxin under anaerobic conditions in the presence of FAD (200μM) before further analysis as above. D – The redox state of thioredoxin was monitored in the absence of Ero1α. E - Schematic diagram showing that the initially oxidised Ero1α is reduced by reduced thiredoxin. The thioredoxin present is completely oxidised by Ero1α.

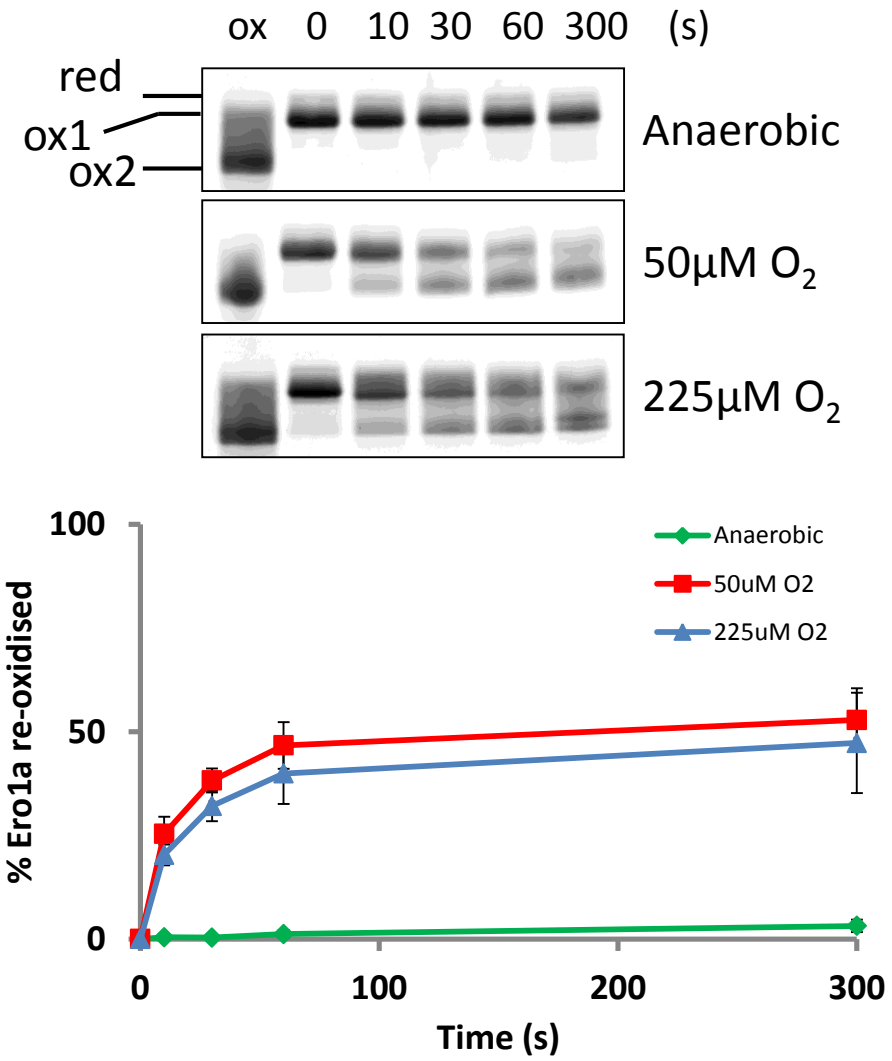

Figure 3.10 – Oxygen drives incomplete intramolecular disulphide exchange within Ero1α. Ero1α was reduced with DTT before passing through a Spin Column with a molecular weight cut-off of 6 kDa to remove the reducing agent. Reduced Ero1α was incubated under anaerobic conditions before titrating increasing concentrations of oxygen into the assay mix. The redox state of Ero1α was frozen by alkylating with NEM, then analysed by SDS-PAGE in the absence of reducing agent. Ero1α was then visualised by silver staining. Densitometry analysis was performed on the results of three separate and independent experiments and mean oxidised Ero1α, as a percentage of total Ero1α per lane, is plotted against time. Error bars represent standard deviation.

acceptor. Reduced Ero1α was incubated with increasing concentrations of oxygen, from 50-225 μM, for 300 s. Samples were taken at the given time points, alkylated with NEM, analysed by SDS-PAGE and silver stained. Ero1α existed in its reduced form under anaerobic conditions, however in the presence of oxygen (50 μM), thought to be approximately equal to the physiological oxygen tissue concentration, approximately 53 ± 7.6% (standard deviation, n=3) of the Ero1α was oxidised after 300 s (Figure 3.10). Incubating Ero1α with 225 μM did not allow complete re-oxidation of Ero1α; indeed Ero1α oxidation after 300 s was approximately 47 ± 12% (standard deviation, n=3) oxidised. It can be concluded that internal disulphide exchange may play a role in the inactivation of Ero1α *in vivo* but is unlikely to be the main or sole mechanism.

3.6 Discussion.

During this study, a recombinant version of Ero1α containing an N-terminal GST and His-tag was successfully expressed, purified and characterised. Previous studies have produced Ero1α with similar characteristics (Baker et al., 2008). Ero1α was successfully expressed in a bacterial expression system. Purification by nickel affinity and ion exchange chromatography yielded a clean product of approximately 55 kDa. An established method of confirming native folding of Ero1α is to measure the ratio of protein: bound FAD cofactor (Baker et al., 2008). This study produced a ratio of approximately 7:9, or 78% of bound FAD, hence natively folded Ero1α, and compares well to the ratio previously described (85%) (Baker et al., 2008). Another test of Ero1α folding is to compare the mobility of the reduced and oxidised forms during SDS-PAGE. In agreement with previous studies, a decrease in mobility was observed upon reduction of Ero1α with DTT, confirming the presence of disulphide bonds (Benham et al., 2000). One further test of folding was carried out using size-exclusion gel filtration chromatography. Ero1α exists mainly as a monomer of approximately 41 kDa with some dimer formation which elutes at approximately 87 kDa (Figure 3.2C, Appendix 1). This compares well with previous results(monomer: 44 kDa, dimer: 100 kDa) (Wang et al., 2009). The remaining absorbance peaks at 280 nm eluting at approximately 7.5 ml and 13.5 ml are most likely aggregates and preparation contaminants, respectively, as they do not absorb at 454 nm.

Having confirmed that Ero1α had bound FAD, contained disulphides and existed at the correct size, it was possible to characterise its activity towards a number of substrates. Ero1α activity has previously been characterised towards DTT thus providing a comparison (Araki and Nagata, 2011, Wang et al., 2009). The Ero1α prepared during this study was comparatively active towards DTT. The results in Figure 3.3A highlight the necessity for Ero1α activity modulation as Ero1α activity can produce significant

concentrations of hydrogen peroxide in a short time. Interestingly, this hydrogen peroxide is unable to prevent further Ero1α activity and so does not provide a reliable regulatory mechanism. This lack of regulation may be as a result of using such a strong reducing agent as a substrate. DTT, therefore, is a good substrate to test activity of Ero1α but may mask any regulatory effects that are the focus of this study.

Using PDI as a substrate for Ero1α, more information can be drawn on the regulation of Ero1α activity (Figure 3.3B). As expected, Ero1α shows limited activity towards PDI in the absence of GSH. This is consistent with previous findings (Baker et al., 2008) and is likely a result of available reduced substrate being consumed without regeneration of reduced PDI. It is interesting that Ero1α shows limited activity towards PDI in the presence of 350 μM GSH. 350 μM GSH is theoretically enough to recycle the oxidised PDI, however the PDI redox state is sensitive to the ratio of reduced: oxidised glutathione (Chambers et al., 2010). This may provide an insight into the lack of recycling, hence Ero1α activity. The consumption of 20 μM oxygen may indicate that Ero1α is oxidising both active sites of 10 μM PDI and consuming 20 μM oxygen as a result, or 10 μM of oxidised PDI may be turned over by GSH. This could potentially result in the oxidation of 40 μM GSH, creating a GSH: GSSG ratio of approximately 16:1 (310 μM: 20 μM). In the presence of 1 mM GSH approximately 50 μM oxygen is consumed; theoretically 100 μM GSH would be required to recycle the substrate resulting in a GSH: GSSG ratio of 18:1 (900 μM: 50 μM). Including 2 mM GSH in the chamber resulted in the consumption of approximately 90 μM oxygen or 180 μM GSH. This would create a GSH: GSSG ratio of approximately 20:1. Finally in the assay containing 10 mM GSH, the oxygen in the chamber was completely consumed within 200 s and so a GSH: GSSG equilibrium could not be established. This observation may reveal a regulatory mechanism – Ero1α activity may be stopped as the balance of glutathione is restored at a ratio of between 16:1 and 20:1, or Ero1α is able to drive oxidation of glutathione until this ratio is reached. Furthermore, 1 mM or 2 mM GSH should provide enough reducing equivalents to completely consume the oxygen in the electrode. The fact that this does not occur indicates that glutathione is acting to shut down Ero1α activity. The glutathione ratio within the ER is thought to be around 10:1 and so perhaps Ero1α is responsible, in part, for this. Further contribution may come from other oxidative pathways such as that of PrxIV or VKOR. It is important to note, however, that equilibrium may not have been reached before completion of the assay at 900 s. This could potentially result in an underestimation of oxygen consumption and thus affect the glutathione ratios.

An alternative source of Ero1α regulation in Figure 3.3B could potentially come from

hydrogen peroxide-mediated sulphenylation. Up to 20 μM hydrogen peroxide would be produced in the Ero1α - PDI and assay and in the assay containing 350 μM GSH; 50 μM in the assay with 1 mM GSH; 90 μM hydrogen peroxide in the assay with 2 mM GSH; and 220 μM hydrogen peroxide in the assay with 10 mM GSH. There is, therefore, the potential for the production of a large concentration of hydrogen peroxide within the chamber which may influence the redox state of PDI or Ero1α, thus influencing activity and oxygen consumption.

One further interesting observation is the apparent delay in reaching the maximum rate of oxygen consumption, or lag-phase, after initiating the reaction. This observation has been described previously as an Ero1 phenomenon; a consequence of regulatory disulphide reduction prior to enzyme activation (Araki and Nagata, 2011, Baker et al., 2008, Gross et al., 2006, Heldman et al., 2010, Wang et al., 2009). This lag-phase is present in assays using both DTT and PDI as substrates thus confirming observations in previous studies.

The results from the thioredoxin assay in Figure 3.4 provide data in agreement with previous studies (Baker et al., 2008, Heldman et al., 2010). The characteristic lag phase is observed. Trx oxidation in this assay is quicker than in previous studies, likely due to the concentrations used (0.5 μM Ero1α was used previously compared to 2 μM in this study) (Baker et al., 2008). It is also interesting to note that Ero1α does not return to its fully re-oxidised OX2 form in Figure 3.4, in contrast to previous studies with Ero1α (Baker et al., 2008) and Ero1p (Heldman et al., 2010). The reasons for this are unknown. The appearance of a double band upon AMS alkylation of non-reduced Ero1α samples may be explained by incomplete alkylation, resulting in a heterogeneous population of Ero1α molecules.

Characterisation of the sulphenic acid probe dimedone was carried out using peroxiredoxin IV as a model system. The assay depicted in Figure 3.5 successfully showed that dimedone reacts specifically with cysteine sulphenic acid. It also highlights the reactivity of PrxIV with hydrogen peroxide, as significant sulphenylation occurred in the absence of added hydrogen peroxide. Dimedone reactivity is confirmed to be sulphenic acid specific as increased hyperoxidation of PrxIV was coupled to decreased dimedone labelling.

The labelling of Ero1α with dimedone paints a somewhat confusing picture. Under the conditions tested, Ero1α was clearly labelled with dimedone (Figure 3.6). At high concentrations of hydrogen peroxide (60 μM), dimedone-labelling of Ero1α decreases. This is presumably due to hyperoxidation of the cysteines and so dimedone can no longer react, as seen in Figure 3.5B. However, dimedone reactivity does not interfere with Ero1α

regulation as Ero1α was not trapped in an active, or reduced, form by dimedone (Figure 3.7). This would suggest that Ero1α is sulphenylated on one or more cysteine residues uninvolved in regulation of activity or formation of Ox1 or Ox2. The fact that activity is not inhibited suggests that catalytic residues (cyteines 94, 99, 394 and 397) are not sulphenylated. It is possible that sulphenylation occurs on one or more of cysteines 35, 37, 46, 48, 166, 208 or 241. There may be a slight delay in the completion of Trx oxidation when compared to activity of Ero1α in the absence of dimedone (Figure 3.4), however it can be concluded that the regulatory disulphides are not modified by dimedone thus unlikely to be sulphenylated as part of the regulatory inactivation mechanism.

In contrast to the data presented in Figure 3.4, Figure 3.8 clearly shows that hydrogen peroxide induces disulphide formation. 100 µM hydrogen peroxide induces oxidation more quickly than 10 µM, however the oxidised band appears smeared. This may indicate the formation of non-native disulphides or the incomplete formation of disulphides due to thiol hyperoxidation. Disulphide formation in Ero1p by 100 µM hydrogen peroxide does not occur, nor does the inclusion of catalase slow oxidation (Kim et al., 2012). Ero1p does not display peroxidase activity (Gross et al., 2006). There is currently no data which quantifies physiological cellular concentration of hydrogen peroxide, either at steady state or under stress conditions. The concentrations of hydrogen peroxide used in this study, therefore, are thought to be roughly physiological; 100 µM is thought to be excessive (Song et al., 2007).

The fact that 100 µM hydrogen peroxide induces Ero1α re-oxidation in this assay is interesting, as the Ero1α-thioredoxin assay (Figure 3.4) would theoretically produce 100 µM hydrogen peroxide. This, however, does not induce Ero1α re-oxidation, possibly due to the gradual build up of hydrogen peroxide. The fact that Ero1α shifts from Ox1 to Ox2 suggests that the disulphides formed are regulatory in nature as the C94-C131 disulphide is formed during the Ox1-Ox2 transition (Appenzeller-Herzog et al., 2008). In conclusion, sulphenic acid may play a role in Ero1α re-oxidation and inactivation but this mechanism may produce non-natively folded intermediates which would require isomerisation by the PDI family.

It is interesting to note that DTT treatment is not sufficient to completely reduce Ero1α as a mixture of Ox1 and reduced forms can be seen (Figure 3.8 and Figure 3.10). This may be explained by the fact that DTT can be used as a substrate by Ero1α, thus generating disulphides within the Ero1α molecule.

The techniques used in this study to investigate the process of intramolecular disulphide exchange within Ero1α cannot exclude the contribution of autonomous oxidation, which has been described in Ero1p (Kim et al., 2012).

The ability of Ero1α to utilise exogenous FAD was tested using an SDS-PAGE based assay performed under anaerobic conditions to prevent *de novo* disulphide formation (Figure 3.9). The fact that thioredoxin oxidation reaches approximately 54% is puzzling; theoretically if 2 μM Ero1α is present then only 14 μM Trx should be oxidised during the assay if there are 7 disulphides reduced in each molecule of Ero1α. A small concentration of oxygen may be present which could drive a limited amount of oxidation. FAD clearly cannot act as a terminal electron acceptor for Ero1α, directly contrasting work carried out on Ero1p (Gross et al., 2006) but complementing results witnessed with Ero1α (Wang et al., 2009).

Addition of molecular oxygen to the anaerobic assay restores the ability of Ero1α to generate disulphides. Oxygen is able to induce Ero1α re-oxidation, although no increase in oxidation is witnessed when comparing physiological and excessive oxygen concentrations (Figure 3.10). Oxidation driven by oxygen is slow and incomplete compared to hydrogen peroxide-driven oxidation, although the oxidised Ero1α bands appear sharper. This data suggests that Ero1α re-oxidation and inactivation by intramolecular disulphide exchange is possible, but is slow and incomplete.

Taken together, the data presented in this chapter show that Ero1α has been successfully expressed and purified using a bacterial expression system. Ero1α is active towards the substrates DTT, thioredoxin and PDI, and displays key characteristics unique to the Ero1 family of enzymes. Ero1α is sulphenylated and reacts with dimedone. After developing a system where Ero1α could be stabilised in the reduced form, it was shown to be oxidised and inactivated by hydrogen peroxide, and slowly and incompletely oxidised by an intramolecular disulphide exchange mechanism. Furthermore, exogenous FAD is determined to be a poor terminal electron acceptor for Ero1α.

Chapter 4.0
Dithiol disulphide exchange between Ero1α and ER oxidoreductases

4.1 Introduction.

4.1.1 The PDI domain structure and active sites.

The redox activity of PDI is mediated by four thioredoxin-like domains, two of which contain the redox active CxxC motif. The remaining two thioredoxin-like domains are redox inactive but are thought to contribute to binding of substrate proteins and interacting partners. The PDI thioredoxin-like domains are arranged in the fashion a-b-b′-a′, where the a and a' domains contain a CGHC motif. The PDI active site disulphides are thought to be relatively unstable within the ER and are found in the reduced form at steady state. Dictating disulphide stability is the chemical properties of the two residues positioned between the active site cysteines. In PDI these residues are glycine and histidine; glycine is the smallest amino acid with only a hydrogen molecule sidechain, histidine has a bulky sidechain with delocalised electrons. These delocalised electrons are thought to disfavour an electron rich disulphide bond from forming, compared to other amino acids such as proline. The measure of the propensity for a disulphide to form is known as the reduction potential, where an increased reduction potential denotes a decreased stability for the disulphide, or a more stable dithiol. A histidine to proline mutation within the PDI CGHC motif lowers the reduction potential of the disulphide, which has been confirmed as PDI CGPC mutants are better substrates for Ero1α during oxidative protein folding (Chambers et al., 2010).

4.1.2 Diversity within the PDI family.

While PDI exclusively contains CGHC active site motifs, many other PDI family members have variations of this sequence, giving rise to a family of oxidoreductases with diverse functions. There are four main properties that differentiate between the PDI family members and their enzymatic activity: (i) the active site CxxC motif sequence, (ii) the pKa of the active site cysteines which is governed by neighbouring residues, (iii) the presence or absence of a glutamate-lysine charged pair for proton transfer reactions, (iv) and the presence of a binding site and its affinity for substrates. The CGHC is a motif found in many oxidoreductases, including PDI, ERdj5, PDIr, ERp57, ERp72, P5 and ERp46. ERdj5 contains three CxPC active sites (Cunnea et al., 2003). Other active site motifs include CSMC in PDIr, CPAC in TMX and CPSC in TMX4. The specific functions and characteristics of these motifs are yet to be confirmed. Further diversity within the active sites includes the replacement of either the first or second cysteine within the active site for

a serine, as in SNDC in TMX2, CRFS in ERp44 and SKQS or SKKC in PDILT. Although these sequences cannot harbour a disulphide, these proteins are known to be redox active due to the remaining cysteine residues. ERp44 lacks the second 'resolving cysteine' and forms more stable, less transient mixed disulphides with other cysteine containing proteins (Anelli et al., 2003, Anelli et al., 2002).

Further diversity within the PDI family stems from the catalytically inactive domains within the PDI family. PDI contains two redox inactive domains, as do ERp57, ERp72 and ERp27 amongst others. PDIr and ERp28 have one redox inactive domain, while ERp18, ERp44, ERdj5 and others lack a homologous binding domain. The significance of the binding domain is currently unknown but may provide a means of ensuring the PDI family can interact with the variety of client proteins entering the ER.

Further structural diversity within the PDI family arises from the presence or absence of a fairly well conserved argninine residue which can move into the proximity of the active site (Lappi et al., 2004).This modulates the pKa of the active site cysteines, stabilising the active site N-terminal cysteine thiolate ion and destabilising the active site C-terminal cysteine thiolate ion. N-terminal cysteines, therefore, have a lower pKa value than C-terminal cysteines, ensuring that nucleophilic attack by the N-terminal cysteine forms mixed disulphides. These mixes disulphides are then resolved by the C-terminal cysteine.

Several factors, therefore, influence the activity and specificity of the PDI family, ensuring that a wide range of substrates can be oxidised or isomerised efficiently. This contributes to oxidative protein folding and ensures the health and fidelity of the cell.

4.1.3 Ero1α – PDI interactions.

The interaction between Ero1α and PDI was first described by Benham et al. in 2000 where PDI co-immunoprecipitated with Ero1α. This study described the Ero1α OX2-dependent nature of the interaction, suggesting the Ero1α-PDI complex occurs specifically during oxidative protein folding and not during the oxidative folding steps of Ero1α maturation (Benham et al., 2000). Ero1α-PDI interactions are dependent on Ero1α Cys94 (Bertoli et al., 2004). Ero1α preferentially oxidises the a′ domain of PDI (Baker et al., 2008), similar to the oxidation witnessed in PDIp by Ero1p (Kulp et al., 2006). In cells, Ero1α oxidation of PDI was confirmed as oxidation of both PDI active sites increases with overexpression of deregulated Ero1α (Appenzeller-Herzog et al., 2008).

The reduction potential of the PDI active site disulphides is crucial to their Ero1α-mediated oxidation. PDI mutants with lowered reduction potentials are oxidised more readily than wild type PDI (Chambers et al., 2010).

The PDI binding pocket is located on the b′ domain and contains a negatively charged surface which binds Ero1α more efficiently than the same domain from the closely related ERp57, suggesting specificity among the PDI family (Inaba et al., 2010). In addition, mutation of a cluster of positively charged residues positioned near the shuttle cysteine-containing loop of Ero1α has an inhibitory effect on disulphide transfer with PDI. High concentrations of sodium chloride enhance binding of Ero1α to PDI and Triton X-100 inhibits binding (Inaba et al., 2010). A PDI mutant containing no cysteine residues was able to bind Ero1α with near wild type kinetics, further evidence to suggest that non-covalent interactions may mediate this interaction (Inaba et al., 2010).

Docking simulations predicted that a β-hairpin structure protruding from Ero1α binds to the PDI hydrophobic b′ domain binding pocket. Experimental data confirmed this, as interactions between the two molecules were impaired upon deletion of the β-hairpin residues (Masui et al., 2011). Mutation of hydrophobic phenylalanine residues within the PDI binding pocket impaired interactions and compromised disulphide transfer between Ero1α and PDI, and disrupted folding of JcM in cells.

Interactions between Ero1α and PDI have therefore been well studied and documented. Binding occurs exclusively between the b′ domain of PDI and Ero1α, facilitating disulphide transfer between the shuttle cysteines and the PDI a′ active site. These previous studies have investigated the binding of oxidised Ero1α and the reduced form of PDI, however, and so do not necessarily represent the mechanisms governing the potential oxidation of Ero1α by PDI.

4.1.4 Autonomous and PDI-mediated oxidation of Ero1p.

While the regulatory disulphides of Ero1p are known to be reduced by substrate enzymes, the mechanism of re-oxidation of the disulphides and subsequent inactivation of Ero1p is less well understood. However, PDIp and autonomous oxidation are emerging as potential regulators of Ero1p activity. Ero1p is capable of autonomous oxidation, where one Ero1p molecule oxidises another via the C100-C105 shuttle disulphide (Kim et al., 2012). PDIp-mediated oxidation is more efficient, however, and provides a means of feedback regulation of Ero1p by linking Ero1p oxidation to the glutathione balance (Kim et al., 2012). The implications of this finding are that Ero1p activity can be regulated by these molecules to prevent the formation of a hyperoxidising environment, which can impair protein folding in the ER and stress cells (Chapters 1.2.7 and 1.2.8). PDIp will be reduced due to the availability of nascent client proteins and the relative abundance of reduced glutathione – which keeps Ero1p in an active state. Ero1p works to oxidise PDIp and GSH

indirectly until the redox balance becomes more oxidising and Ero1p is subsequently inactivated through the re-oxidation of its regulatory disulphides. Regulation of Ero1α activity by PDI has not yet been studied.

4.2 *In vitro* Ero1α re-oxidation and inactivation is carried out by specific ER oxidoreductases.

With over 20 PDI family members discovered so far, many acting as oxidases to transfer disulphides to reduced proteins, it is possible that one or more function to regulate the activity of Ero1α by re-oxidising and inactivating it. This hypothesis was tested using an SDS-PAGE based approach, where DTT-reduced Ero1α was incubated with various oxidants and PDI family members at the indicated concentrations for 300 s. This was done under anaerobic conditions, ensuring that oxidation of Ero1α was a result of oxidation by the indicated oxidants or PDI enzymes. Samples from the time courses were NEM alkylated at the given time points and analysed by SDS-PAGE before silver staining or Western blotting with an α-Ero1 antibody. The Ero1α redox state was then visualised (Figure 4.1A).

Ero1α remained reduced under anaerobic conditions over the duration of the assay. The inclusion of oxidised glutathione (10 mM) induced some oxidation of Ero1α, as did Trx (100 μM). ERp18 (50 μM) and PDIr (10 μM) were both able to oxidise Ero1α almost completely within 300 s. PDI (10 μM) and ERp46 (10 μM) were relatively more efficient at oxidising Ero1α, however. PDI (10 μM) oxidised Ero1α almost completely within 30 s, while ERp46 (10 μM) was able to oxidise it almost completely within 10 s.

Densitometry analysis of the oxidation of Ero1α by the ER oxidoreductases PDI and ERp46 was carried out to quantify the percentage of Ero1α oxidised at each time point (Figure 4.1B). Each experiment was carried out three times independently. ERp46 oxidised 75 ± 11% (standard deviation, n=3) of the Ero1α within 10 s, 84 ± 15% within 60 s and 91 ± 8% of the Ero1α after 300s. In comparison, PDI oxidised approximately 28 ± 15% of the Ero1α within 10 s, 81 ± 12% after 60 s and 89 ± 8% after 300 s. Specific oxidoreductases therefore can act to shut down Ero1α activity *in vitro*. In comparison, PDIr oxidised only 13 ± 3% of Ero1α within 10 s, 40 ± 4% after 60 s and 72 ± 7% after 300 s.

4.3 Investigating the PDI mediated oxidation of Ero1α.

Interactions between Ero1α and PDI have not been studied with regards to regulation of Ero1α activity. Interactions during oxidative protein folding involve reduction of Ero1α by the PDI a′ active site and the subsequent oxidation of the PDI a′ active site. During Ero1α

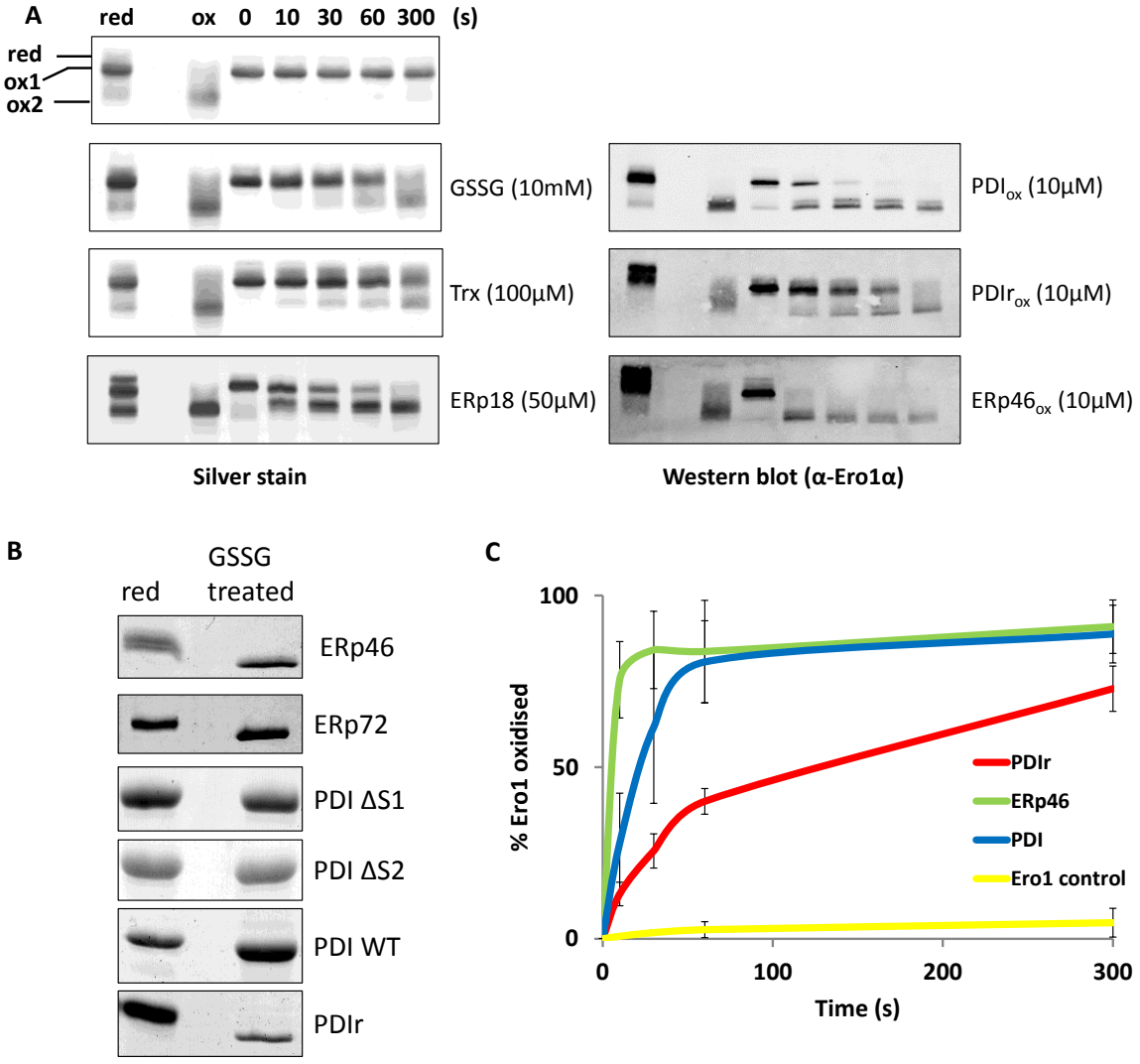

Figure 4.1 - Ero1α is oxidised completely and rapidly by the oxidised forms of PDI and ERp46. A - Ero1α was reduced with DTT before removal of the reducing agent. 2µM reduced Ero1α was then incubated alone or with oxidised glutathione (GSSG), Trx, ERp18, PDI, PDIr or ERp46. Incubations were carried out under anaerobic conditions with samples taken at the given time points and alkylated with NEM to freeze the redox states of the enzymes. Analysis was carried out via SDS-PAGE with gels either silver stained or Western blotted. B – The redox state of various PDI family members were analysed after 15 min incubation with 20 mM GSSG. Samples were AMS alkylated before analysing via non-reducing SDS-PAGE. Gels were Coomassie stained to visualise. C – Assays in A were repeated independently and gels were subject to densitometry quantification. Total oxidised Ero1α was calculated as a percentage of oxidised material/ total material and results were plotted against time. PDI and ERp46 oxidation of Ero1α is compared to PDIr and the Ero1α control assay. Error bars represent standard deviation (n=3).

regulation, oxidised PDI must interact with the reduced form of Ero1α; an interaction thought unfavourable due to the reduction potentials of the Ero1α and PDI disulphides (-275 mV and -180 mV, respectively) (Baker et al., 2008). In favour of the regulatory interaction is the affinity of PDI for reduced substrates, driven by hydrophobic and electrostatic interactions (Masui et al., 2011). It was therefore necessary to investigate the mechanism of interaction between the two molecules to determine if interaction was mediated by the PDI b′ binding domain (Masui et al., 2011) and the a′ active site (Chambers et al., 2010).

4.3.1 Ero1α oxidation by PDI active site mutants.

By eliminating one PDI active site, any disulphide transfer between PDI and Ero1α must occur due to dithiol disulphide exchange with the remaining active site. Two PDI active site mutants, prepared previously (Chambers et al., 2010), were utilised to determine whether Ero1α is oxidised specifically by either domain. ΔS1 PDI has the a domain active site mutated from CGHC to AGHA, while ΔS2 PDI has the a′ active site mutated to AGHA (Figure 4.2A). Each mutated active site can no longer form the active site disulphide. Under anaerobic conditions, oxidised forms of both ΔS1 and ΔS2 PDI were incubated with reduced Ero1α and the redox state of Ero1α was monitored over time (Figure 4.2B). The ΔS2 mutant was able to oxidise 18 ± 0.6% (standard deviation, n=3) of Ero1α after 10 s, 60 ± 1% of Ero1α after 60 s, and 82 ± 12% after 300 s. The ΔS1 PDI mutant was able to oxidise 18 ± 10% (standard deviation, n=3) of Ero1α after 10 s, 67 ± 10% after 60 s and 87 ± 10% after 300 s.

To study the effect of lowering the reduction potential of the PDI active sites on the interaction with Ero1α, two further mutants were used. Lowering the reduction potential makes the disulphide more stable, thus the mutants are less likely to act as oxidases. The ΔS1 HP and ΔS2 HP mutants have the remaining CGHC active site histidine mutated to a proline (Figure 4.3A). Reduced Ero1α was incubated with oxidised ΔS1 HP or ΔS2 HP PDI and the redox state of Ero1α was monitored over 300 s (Figure 4.3B). Densitometry analysis was performed to quantify the levels of Ero1α oxidised over the time course. Assays were performed independently at least twice and the mean value of oxidised Ero1α, as a percentage of the total Ero1α per lane, was plotted against time (Figure 4.4).

The ΔS1 HP mutant was able to oxidise 16 ± 3% (standard deviation, n=4) of Ero1α within 10s , 57 ± 10% within 60 s and 84 ± 12% after 300 s. The ΔS2 HP mutant was able to oxidise 13 ± 4% (range, n=2) of Ero1α after 10 s, 13 ± 18% after 60 s and 23 ±

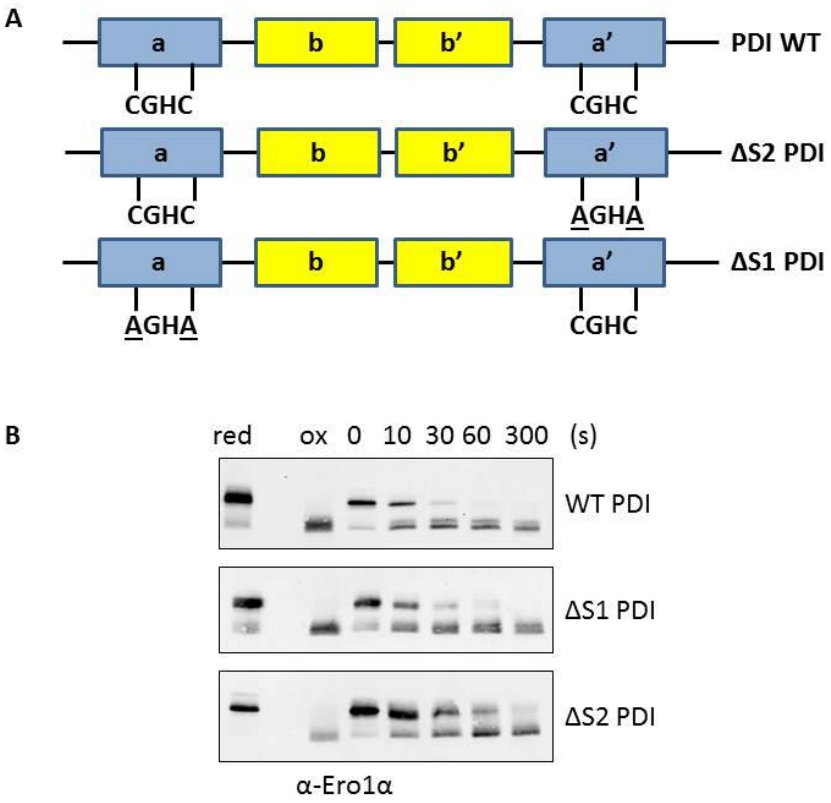

Figure 4.2 – Ero1α is preferentially oxidised by the PDI a′ active site domain. A – Schematic diagram showing the PDI domain structure and the cysteine to alanine mutations within the active sites in each of the ΔS1 and ΔS2 PDI mutants. B – Reduced Ero1α was incubated with oxidised PDI ΔS1 or ΔS2 mutants for 300 s under anaerobic conditions. Samples were taken at the given time points and alkylated with NEM to freeze the redox states of the enzymes. Samples were then analysed via SDS-PAGE and Western blot, probing with the α-Ero1α antibody. Ero1α re-oxidation by wild type PDI is included for comparison.

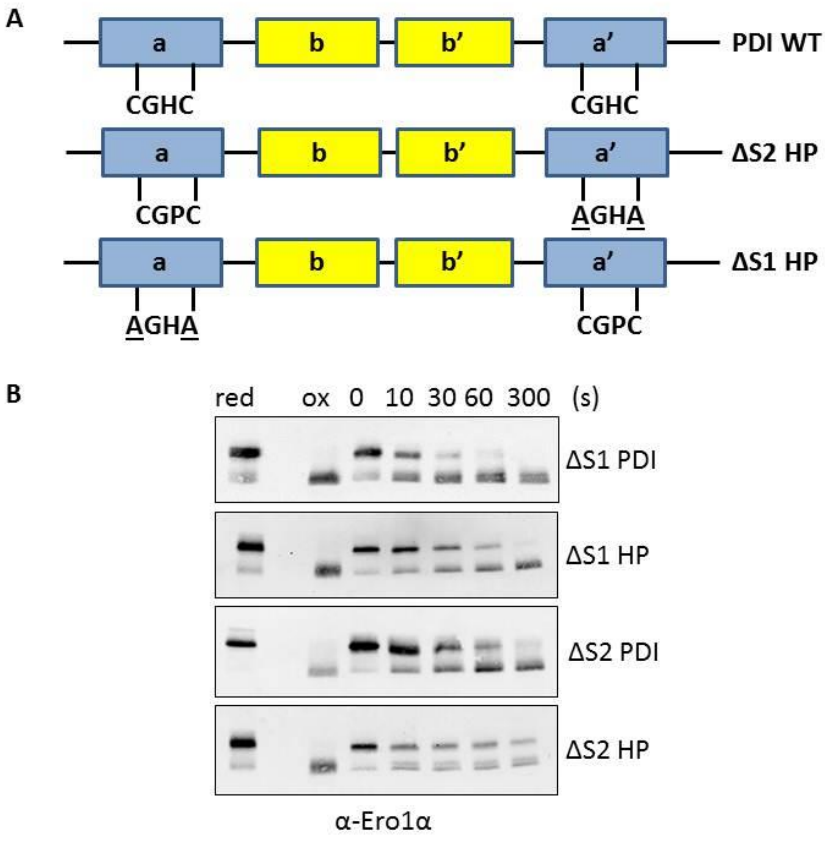

Figure 4.3 – Lowering the reduction potential of the PDI active sites lowers oxidase activity thus slowing oxidation of Ero1α. A – Schematic diagram of the PDI domain structure and the histidine to proline mutations in the remaining intact active sites of ΔS1 HP and ΔS2 HP PDI. B - Reduced Ero1α was incubated with oxidised PDI ΔS1 or ΔS2 mutants for 300 s under anaerobic conditions. Samples were taken at the given time points and alkylated with NEM to freeze the redox state of the enzymes. Samples were then analysed via SDS-PAGE and Western blot, probing with the α-Ero1α antibody. Ero1α re-oxidation by the ΔS1 and ΔS2 PDI mutants is included for comparison.

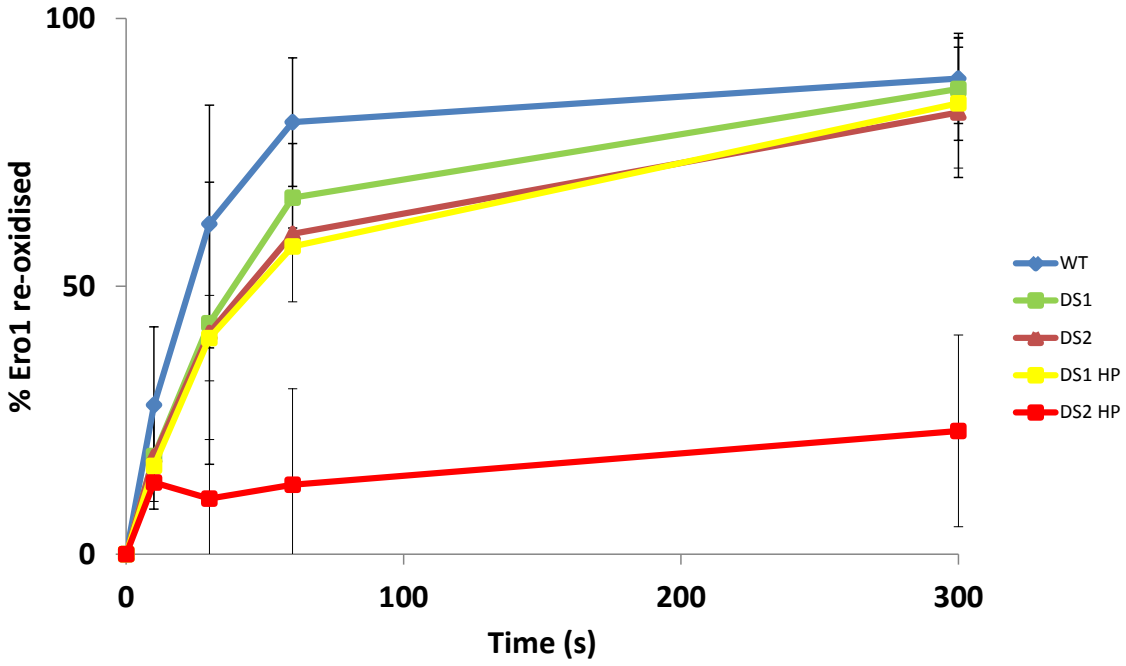

Figure 4.4 – Quantification of Ero1α re-oxidation by the PDI mutants. Densitometry analysis of the results presented in Figures 4.2 and 4.3 was performed to quantify oxidation of Ero1α as a percentage of the total, per lane, and plotted against time. The assays were performed and repeated independently. Error bars represent standard deviation (n=3) except DS2 HP mutant where error bars represent the range (n=2).

18% after 300 s.

4.3.2 The role of the PDI b′ domain in Ero1α re-oxidation.

Ero1α binds to the PDI b′ domain prior to PDI oxidation. To explore the binding mechanism during the regulatory interaction between Ero1α and PDI, an oxidised PDI binding mutant (Appendix 2) was incubated with reduced Ero1α. Samples were taken at the given time points, NEM alkylated and the Ero1α redox state was analysed by SDS-PAGE and Western blot (Figure 4.5A). Densitometry analysis was performed on the resultant blots to quantify the oxidation of Ero1α during the time course. Oxidised Ero1α was calculated as a percentage of the total, per lane, and plotted against time (Figure 4.5B). The PDI binding mutant (BM) was able to oxidise 10 ± 6.5% (standard deviation, n=6) of Ero1α after 10 s, 33 ± 12% after 60 s and 67 ± 18% after 300 s.

4.4 *In vivo* investigation of Ero1α re-oxidation.

Having analysed the data from Chapters 3 and 4, it seemed that the most likely mechanism of Ero1α re-oxidation and inactivation would be enzymatic oxidation by members of the PDI family, particularly PDI and ERp46. These two enzymes rapidly and completely oxidised Ero1α *in vitro* while intramolecular disulphide exchange and sulphenylation mechanisms are not as efficient. This conclusion warranted the progression of investigation into living cells.

4.4.1 Ero1α recovery from a DTT challenge.

An investigation into the *in vivo* re-oxidation of Ero1α by several ER oxidoreductases was carried out. The presence of PrxIV and the Gpx7/8 enzymes within the ER should theoretically remove hydrogen peroxide, thus hydrogen peroxide should not affect Ero1α re-oxidation. The contribution of intramolecular disulphide exchange to Ero1α inactivation cannot be eliminated due to the availability of oxygen. It was hypothesised that Ero1α and the ER proteins would be reduced by treatment with DTT (10 mM). Ero1α would then re-establish the redox balance by generating disulphide bonds *de novo* prior to returning to its OX2 conformation. It was hypothesised that overexpression of PDI and ERp46 would accelerate the re-oxidation of Ero1α. Cells overexpressing ERp18 were included for comparison, as oxidation of Ero1α by ERp18 was slow *in vitro* (Figure 4.1). Cells were treated with DTT before washing and allowing recovery over 60 min. At the appropriate time points, cells were washed with NEM and lysed. The Ero1α redox state was analysed by SDS-PAGE and Western blot (Figure 4.6).

The results show that in untreated HT1080 cells (UNT), Ero1α existed in its fully oxidised

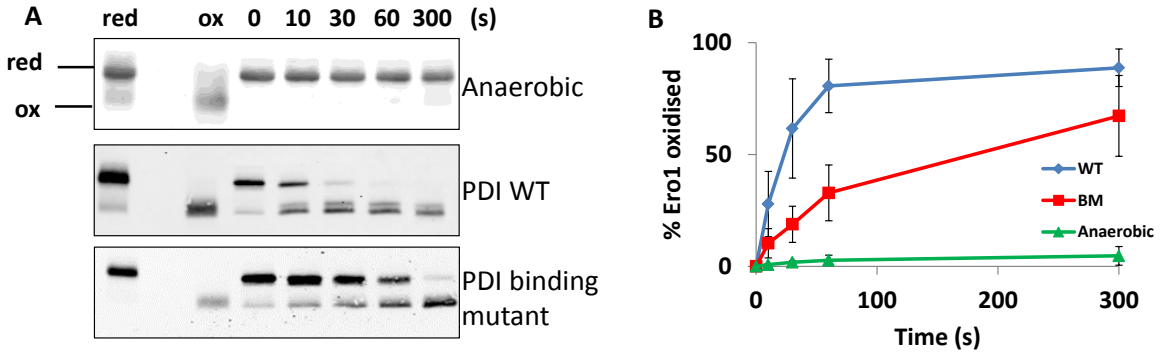

Figure 4.5 – The PDI b′ domain influences the oxidation of Ero1α. A – Reduced Ero1α was incubated under anaerobic conditions with an oxidised PDI mutant containing three point mutations which abolish binding of Ero1α. At the given time points, samples were alkylated with NEM before SDS-PAGE analysis and Western blotting using an α-Ero1α antibody. Results of Ero1α incubation alone and with wild type PDI are included for comparison. B – Densitometry analysis was performed on the results of the PDI binding mutant incubation with Ero1α. The results shown are representative of three independently performed assays. The percentage of Ero1α re-oxidised during the binding mutant assay (green) is compared to the results of wild type PDI (red) and Ero1α control (blue) assays. Error bars represent standard deviation (n=3).

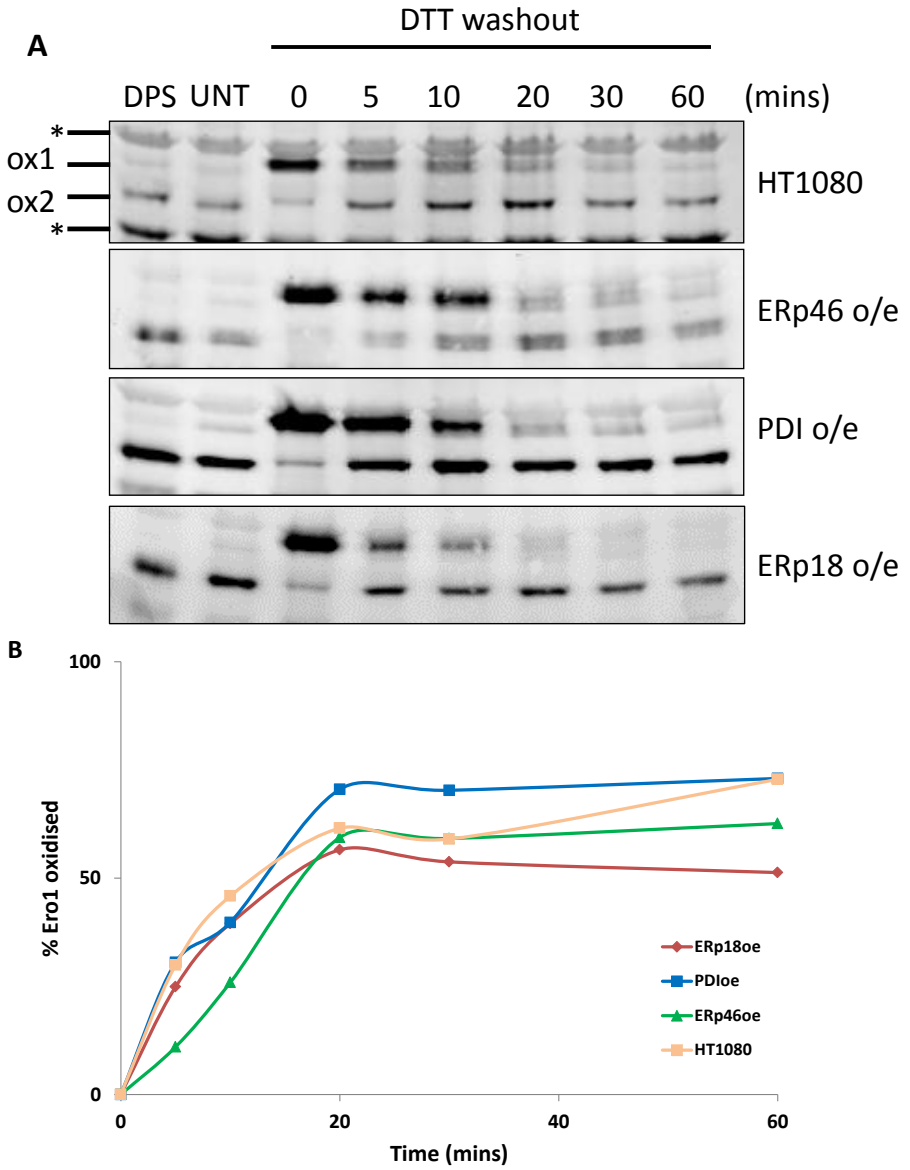

Figure 4.6 – Overexpression of PDI and ERp46 do not improve Ero1α recovery from a DTT challenge. A – HT1080 cells or HT1080 cells overexpressing ERp46, PDI or ERp18 were treated with DTT (10 mM) for 5 min before washing out the DTT for the given time. Untreated cells (UNT) or cells treated with DPS (1mM) were included as controls. At each time point, cells were washed in PBS containing NEM (20 mM) to prevent further disulphide transfer. Cells were lysed and the supernatant resuspended in SDS sample buffer before analysis by non-reducing SDS-PAGE and Western blot using an α-Ero1α antibody (* = cross reactive band). Representative results are shown. B – Densitometry analysis was performed on the results in A. Oxidised Ero1α was calculated as a percentage of total Ero1α, per lane, and plotted against time for each cell line tested.

form and ran with mobility comparable to Ero1α in DPS-treated cells. After DTT treatment, Ero1α ran with a decreased mobility through the gel. Within 5 min Ero1α began to recover back to its oxidised form and within 20 to 30 min Ero1α had recovered to its untreated state. Densitometry analysis of the results was performed to quantify oxidised Ero1α as a percentage of the total Ero1α in each lane. The percentage of oxidised Ero1α was plotted against time and representative values are shown for each cell line (Figure 4.6B).

4.4.2 Ero1α recovery from DTT in PDI, ERp46 and PrxIV knockdown cells.

The effect of knocking down ERp46 and PDI on Ero1α recovery from DTT challenge was investigated to determine whether the absence of the main source of Ero1α oxidation may prevent or impair this process. PDI and ERp46 knockdown cells were created by transfecting HT1080 cells with specifically targeted shRNA constructs; the resultant expression levels 5 days post-transfection were quantified after lysing cells and analysing samples by SDS-PAGE and Western blot. Expression of each target protein was compared with mock transfected cells (cells transfected using scrambled shRNA, sh13). GAPDH was used as a loading control (Figure 4.7). Bands were quantified by densitometry analysis.

PDI expression levels in the PDI shRNA transfected cells were 48% of control levels (Figure 4.7A). In cells transfected with ERp46 targeted shRNA, ERp46 expression was lowered to 21% of control levels (Figure 4.7B).

In an additional knockdown assay, cells stably transfected with shRNA targeted at PrxIV previously prepared by Dr. Timothy Tavender were tested for PrxIV expression levels (Figure 4.7C). PrxIV expression in PrxIV knockdown cells were 18% of that in control cells. PrxIV knockdown cells were used as PDI and ERp46 rapidly reduce PrxIV *in vitro* and in cells, therefore PrxIV may be a major source of disulphides for PDI and ERp46 (Tavender et al., 2010, Zito et al., 2010). Disrupting this disulphide source may prevent re-oxidation and inactivation of Ero1α by these oxidoreductases.

To address the potential issue of functional degeneracy within the PDI and ERp46 knockdown cells, a PDI-ERp46 shRNA co-transfection was carried out. This produced cells with PDI expression levels of 29.5 ± 4% of control levels, and ERp46 expression levels between 30 ± 3% when using GAPDH as a reference (Figure 4.7D).

Having successfully produced cells expressing lower levels of PDI, ERp46, PrxIV and ERp46-PDI compared to the scrambled shRNA control, these cells could be used in the DTT-recovery assay to determine whether or not lowered levels of these enzymes

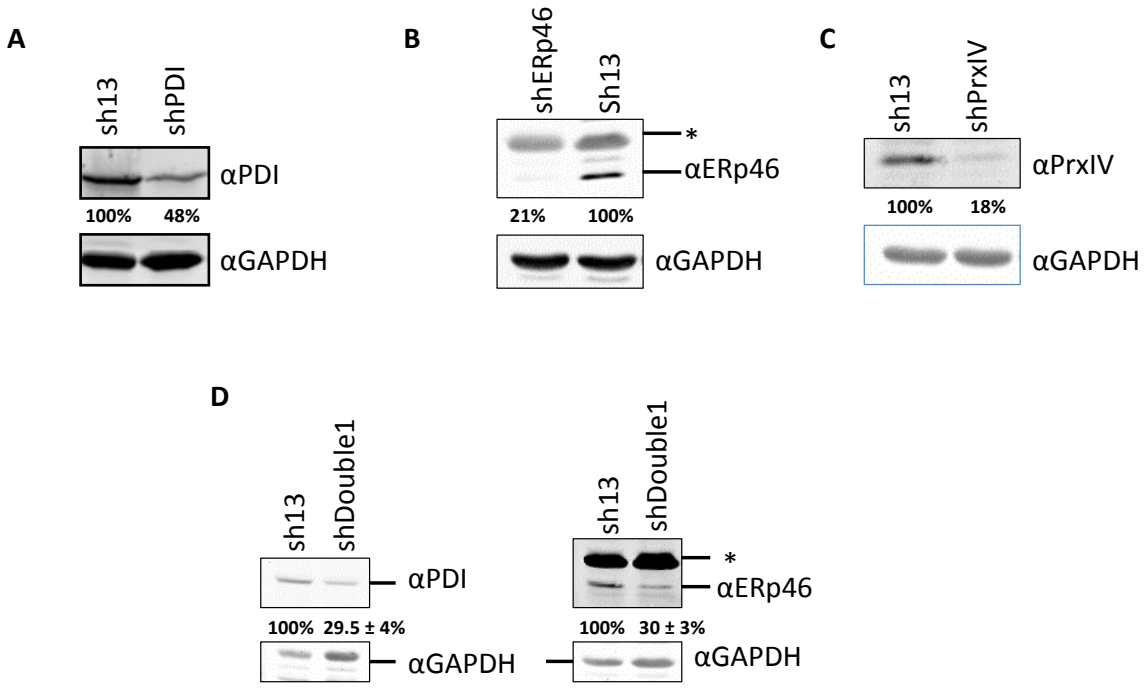

Figure 4.7 – Knockdown of PDI, ERp46 and PrxIV expression in HT1080 cells. Knockown of A – PDI and B – Erp46 by shRNA transfection. HT1080 cells were grown to approximately 80% confluence prior to transfection with shRNA. Cells were grown for 5 days under antibiotic selection to eliminate untransfected cells. Post-selection, cells were lysed and analysed by SDS-PAGE and Western blot probing with αPDI, αERp46 or αGAPDH antibodies. Densitometry analysis was performed to determine relative expression levels using GAPDH as a reference. C – A PrxIV stable knockdown cell line created previously was analysed to determine expression levels of PrxIV using similar methods to those in A and B. D – A PDI-ERp46 double knock down cell line was created by co-transfecting shRNA targeted to both oxidoreductases. Antibiotic selection was applied for 5 days post-transfection then cell lysates were analysed as in A, B and C. Knockdown was tested and expressed as a percentage of expression in control cells ± standard deviation (n=3). (* = cross reactive band). Control cells were transfected with sh13 vector containing a scrambled, non-specific shRNA construct.

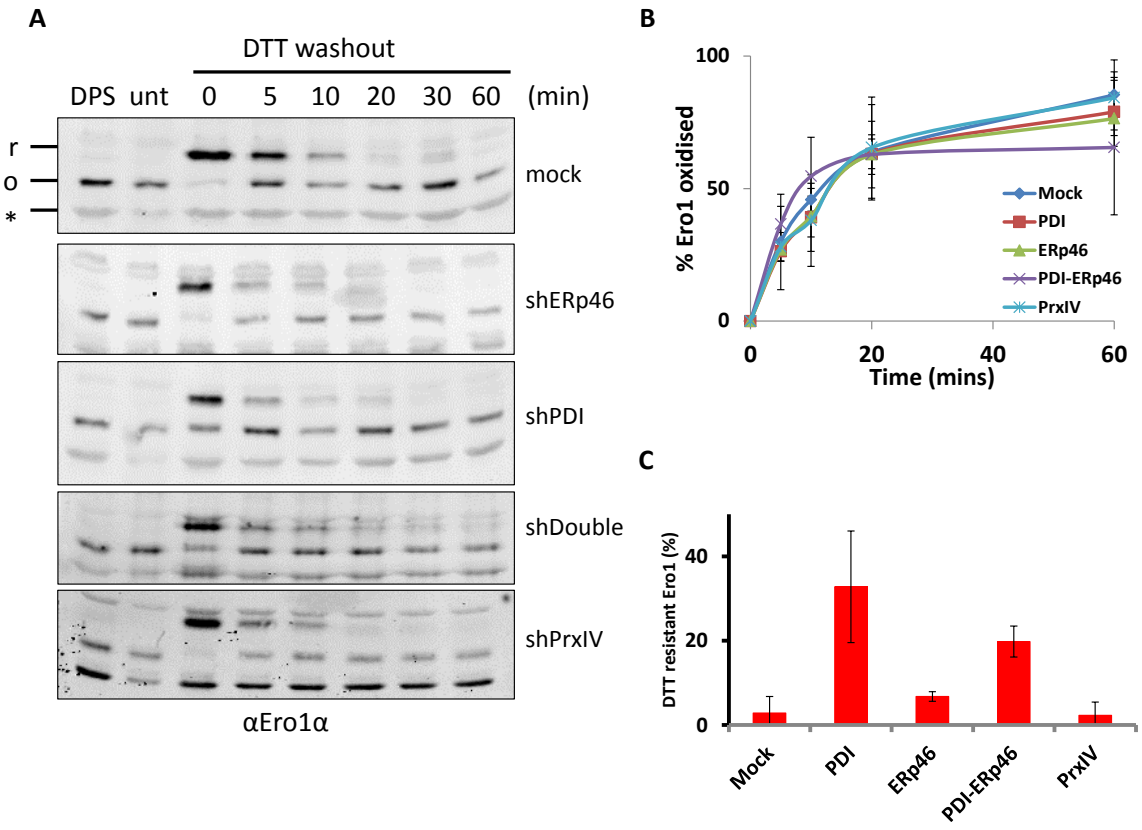

Figure 4.8 – Knockdown of PDI and ERp46 expression does not significantly affect Ero1α re-oxidation after a DTT challenge. A - Knockdown cells prepared as previously described were grown to approximately 80% confluence before a 5 min treatment with media containing DTT (10 mM). DTT-media was washed out with fresh media for the indicated time before washing for 5 min with PBS containing 20 mM NEM. Cell lysate was analysed via SDS-PAGE and Western blot, probing with αEro1α antibody (* = cross reactive band). B – Assays in A were independently repeated and densitometry analysis was performed to quantify levels of Ero1α oxidation. The percentage of Ero1α oxidised was plotted against time for each shRNA knockdown cell line. Error bars represent standard deviation (shPDI, n=3; shERp46, n=3; shPDI-ERp46, n=3) or range (mock, n=2; shPrxIV, n=2). C – Ero1α DTT-resistance in shRNA transfected cells. The mean absolute percentage of Ero1α remaining oxidised during DTT treatment was calculated as a percentage of the total Ero1α from A. Error bars represent standard deviation (shPDI, n=3; shERp46, n=3; shPDI-ERp46, n=3) or range (mock, n=2; shPrxIV, n=2).

influence re-oxidation of Ero1α. Knockdown cells were treated with DTT before washing with media for up to 60 min. At each given time point, cells were washed with PBS containing NEM to freeze the redox state of Ero1α before SDS-PAGE and Western blot analysis. Blots were probed with αEro1α antibody (Figure 4.8A). Densitometry analysis was performed to quantify oxidised Ero1α as a percentage of the total in each lane, and values were plotted against time (4.8B).

Results from the mock transfection show that Ero1α existed almost exclusively in the Ox1 state at the 0 time point, with only a small fraction remaining oxidised. Re-oxidation reached 46 ± 4% (range, n=2) after 10 min and 85 ± 5% after 60 min. The same assay performed in shERp46 treated cells resulted in Ero1α oxidation reaching 39 ± 7.5 % (standard deviation, n=3) after 10 min and 76 ± 11% after 60 min. In PDI knockdown cells, 39 ± 13% (n=3) of Ero1α was oxidised after 10 min and 79 ± 28% after 60 min. Ero1α oxidation in PDI-ERp46 double knockdown cells reached 55 ± 15% (n=3) after 10 min and 65.5 ± 6% after 60 min. In PrxIV knockdown cells, 38 ± 17% (n=2) of Ero1α was oxidised after 10 min, and 84 ± 3% after 60 min.

One interesting result visible in Figure 4.8A was the significant portion of Ero1α, 33 ± 13%, which remained oxidised during DTT treatment (t=0) of PDI knockdown cells (Figure 4.8C). The DTT-resistant band could also been seen at the 0 time point in the PDI-ERp46 shRNA co-transfected (shDouble) cell assay; 19.8 ± 3.7% remained reduced. In ERp46 knockdown cells, 6.8 ± 1.1% of Ero1α was DTT-resistant, in PrxIV knockdown cells 2.8 ± 2.6% and in mock transfected cells 2.8 ± 2.1%.

4.5 Discussion.

Enzymatic re-oxidation of Ero1α is quicker and more complete than the intramolecular disulphide exchange mechanism and oxidation by hydrogen peroxide (Figures 3.8 and 3.9). Enzymatic oxidation of Ero1α results in well-resolved bands. Ero1α is preferentially oxidised by PDI and ERp46 (Figure 4.1) suggestive of a specific function for these enzymes. High concentrations of oxidised glutathione have no direct effect on Ero1α activity regulation. The results imply that there may be a feedback system; Ero1α will oxidise PDI to drive oxidative protein folding, but PDI will oxidise Ero1α to prevent hyperoxidising conditions. ERp46 seems to be a more efficient oxidase of Ero1α than PDI, however the reasons for this are unknown given the similarities in the CxxC motifs between the two oxidoreductases. Furthermore, the CGHC motif is shared by ERp18 and PDIr and so the reason that these PDI family members are poor oxidases of Ero1α remains to be determined. Binding and interactions between Ero1α and the oxidases may prove

crucial. In the reduced state, the region of cys94-131 is unstructured in Ero1α which would facilitate interaction with PDI and therefore oxidation, changing redox state of Ero1a from OX1 to OX2 (Inaba et al., 2010).

Interestingly, the rapid and complete oxidation of Ero1α by PDI mirrors the oxidation of Ero1p by PDIp (Kim et al., 2012). Aside from the differences in isoforms used during the studies, Kim et al. use PDIp concentrations of 20 to 50 times that of Ero1p. This study shows that PDI oxidation of Ero1α occurs at concentrations only 5 times higher, thus proving that Ero1α re-oxidation is more sensitive than previously thought.
It is interesting to note the two separate Ero1α bands clearly visible after re-oxidation in the ERp18 and PDI assays (Figure 4.1, also witnessed in Figures 4.5, 4.3 and 4.2). This may be two separate Ero1α redox species, the identities of which could be determined by mass spectrometry.

The fact that Ero1α is oxidised differentially by the PDI active site mutants (Figure 4.5) is somewhat expected given recent studies exposing the preferential interactions between Ero1α and the a′-b′ domains. Ero1α has been shown to oxidise the a′ active site of PDI (Baker et al., 2008, Chambers et al., 2010) during the process of oxidative protein folding. This study reveals a similar interaction occurs during Ero1α activity regulation, as the a′ active site oxidises Ero1α as well as the wild type. Oxidation of Ero1α by the a domain active site is slightly slower. The binding of PDI to Ero1α occurs via a protruding Ero1α β-hairpin structure and a hydrophobic binding pocket within the PDI b′ domain (Masui et al., 2011); the same is true during Ero1α activity regulation. It can therefore be concluded that a similar interaction occurs during the oxidation of Ero1α by PDI (Figure 4.1). Oxidation of Ero1α by the PDI binding mutant is not completely impaired, however, and so the b′ domain is important but not essential for regulation of Ero1α.

Previous work has showed that lowering the reduction potential of the PDI active site, by mutating the sequence from CGHC to CGPC, stabilises the disulphide and enhances PDI oxidation by Ero1α (Chambers et al., 2010). The data presented in Figures 4.2 and 4.3 confirm this effect, as the PDI histidine to proline mutants display impaired oxidase activity; the active site disulphide has been stabilised thus is less likely to be reduced by Ero1α. Although the data in Figure 4.4 shows small differences in the oxidase activity of these PDI mutants, the differences are consistent and reproducible. Interestingly, the ΔS1 HP mutant was more able to oxidise Ero1α than the ΔS2 HP mutant, confirming that the a′ domain active site is more active in this respect. Taken together, this suggests that lowering the reduction potential of the PDI active sites results in their impaired ability to oxidise

Ero1α. The b′ domain of PDI seems to bind both the oxidised and reduced forms of Ero1α, and the a′ domain of PDI then participates in a dithiol-disulphide exchange reaction.

Ero1α recovery from a DTT challenge was investigated in cells and generated interesting results (Figure 4.6). The Ero1α recovery rate is much slower *in vivo* than *in vitro*. This is most likely due to the large ER proteome which has been reduced during DTT treatment. Ero1α can only recover once its substrate proteins and the glutathione balance has been restored. This could also explain why there is no increased Ero1α recovery rate in the PDI and ERp46 overexpressing cell lines when compared to the HT1080 and ERp18 overexpressing cell lines.

One problem with the knockdown approach used in Figures 4.7 and 4.8 is that functional degeneracy exists within the ER oxidoreductases; phenotypic traits can be masked due to the compensatory actions of other ER proteins. Although PDI and ERp46 expression levels were successfully lowered, other oxidoreductases may compensate for this lowered expression. Previous knockdown studies on PDI have yielded variable results – from 55% knockdown using a similar shRNA approach (Tavender and Bulleid, 2010) to 100% knockdown using siRNA (Rutkevich et al., 2010), although this is questionable given the suggestion that the PDI gene is essential in yeast (LaMantia and Lennarz, 1993). Further studies suggest PDI knockdown is limited to approximately 40-50% using siRNA (Gilbert et al., 2006, Tian et al., 2009). Knockdown of ERp46 expression has previously been reported at 77% (Tavender and Bulleid, 2010); the knockdown described in this study is therefore comparable. Production of a PDI-ERp46 double knockdown shows that PDI expression is 29.5 ± 4% of mock transfected cells, while ERp46 expression is 30 ± 3%. The reason for slighty lower PDI expression in the double knockdown compared to the PDI single knockdown is unknown. ERp46 expression in the double knockdown was slightly higher than in the ERp46 single knockdown, which could possibly be as a result of compensation for the lowered PDI levels.

After carrying out the DTT recovery assay on PDI, ERp46 and PDI-ERp46 knockdown cells, it became apparent that there is no significant difference in Ero1α recovery between transfected and mock transfected cells (Figure 4.8). This may be due to functional degeneracy within ER oxidoreductases or may be due to additional mechanisms acting to oxidise Ero1α such as hydrogen peroxide or internal disulphide exchange. A failsafe mechanism may be in place to prevent excessive Ero1α activity in the absence of its two principle oxidases. Ero1α recovery in PrxIV knockdown cells is unaffected, compared to mock transfected cells, and could possibly be due to the fact that PrxIV oxidation of PDI and ERp46 is relatively slow, occurring on the minute scale (Tavender and Bulleid, 2010),

and so would be unlikely to impact upon Ero1α regulation. Alternatively, the lack of oxidising equivalents being introduced into PDI and ERp46 by PrxIV may again be masked by functional degeneracy.

Recent evidence has questioned the role of Ero1α as the main source of oxidising equivalents within the ER, implicating PrxIV in this process as it can drive oxidative folding of RNAse and is reduced by several PDI enzymes (Tavender et al., 2010, Zito et al., 2010). The PrxIV-PDI pathway could constitute a feedback regulation system where the hydrogen peroxide generated by Ero1α could be utilised by PrxIV to generate *de novo* disulphide bonds. Excessive Ero1α activity, leading to increased hydrogen peroxide concentrations, results in disulphide formation within PrxIV before reduction by PDI, ERp46 or P5. From here the disulphides could be used to re-oxidise Ero1α and prevent hyperoxidation of the ER environment.

One potentially important result can be seen in Figure 4.8 and relates to the apparent partial DTT-resistance of Ero1α in PDI knockdown and PDI-ERp46 double knockdown cells. Ero1α displays lowered sensitivity to DTT reduction in cells expressing lowered levels of PDI, as has been suggested in yeast (Kim et al., 2012). Hydrogen peroxide-mediated or autonomous oxidation of Ero1α cannot be ruled out in cells and so may mask effectsof ERp46 and PDI knockdown on Ero1α re-oxidation. Furthermore, levels of PDI and ERp46 may not be low enough in each of the knockdowns to see an effect; it is possible that these low levels of PDI and ERp46 expression are sufficient to carry out the function of re-oxidising Ero1α. Ero1α re-oxidation in PrxIV knockdown cells does not differ significantly from re-oxidation in control cells. This could suggest that knockdown of PrxIV increases Ero1α sensitivity to sulphenylation, or more likely PrxIV involvement in this pathway is not significant.

There are a number of potential caveats associated with the overexpression and knockdown assays carried out in Figures 4.6 – 4.8. The cell lines overexpressing ERp18, PDI, ERp46 were not confirmed as overexpressing the relevant PDI family member, which could be done by Western blot. In using shRNA to carry out a transient transfection, the individual cells may be affected in different ways and some may express lower levels of the target protein than others. Furthermore, the cells may compensate for the lowered expression levels of specific PDI family members by upregulating expression of others. Transfection of the cells with shRNA could also potentially result in off-target effects such as the unwanted knockdown of other related PDI family members. These factors could potentially mask any effect during the DTT recovery assay or could produce an artefactual effect.

Taken together, the data in this chapter suggests strongly that the oxidation and inactivation of Ero1α is catalysed efficiently by PDI and ERp46 *in vitro*. Interactions between reduced Ero1α and oxidised PDI have been characterised and shown to be mediated by interactions with the PDI b′ binding domain and the a′ active site. These interactions can be impaired by lowering the reduction potential of the active site disulphides. Unfortunately the inactivation of Ero1α by PDI and ERp46 is more difficult to investigate in cells, as overexpression and knockdown of PDI and ERp46 did not generate significant acceleration or deceleration of Ero1α re-oxidation following DTT challenge. The results may, however, implicate PDI further in the regulation of the Ero1α redox state as Ero1α is less sensitive to DTT in cells with lowered PDI expression.

Chapter 5.0
The roles of Ero1α and glutathione in ER redox homeostasis

5.1 Introduction.

After the landmark study by Hwang et al. in 1992, glutathione was thought to provide the source of oxidising equivalents for disulphide bond generation within the ER due to the skewed ratio of GSSG: GSH (approximately 1:10) in comparison with the cytosol (1:100). With a relative abundance of GSSG, it was thought that this could support oxidative protein folding. However, evidence is now mounting that glutathione actually provides a buffer not to facilitate oxidative processes, but to facilitate the reduction of the oxidative protein folding enzymes enabling the reduction and isomerisation of non-native disulphides. Glutathione has been shown to support the reduced redox states of PDI family members and acts to counter the oxidative power of Ero1 and hydrogen peroxide, thus preventing ER hyperoxidation.

5.1.1 Glutathione provides a reducing pathway within the ER to support isomerisation of non-native disulphides.

Yeast cells are able to re-establish the balance of glutathione after reductive challenge with DTT. This balance is dependent on the activity of Ero1 which regenerates GSSG via the oxidation of GSH (Cuozzo and Kaiser, 1999). Mutations in the glutathione synthesis gene, GSH1, complement the *ero1-1* thermosensitive yeast mutant. This suggests that glutathione acts as a net reductant and that preventing yeast from generating GSH could protect the cells from the effects of a compromised oxidative pathway. Glutathione seems to exert an extra load on the oxidative pathway as *ero1-1: gsh1* double mutant cells are more able to facilitate oxidative folding of CPY compared to e*ro1-1* cells. Removing this extra load allows a compromised oxidative pathway to cope. Overexpression of GSH1 does not impair the oxidative folding of CPY, although the UPR is induced in GSH1 overexpressing cells indicating an accumulation of unfolded proteins within the ER. Disrupting the GSH1 gene in *ero1-1* cells results in the decreased activation of the UPR, while the inclusion of GSH in the growth medium of *ero1-1: gsh1* cells results in an increased UPR induction. Glutathione therefore acts as a reductant in the yeast ER and opposes the oxidative activity of Ero1p.

The reductive function of glutathione has been investigated in mammalian cells. Oxidative protein folding and subsequent secretion of tissue type plasminogen activator (tPa) is accelerated in cells overexpressing Ero1α. In glutathione-depleted buthionine sulphoximine (BSO) treated cells, where γ-glutamylcysteine synthetase is inhibited,

disulphide formation within tPa is accelerated but secretion is impaired due to the formation of non-native disulphides. Secretion is coupled to the resolution of these non-native disulphides (Chakravarthi and Bulleid, 2004). Furthermore, disulphide formation within the JcM is accelerated in SP cells compared to intact cells. Restoring glutathione to the SP cell system has an inhibitory effect on folding in a concentration-dependent manner. Disruption of the glutathione balance with GSH-synthesis inhibitors also results in accelerated JcM folding although this leads to the formation of high-molecular weight aggregates (Molteni et al., 2004). Lower levels of glutathione therefore impair isomerisation and result in the hyperoxidation of the ER. This effect is likely due to the lack of reduction of the ER oxidoreductases required to carry out isomerisation reactions. GSH within the cytosol opposes the oxidative folding pathway within the ER, although this system can be saturated as GSH added to intact cells has no effect on JcM folding. Without glutathione, cells are susceptible to the powerful oxidative activity of Ero1α.

5.1.2 Glutathione maintains ERp57 in a reduced state.

Direct evidence of the reduction of ER oxidoreductases by glutathione has been shown with ERp57. Numerous oxidoreductases were confirmed to exist in a reduced state in cells, while ERp57 specifically was shown to recover from an oxidative challenge. This recovery is not seen in microsomes thus the reductive pathway is not functional within the closed microsomal system (Jessop and Bulleid, 2004). Recovery is restored, however, when microsomes are incubated in the presence of cytosolic glutathione. Carmustine-inhibition of glutathione reductase, thus GSSG reduction, prevents the reduction of ERp57. A similar effect is seen with BSO treatment, strongly suggesting that cytosolic GSH is a major reductant within the ER. However, this does not imply that glutathione directly reduces ERp57.

Complementary data showed that ERp57 reduction is accelerated in the presence of glutathione, in a concentration-dependent manner. Purified recombinant ERp57 was oxidised using DPS and was sensitive to GSH treatment. Interaction between GSH and ERp57 was confirmed *in vivo*, thus GSH can directly reduce ERp57. Maintaining the intracellular glutathione pool and balance is essential, therefore, to keep members of the oxidoreductase family in the reduced state. Glutathione provides a reductive pathway within the ER which is essential to the reduction and isomerisation of disulphides during oxidative protein folding.

5.1.3 The dynamic relationship between glutathione, Ero1 and PDI.

While glutathione contributes to the regulation of the ERp57 redox state, its influence on the Ero1-PDI pathway has been widely studied due to the central role of this pathway in oxidative protein folding. Glutathione has an indirect effect on Ero1α activity by modulating the redox state of PDI. Glutathione therefore acts as a redox buffer that governs ER oxidative capacity. Hyperoxidation of the glutathione equilibrium pushes Ero1 towards its inactive Ox2 state, while Ero1 is pushed towards the reduced, active form when the glutathione balance is reducing.

Ero1p drives oxidative protein folding in the presence of GSH, generating GSSG through the oxidation of PDI by Ero1p and the subsequent reduction of PDI by glutathione (Tu et al., 2000). Regulatory disulphides within Ero1p are reduced more slowly in BSO treated cells following DTT treatment, compared to untreated cells, suggesting that the presence of a pool of GSH can accelerate the reduction of Ero1p regulatory disulphides (Kim et al., 2012). Glutathione, therefore, can influence the activity of Ero1p through PDI.

Incubation of Ero1p with both PDIp and GSH enhances Ero1p reduction and activation, suggesting that the pool of reduced PDIp required to activate Ero1p is maintained by GSH (Kim et al., 2012, Sevier et al., 2007). This reaction generates GSSG in an Ero1p-dependent fashion, as no GSSG is produced in the presence of an inactive Ero1p mutant (Kim et al., 2012). Furthermore, PDIp oxidation by Ero1p is fastest in a GSSG free environment, compared to oxidation in the presence of various ratios of GSH: GSSG. The initially quick rate of PDIp oxidation decreases as GSSG is produced, again suggesting this can influence Ero1p activity (Kim et al., 2012). The ratio of GSH: GSSG where Ero1p is oxidised has been estimated at 3: 1, above which Ero1p would be reduced and activated. The glutathione ratio therefore controls Ero1p activity through regulation of the PDIp redox state. The glutathione ratio at which Ero1α is oxidised has yet to be determined.

There is a growing body of evidence to suggest that Ero1α activity is modulated by glutathione. After DTT treatment, Ero1α is stable in the OX1 form in cells. In the absence of cytosolic GSH, in SP cells, the OX2 form of Ero1α is rapidly generated. GSH addition to SP cells results in the slowing of OX2 formation in a dose-dependent manner. Oxidation of Ero1 α is due to the oxidised state of PDI in SP cells, which is counteracted by the presence, or addition, of GSH (Molteni et al., 2004). In BSO-treated cells expressing the hyperactive C131A Ero1α mutant, the hyperoxidised phenotype is exacerbated and ER oxidoreductases ERp57 and TMX3 exist in the oxidised form (Appenzeller-Herzog et al., 2008). Upregulation of GSH has been described in cells expressing the Ero1α C131A mutant, however there is currently contradictory evidence regarding this phenomenon in Ero1α-overexpressing cells (Appenzeller-Herzog et al., 2008, Molteni et al., 2004).

Expression of a deregulated Ero1α mutant, C104/131A, leads to increased ER oxidoreductase oxidation which is alleviated by treatment with the glutathione precursor N-acetylcysteine (NAC), or aggravated by treatment with BSO (Hansen et al., 2012). The same result is seen in yeast cells (Cuozzo and Kaiser, 1999). GSH, therefore, buffers the ER oxidoreductases from Ero1α-mediated oxidation. GSH, PDI and Ero1α are involved in a close, elegant relationship which influences redox regulation within the ER.

5.2 Removal of the cytosol induces PDI and ERp57 oxidation.

5.2.1 Depletion of cellular glutathione following digitonin permeabilisation of the plasma membrane.

Semi-permeabilisation of cells has been described previously and widely adopted to investigate the functions of glutathione and cytosolic components. Digitonin, a cholesterol-specific detergent, acts to permeabilise cholesterol-rich membranes while leaving others intact. The ER and nuclear envelope both surivive digitonin treatment while the plasma membrane is permeabilised. By subsequently washing the semi-permeabilised cells, the cytosolic components can be removed, including proteins and glutathione. To confirm that treatment of cells with digitonin caused a release of cytosolic glutathione content, the glutathione content of cells was quantified in cells treated with digitonin or left untreated. To assay this, protein was precipitated from cell lysate before adding the soluble fraction to DTNB, NADPH and glutathione reductase in buffer. DTNB is reduced by GSH resulting in the release of 2-nitro-5-thiobenzoate which absorbs at 405 nm, thus its production can be followed spectrophotometrically. Glutathione reductase turns over oxidised glutathione thus providing a means of quantifying the total glutathione content. The initial rate of change in absorption at 405 nm can be compared to standard samples of known glutathione content, allowing quantifaction of the content in cell samples. After plotting the initial rate of change in absorption against glutathione content standards in nmol, a line of best fit was drawn (Figure 5.1). This line had the equation $y = 0.3496x + 0.3113$, where y is the rate of change in absorption and x is the glutathione content in nmol. After assaying 3 million cells for glutathione content, glutathione content was determined to be 7.16 ± 2.41 nmol (standard deviation). Assaying 3 million digitonin-treated cells resulted in a glutathione content of 0.77 ± 0.16 nmol, while 8 million digitonin-treated cells contained 1.50 ± 0.61 nmol glutathione. Thus digitonin treatment of cells greatly depletes glutathione content.

5.2.2 ERp57 and PDI are oxidised after digitonin treatment.

The use of microsomal vesicles has been described previously to specifically investigate the role of glutathione in the redox maintenance of the ER oxidoreductase ERp57

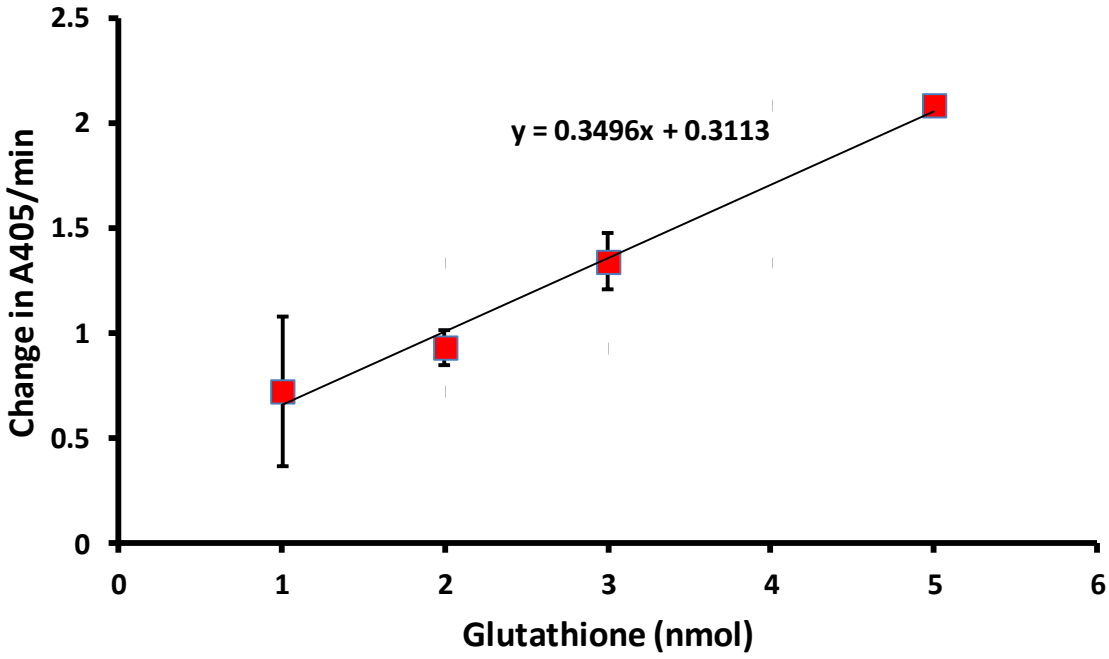

Figure 5.1 – Glutathione content standard curve. SP cells were lysed in 1% 5-sulfosalicyclic acid and proteins were removed by centrifugation. Supernatant was added to a reaction mixture of 0.2 mM NADPH, 0.6 mM Ellman's reagent and 1 unit glutathione reductase in 150 mM sodium phosphate buffer. Absorbance at 405 nm was recorded and the rate of change of absorbance was plotted against standard glutathione content. This assay was carried out twice and error bars show standard deviation. The line of best fit was used to determine glutathione content in cells and SP cells.

(Jessop and Bulleid, 2004). In this study, the SP cell preparation technique was used to consolidate and contribute to this knowledge with the investigation of PDI and ERp57 redox states. SP cells were created and the remaining intact ER was treated with DTT (10 mM), DPS (1 mM) or left untreated for 10 min. Thiols were alkylated in buffer containing NEM (20 mM). Differential alkylation was carried out after lysing the cells, treating with the reducing agent TCEP and AMS. This results in the AMS modification of thiols which were originally in an oxidised state, and produces a greater shift in mobility between the oxidised and reduced forms of ERp57 and PDI. These samples were compared to the equivalent treatments in intact cells which were incubated in the absence of digitonin (Figure 5.2A).

In DTT treated samples, both PDI and ERp57 ran faster through the gel than DPS-treated samples in both SP cells and in intact cells. The difference in mobility reflects either the absence or presence of disulphides following treatement with DTT or DPS respectively. PDI was approximately 36 ± 6% (standard deviation, n=3) oxidised in untreated, intact cells, or 79 ± 4.6% oxidised in untreated SP cells. ERp57 also displayed an oxidative shift between intact cells and SP cells. ERp57 was 23 ± 1% (range, n=2) oxidised in untreated, intact cells, or 61 ± 5.5% oxidised in untreated SP cells. The redox states of PDI and ERp57, therefore, shifted from reduced to oxidised during the SP cell preparation.

The SP cell preparation contained a number of steps with several washes, therefore the oxidation of PDI and ERp57 could occur at a specific stage within the protocol. To determine at which stage the oxidation of these enzymes occurred, samples were taken at several time points throughout the preparation and NEM alkylated to freeze the redox state. They were then differentially alkylated with AMS to produce the necessary gel shift and analysed by SDS-PAGE and Western blotting (Figure 5.2B).

Upon addition of digitonin, ERp57 existed in the reduced form while PDI existed as a mixture of reduced and oxidised species. The reason for this is unknown; however it seems unlikely that the PDI redox state would be altered immediately upon plasma membrane permeabilisation. After 5 min of incubation with digitonin, both ERp57 and PDI were slightly more oxidised. ERp57 and PDI were both oxidised further between the digitonin treatment step and the HEPES wash. ERp57 was further oxidised over the course of this wash step, whereas PDI seemed to be almost completely oxidised between these steps. It is possible to conclude that PDI and ERp57 were oxidised during the course of the SP cell preparation with much of the oxidation occurring between the digitonin treatment and the HEPES wash. These findings were confirmed by densitometry analysis. This observation is interesting as the cytosolic components, which would be released during the digitonin

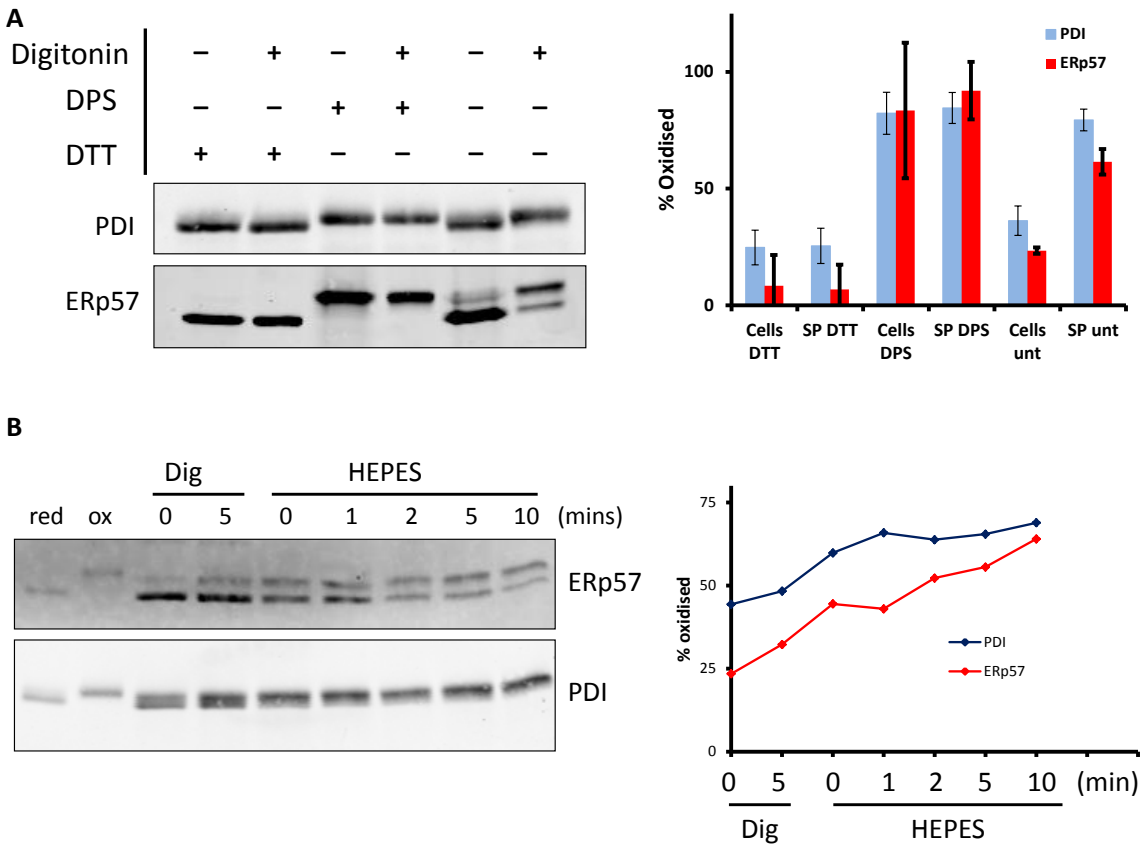

Figure 5.2 – PDI and ERp57 are oxidised during the SP cell preparation. A – SP cells or intact cells were treated with either DTT, DPS or left untreated for 10 min. All cells were then alkylated in 10 mM NEM, washed and lysed in NEM-free lysis buffer. Samples were then added to SDS sample buffer, treated with 10 mM TCEP and incubated with 20 mM AMS for 20 min. Samples were analysed by SDS-PAGE and Western blotted using α-PDI or α-ERp57 antibodies. Densitometry analysis was carried out and oxidised protein was calculated as a percentage of the total in each lane; shown as a histogram with error bars representing standard deviation (PDI, n=3) or range (ERp57, n=2). B – To determine at which point oxidation occurred during the SP cell preparation, samples were taken immediately upon addition of digitonin and after 5 min incubation. Samples were also taken during incubation with HEPES buffer at 0, 1, 2, 5 and 10 min. Samples were alkylated immediately in NEM before washing, differentially alkylating with AMS and analysing via SDS-PAGE and Western blot as above. Densitometry analysis was performed on the blots in B and represent oxidised PDI or ERp57 as a percentage of the total material in each lane.

treatment, are removed at this point - including glutathione which was shown previously to affect the ERp57 redox state (Jessop and Bulleid, 2004). We subsequently hypothesised that the increased oxidation of PDI and ERp57 was due to one or both of the following; the removal of reduced glutathione from the cytosol or oxidation directly or indirectly by Ero1α.

5.3 Ero1α knockdown impairs PDI and ERp57 oxidation in SP cells.

To test the hypothesis that Ero1α could drive oxidation of PDI and ERp57 during the SP cell preparation, an Ero1 knockdown cell line previously used to investigate the ER redox state was used (van Lith et al., 2011). This cell line expresses only 5% of endogenous levels of Ero1α and so any oxidation of PDI and ERp57 will likely be from another source i.e. PrxIV-mediated oxidation, although the contribution of the remaining Ero1α cannot be ruled out. The redox states of PDI and ERp57 were investigated in SP cells, created from Ero1α knockdown cells, or intact Ero1α knockdown cells (Figure 5.3).

In intact cells and SP cells treated with DPS, ERp57 and PDI both existed in an oxidised state indicated by their reduced mobility through the gel due to AMS alkylation. In intact cells and SP cells treated with DTT, both ERp57 and PDI existed as reduced species and ran comparatively slowly through the gel. In untreated intact cells PDI and ERp57 were 18 ± 9.7% and 10 ± 6% oxidised, respectively, however in untreated SP cells PDI was 49 ± 4.5% oxidised and ERp57 was 26 ± 7.6% oxidised. Knocking down Ero1 expression, therefore, results in a decreased level of oxidation of PDI and ERp57 in SP cells.

5.4 PDI and ERp57 redox state after cell lysis.

Having shown that Ero1α oxidised PDI and ERp57 during the SP cell preparation, it was necessary to confirm that this process was enzymatic and occured on a much quicker scale than it would do by air oxidation. SP cells were therefore lysed immediately upon their preparation (after digitonin treatment and HEPES wash step) and the oxidation state of PDI and ERp57 was monitored over the course of 60 min. The redox state after cell lysis was compared to that of intact cells, SP cells after 2 min of incubation with digitonin and after2 min of incubation in HEPES buffer. Samples were analysed via SDS-PAGE as above (Figure 5.4).

The blots reveal that the redox states of both PDI and ERp57 did not shift during the assay, remaining reduced in each sample. This finding confirmed that oxidation of these enzymes was catalytic rather than being driven by air oxidation as ERp57 and PDI were both stable in the reduced state after cell lysis.

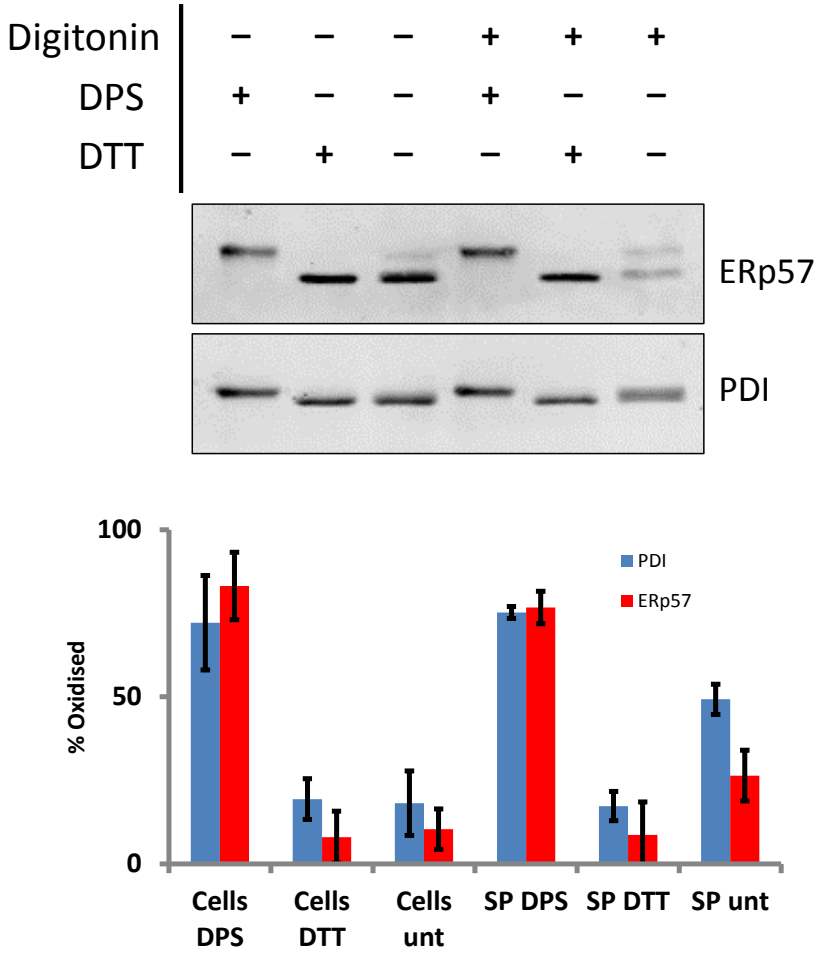

Figure 5.3 – Oxidation of ERp57 and PDI during the SP cell preparation is highly dependent on Ero1α. SP cells were generated using Ero1 knockdown cells. These were treated with DTT, DPS or left untreated for 10 min and compared to intact Ero1 knockdown cells. All cells were alkylated with 20 mM NEM after treatment before differential alkylation using TCEP and AMS for 20 min. Samples were analysed via SDS-PAGE and Western blotted using α-PDI or α-ERp57 antibodies. Densitometry analysis was carried out and oxidised protein was calculated as a percentage of the total in each lane; shown as a histogram. Error bars represent standard error (ERp57, n=3) or range (PDI, n=2).

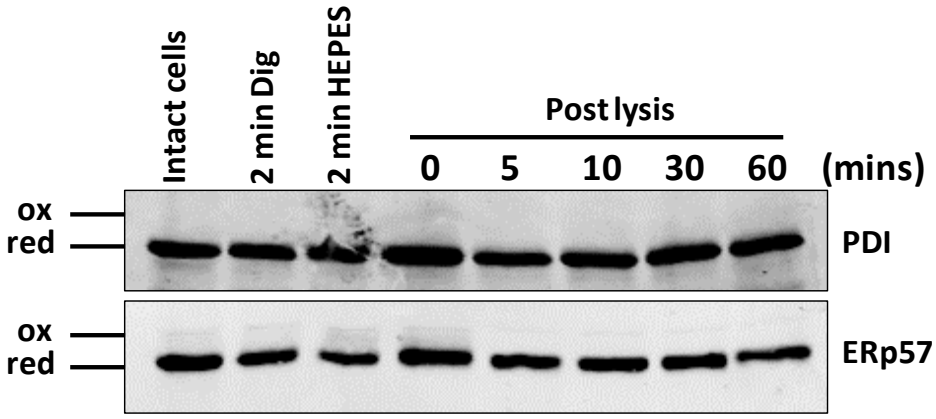

Figure 5.4 – PDI and ERp57 are not oxidised after lysis of SP cells; confirmation that oxidation of the SP cell ER environment is an enzymatic process. Samples were taken after 2 min of digitonin treatment, after 2 min of incubation with HEPES buffer, or from intact cells and NEM alkylated. Samples were also NEM alkylated at 0, 5, 10, 30 and 60 min from cells post-lysis. Alkylated samples were precipitated in 10% TCA, resuspended in SDS sample buffer, reduced with TCEP and differentially alkylated with AMS. Samples were then analysed by SDS-PAGE and Western blotted with α-PDI or α-ERp57 antibodies.

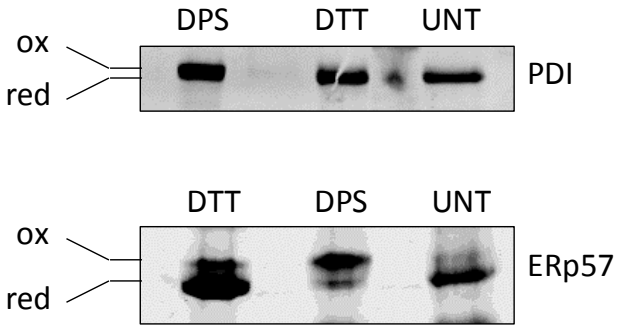

Figure 5.5 – PDI and ERp57 both remain in the reduced state in microsomes. Microsomes were prepared from HT1080 cells. Microsomes were treated with DTT, DPS or left untreated for 10 min before alkylating samples with 20 mM NEM. Microsomes were washed, treated with TCEP and differentially alkylated with AMS for 20 min. Samples were analysed via SDS-PAGE and Western blot using α-PDI and α-ERp57 antibodies.

5.5 Microsomal redox state comparison with cells and SP cells.

Microsomes have been used in a number of previous studies to investigate the impact of glutathione on the ER redox state. Previous studies have suggested that ERp57 remains in the reduced state in microsomes, contrary to the redox state of ERp57 in SP cells. To clarify the redox state of ERp57 and PDI in microsomes, a similar differential alkylation assay to that used above was adopted. Microsomes were gifted by Greg Poet (PhD student, University of Glasgow), having been isolated from dog pancreas. Microsomes were treated with DTT, DPS or left untreated for 10 min before alkylating with NEM. Samples were then precipitated in 10% TCA before resuspending the protein pellet in SDS sample buffer. Samples were reduced with TCEP and alkylated with AMS and analysed via SDS-PAGE and Western blot (Figure 5.5).

The PDI blotted samples show a marginal shift between oxidised and reduced species as the gel was not run as long as with previous samples. The DPS treated microsomes show that PDI existed in the oxidised form as it ran slightly higher than PDI in the DTT treated sample. In untreated microsomes, PDI ran alongside the DTT treated sample, suggesting that it was reduced in microsomes. The shift between the reduced and oxidised form of ERp57 was more pronounced and clearly shows the slower migration of ERp57 in the DPS treated microsomes compared to the DTT treated microsome sample. In untreaded microsomes, ERp57 existed in a mainly reduced state. PDI and ERp57 therefore exist in the reduced state in microsomes, unlike in SP cells where they are oxidised.

5.6 Discussion.

The data presented in Chapter 5 both confirm and contribute to knowledge surrounding the role of glutathione and Ero1α in ER redox homeostasis. This study confirms that treatment of cells with digitonin and subsequent washing with buffer strips the cells of cytosolic glutathione. This treatment removes approximately 90% of cellular glutathione (0.77 nmol in 3 million SP cells compared to 7.16 nmol in 3 million untreated cells). This is comparable to the glutathione content found in other cell types (Hwang et al., 1992, Ramos et al., 2005). This method therefore provides a system where the influence of cytosolic glutathione, or other cytosolic factors, on ER redox homeostasis can be investigated.

The redox state of PDI shifts from reduced to oxidised in a glutathione-depleted environment (Mezghrani et al., 2001), as glutathione maintains ER oxidoreductases in a reduced state (Jessop and Bulleid, 2004, Molteni et al., 2004). There are a number of studies describing potential glutathione transport proteins and systems (Banhegyi et al., 2003, Banhegyi et al., 1999) although a definitive report remains elusive. It is currently

unknown, therefore, why cytosolic glutathione alters redox states within the ER. In this study, the redox states of PDI and ERp57 are both confirmed to be sensitive to cytosolic glutathione and are oxidised in SP cells. In addition to this, the time course presented in Figure 5.2B shows for the first time that oxidation occurs almost immediately upon digitonin treatment, presumably as the plasma membrane is permeabilised and cytosolic glutathione is diluted into the buffer. Interestingly, this treatment alone is not sufficient to cause complete oxidation, as oxidation continues during the HEPES buffer incubation. PDI and ERp57 oxidation is therefore highly sensitive to the presence of glutathione.

ERp57 is known to be sensitive to glutathione removal and not the removal of other cytosolic factors (Jessop and Bulleid, 2004). The same cannot be concluded for PDI, which could be further investigated by adding back cytosolic factors and monitoring their influence on PDI redox state.

ERp57 seems to be slightly more resistant to oxidation than PDI during the SP cell preparation. This may be due to the fact that ERp57 is a poor substrate for Ero1α (Mezghrani et al., 2001).

To identify the source of oxidation during the SP cell preparation, SP cells were created using Ero1 knockdown cells. Recent studies have questioned the contribution of Ero1α in ER redox homeostasis, suggesting that PrxIV may play an equal or greater role (Tavender et al., 2010, Zito et al., 2010). Furthermore, the fact that Ero1α is not an essential gene (Zito et al., 2010) would suggest that it is not such a significant source of oxidising equivalents. Oxidation of ERp57 and PDI in Ero1 knockdown SP cells, however, was less than that in HT1080 SP cells, indicating that Ero1 is a major source of oxidation during this process. ERp57 is approximately 35% less oxidised in Ero1 knockdown SP cells compared to HT1080 SP cells. PDI is approximately 30% less oxidised under the same conditions. These significant effects are seen in cells expressing 5% of endogenous Ero1α levels, thus it would be interesting to investigate the effects of an Ero1α knockout which may have a more profound effect on PDI and ERp57 oxidation in SP cells. These findings agree with, and contribute to, results previously obtained on the effects of Ero1α knockdown (van Lith et al., 2011).

The results shown in Figure 5.4 confirm that PDI and ERp57 oxidation is a result of enzymatic activity rather than an artefactual effect of cell lysis or air oxidation. PDI and ERp57 are stable in the reduced state and resistant to air oxidation for over 60 min. There are discrepancies in the data as both PDI and ERp57 exist almost completely reduced throughout the time course. After 2 min of HEPES buffer incubation in Figure 5.2B,

ERp57 is approximately 50% oxidised, while PDI is almost fully oxidised. This is different from what is witnessed in Figure 5.4. An oxidised control would confirm the oxidative shift in mobility. This raises the question of the source of the oxidative power in cells and in Ero1α knockdown cells – it may be provided by the remaining Ero1α, PrxIV or by some other mechanism. This could be investigated by repeating the same assay in PrxIV knockdown or knockout cells, or in Ero1α-PrxIV double knockdown or knockout cells.

The results in Figure 5.5 confirm data previously presented, showing that ER oxidoreductases exist in the reduced state in microsomes; contradicting their SP-cell redox state. ERp57 has previously been shown to exist in the reduced state in microsomes (Jessop and Bulleid, 2004). The reasons for this are likely due to the methods of preparation; microsomes are isolated by ultracentrifugation, whereas SP cells are mechanically disrupted by digitonin. The ER membrane may be affected by the detergent, thus producing a slightly 'leaky' system which could lead to differences in glutathione content between the two. Unfortunately separation of the PDI redox states in this assay was poor due to incomplete electrophoresis.

The results presented in this chapter provide a significant insight into the influence of glutathione and Ero1α on ER redox homeostasis. At a time when the contribution of Ero1α has been questioned, it is clear that it is a source of significant oxidation within SP cells. Oxidation of ER oxidoreductases is shown to be a catalytic process occurring upon removal of cytosolic factors, most importantly glutathione. This implies that cytosolic glutathione may ultimately influence the oxidative protein folding of nascent proteins within the ER. The results also highlight the fact that microsomes and SP cells, although both glutathione-depleted, differ significantly with regards to ER oxidoreductase redox states.

Chapter 6.0
Conclusions and future work

6.1 General discussion.

This novel study aimed to investigate the mechanism of Ero1α re-oxidation and inactivation. Having tested the three hypotheses, listed in chapter 1.4, it is clear that although hydrogen peroxide and internal disulphide exchange can catalyse the oxidation of Ero1α, the most rapid and efficient mechanism is oxidation by specific ER oxidoreductases. At equimolar concentrations of the potential oxidant molecules, internal disulphide exchange seems to be the least favourable mechanism of oxidation, while oxidation by PDI and ERp46 is most favourable. It is interesting to note that, *in vitro*, Ero1α is more sensitive to regulation by PDI than has been previously reported (Kim et al., 2012). This study reveals that Ero1α is completely and rapidly oxidised by PDI at a ratio of 2 μM Ero1α: 10 μM PDI, a much more physiological ratio than that tested on Ero1p (2 μM; 50 μM). As Ero1α oxidation by hydrogen peroxide and internal disulphide exchange is shown to be possible, contribution of these mechanisms to the *in vivo* regulation of Ero1α activity cannot be ruled out under the conditions tested in this study. Furthermore, autonomous oxidation by Ero1α cannot be discounted by the findings of this study. PDI, ERp46, hydrogen peroxide and internal disulphide exchange may work together to prevent excessive Ero1α activity, however PDI and ERp46 would likely drive the vast majority of oxidation. This would explain, in part, the lack of effect of PDI and ERp46 knockdown on Ero1α re-oxidation.

As PDI is a known isomerase, it may be possible that non-native disulphides formed by sulphenylation of Ero1α regulatory cysteines could be isomerised by PDI, thus contributing to the overall goal of preventing Ero1α activity. Alternatively, hydrogen peroxide may cause oxidation of the glutathione pool throught the glutathione peroxidase enzymes. An increased ratio of oxidised: reduced glutathione would influence the PDI redox state, thus preventing Ero1α activity through a lack of substrate or by directly oxidising the regulatory disulphides. It is entirely possible, and indeed sensible, that more than one mechanism exists to regulate Ero1α activity, considering the potentially dire consequences of hyperactivity. Glutathione is likely the ‘master governer’, as glutathione influences the redox state of PDI which can ultimately reduce or oxidise Ero1α.

This study also raises the question of a possible feedback loop existing between ERp46, PDI and PrxIV. This feedback loop would involve the hydrogen peroxide produced by Ero1α acting as an oxidant to create disulphide bonds within PrxIV. As PDI and ERp46 are

known to reduce PrxIV (Tavender et al., 2010), the dislphides could be passed from PrxIV to PDI or ERp46 and on to Ero1α, thus preventing further hydrogen peroxide production.

The 2000 Benham et al. study suggested that PDI prefers to bind a fully folded Ero1α, and did not bind well to a C391A mutant which migrated as a diffuse smear during SDS-PAGE. This data would contradict the findings of this study; however there are important differences in the redox states of Ero1α and PDI which should be taken into account. Crucially, in cells, PDI would be reduced and would interact with oxidised Ero1α, unlike the conditions tested during this study. Furthermore, PDI is known to interact with C94 which could potentially be obscured or inaccessible in the smeared, potentially misfolded C391A mutant.

Interestingly, in addition to the investigations of Ero1α oxidation by PDI, this study adds further evidence that glutathione, Ero1α and PDI are inextricably linked. Lowering PDI expression by shRNA knockdown decreases Ero1α sensitivity to DTT; Ero1α is not reduced as efficiently in PDI deficient cells. Although knockdown of PDI in this study was limited to between 50 and 70%, a significant effect on Ero1α reduction by DTT was witnessed; Ero1α was only approximately 80% reduced by DTT. This is in agreement with the hypothesis that Ero1α redox state is controlled by glutathione via PDI.

Another interesting result from this study is the fact that Ero1α contributes significantly to ER redox homeostasis. Combining results from the oxygen consumption assay (Figure 3.3) and the ERp57 and PDI redox state assay in Ero1 knockdown cells (Figure 5.3), it is clear that Ero1α influences the oxidised: reduced glutathione ratio, via oxidation and recycling of PDI, until the glutathione ratio approaches approximately 1: 20. This is approximately half of the predicted ER glutathione ratio of 1: 10. Furthermore, Ero1α accounts for at least approximately 35% of ERp57 oxidation and 39% of PDI oxidation in SP cells. It can be concluded, therefore, that Ero1α accounts for between 35% and 50% of the oxidation of PDI, ERp57 and glutathione within the ER. This may suggest why Ero1α is necessary for cells to recover from DTT treatment (van Lith et al., 2011).

This study contributes significantly to the field of ER homeostasis and oxidative protein folding as it provides novel data to suggest that Ero1α activity can be rapidly and efficiently controlled specifically by PDI and ERp46. It also provides evidence to suggest that hydrogen peroxide and internal disulphide exchange, or autonomous oxidation, may also play a role. Furthermore, the data provides a novel insight into the interaction between oxidised PDI and reduced Ero1α, an interaction that has never been studied previously in a published article. This study implicates the a′ and b′ domains of PDI in this interaction.

The contribution of Ero1α to redox homeostasis in cells and in SP cells has been partially quantified, and found to be significant with respect to the redox state of important ER oxidoreductases. This study also highlights the differences in the redox states of PDI and ERp57 between microsomes and SP cells – the reasons or which are yet to be discovered.

6.2 Future work.

A number of experiments could be performed to further investigate the findings of this study. With relation to the hydrogen peroxide induced sulphenylation of Ero1α, it may be possible to determine which regulatory cysteines, if any, are particularly susceptible to sulphenylation. This could be done by titrating increasing concentrations of hydrogen peroxide then using mass spectrometry to define the redox state of Ero1α. Low concentrations of hydrogen peroxide may induce specific regulatory disulphide formation. Likewise, a similar approach could be used to determine if any of the regulatory disulphides are particularly susceptible to oxidation by PDI or ERp46, or by internal disulphide exchange or autonomous oxidation.

Mass spectrometry would be a useful approach to determining the disulphide patterns in Ero1α during the activity assay with Trx. This could be used to characterise the reductive and oxidative steps that occur during the activity cycle, in a similar manner to that carried out on Ero1p (Heldman et al., 2010).

It would perhaps be beneficial to determine the concentrations of hydrogen peroxide produced in the assays using the oxygen electrode. If equal concentrations of hydrogen peroxide are generated and recovered, this would be a strong indication that sulphenylation does or does not play a role in Ero1α oxidation.

As an additional control to confirm that cytosolic factors are removed during the SP cell preparation, the removal of well known and characterised cytosolic proteins could be followed by Western blotting samples before and after digitonin treatment and HEPES buffer wash. A more global approach could be adopted by measuring protein content with Bradford's reagent before and after the SP cell preparation.

To investigate the contribution of other oxidative processes during the SP cell preparation, it would be beneficial to determine the redox states of PDI and ERp57 in SP cells generated from, for example, PrxIV knockdown or knockout cells. A similar assay could be carried out in Ero1-PrxIV double knockdown cells to quantify the contribution of both oxidative pathways.

To determine whether autonomous oxidation occurs with Ero1α, a C394/397A active site mutant could be used in conjunction with a myc-tagged Ero1α, similar to the assay carried

out with Ero1p (Kim et al., 2012). The redox state of the C394/397A mutant could be followed during incubation with the myc-tagged version, having selectively removed the myc-tagged version by immunoprecipitation prior to Western blot.

Another potentially interesting assay could be done with a C94A Ero1α mutant, where its interaction with the oxidised form of PDI would indicate whether PDI oxidises the shuttle cysteines which then distribute disulphides to the regulatory cysteines, or whether PDI directly oxidises the regulatory cysteines.

References

ANDERSON, R. G. & PATHAK, R. K. 1985. Vesicles and cisternae in the trans Golgi apparatus of human fibroblasts are acidic compartments. *Cell,* 40**,** 635-43.

ANELLI, T., ALESSIO, M., BACHI, A., BERGAMELLI, L., BERTOLI, G., CAMERINI, S., MEZGHRANI, A., RUFFATO, E., SIMMEN, T. & SITIA, R. 2003. Thiol-mediated protein retention in the endoplasmic reticulum: the role of ERp44. *EMBO J,* 22**,** 5015-22.

ANELLI, T., ALESSIO, M., MEZGHRANI, A., SIMMEN, T., TALAMO, F., BACHI, A. & SITIA, R. 2002. ERp44, a novel endoplasmic reticulum folding assistant of the thioredoxin family. *EMBO J,* 21**,** 835-44.

ANFINSEN, C. B., HABER, E., SELA, M. & WHITE, F. H., JR. 1961. The kinetics of formation of native ribonuclease during oxidation of the reduced polypeptide chain. *Proc Natl Acad Sci U S A,* 47**,** 1309-14.

AOE, T., LEE, A. J., VAN DONSELAAR, E., PETERS, P. J. & HSU, V. W. 1998. Modulation of intracellular transport by transported proteins: insight from regulation of COPI-mediated transport. *Proc Natl Acad Sci U S A,* 95**,** 1624-9.

APPENZELLER-HERZOG, C., RIEMER, J., CHRISTENSEN, B., SORENSEN, E. S. & ELLGAARD, L. 2008. A novel disulphide switch mechanism in Ero1alpha balances ER oxidation in human cells. *EMBO J,* 27**,** 2977-87.

ARAKI, K. & NAGATA, K. 2011. Functional in vitro analysis of the ERO1 protein and protein-disulfide isomerase pathway. *J Biol Chem,* 286**,** 32705-12.

BAKER, K. M., CHAKRAVARTHI, S., LANGTON, K. P., SHEPPARD, A. M., LU, H. & BULLEID, N. J. 2008. Low reduction potential of Ero1alpha regulatory disulphides ensures tight control of substrate oxidation. *EMBO J,* 27**,** 2988-97.

BAKSH, S., BURNS, K., ANDRIN, C. & MICHALAK, M. 1995. Interaction of calreticulin with protein disulfide isomerase. *Journal of Biological Chemistry,* 270**,** 31338-31344.

BANHEGYI, G., CSALA, M., NAGY, G., SORRENTINO, V., FULCERI, R. & BENEDETTI, A. 2003. Evidence for the transport of glutathione through ryanodine receptor channel type 1. *Biochem J,* 376**,** 807-12.

BANHEGYI, G., LUSINI, L., PUSKAS, F., ROSSI, R., FULCERI, R., BRAUN, L., MILE, V., DI SIMPLICIO, P., MANDL, J. & BENEDETTI, A. 1999. Preferential transport of glutathione versus glutathione disulfide in rat liver microsomal vesicles. *J Biol Chem,* 274**,** 12213-6.

BENHAM, A. M., CABIBBO, A., FASSIO, A., BULLEID, N., SITIA, R. & BRAAKMAN, I. 2000. The CXXCXXC motif determines the folding, structure and stability of human Ero1-Lalpha. *EMBO J,* 19**,** 4493-502.

BENITEZ, L. V. & ALLISON, W. S. 1974. The inactivation of the acyl phosphatase activity catalyzed by the sulfenic acid form of glyceraldehyde 3-phosphate dehydrogenase by dimedone and olefins. *J Biol Chem,* 249**,** 6234-43.

BERTOLI, G., SIMMEN, T., ANELLI, T., MOLTENI, S. N., FESCE, R. & SITIA, R. 2004. Two conserved cysteine triads in human Ero1alpha cooperate for efficient disulfide bond formation in the endoplasmic reticulum. *J Biol Chem,* 279**,** 30047-52.

BOTTOMLEY, M. J., BATTEN, M. R., LUMB, R. A. & BULLEID, N. J. 2001. Quality control in the endoplasmic reticulum: PDI mediates the ER retention of unassembled procollagen C-propeptides. *Curr Biol,* 11**,** 1114-8.

BULLEID, N. J. & FREEDMAN, R. B. 1988. Defective co-translational formation of disulphide bonds in protein disulphide-isomerase-deficient microsomes. *Nature,* 335**,** 649-51.

CABIBBO, A., PAGANI, M., FABBRI, M., ROCCHI, M., FARMERY, M. R., BULLEID, N. J. & SITIA, R. 2000. ERO1-L, a human protein that favors disulfide bond formation in the endoplasmic reticulum. *J Biol Chem,* 275**,** 4827-33.

CAO, Z. B., TAVENDER, T. J., ROSZAK, A. W., COGDELL, R. J. & BULLEID, N. J. 2011. Crystal Structure of Reduced and of Oxidized Peroxiredoxin IV Enzyme Reveals a Stable Oxidized Decamer and a Non-disulfide-bonded Intermediate in the Catalytic Cycle. *Journal of Biological Chemistry,* 286**,** 42257-42266.

CHAKRAVARTHI, S. & BULLEID, N. J. 2004. Glutathione is required to regulate the formation of native disulfide bonds within proteins entering the secretory pathway. *J Biol Chem,* 279**,** 39872-9.

CHAMBERS, J. E., TAVENDER, T. J., OKA, O. B., WARWOOD, S., KNIGHT, D. & BULLEID, N. J. 2010. The reduction potential of the active site disulfides of human protein disulfide isomerase limits oxidation of the enzyme by Ero1alpha. *J Biol Chem,* 285**,** 29200-7.

CHEN, B., MARIANO, J., TSAI, Y. C., CHAN, A. H., COHEN, M. & WEISSMAN, A. M. 2006. The activity of a human endoplasmic reticulum-associated degradation E3, gp78, requires its Cue domain, RING finger, and an E2-binding site. *Proc Natl Acad Sci U S A,* 103**,** 341-6.

CHO, S. H., PARSONAGE, D., THURSTON, C., DUTTON, R. J., POOLE, L. B., COLLET, J. F. & BECKWITH, J. 2012. A new family of membrane electron

transporters and its substrates, including a new cell envelope peroxiredoxin, reveal a broadened reductive capacity of the oxidative bacterial cell envelope. *MBio,* 3.

CHOI, H. J., KANG, S. W., YANG, C. H., RHEE, S. G. & RYU, S. E. 1998. Crystal structure of a novel human peroxidase enzyme at 2.0 A resolution. *Nat Struct Biol,* 5**,** 400-6.

CONA, A., CENCI, F., CERVELLI, M., FEDERICO, R., MARIOTTINI, P., MORENO, S. & ANGELINI, R. 2003. Polyamine oxidase, a hydrogen peroxide-producing enzyme, is up-regulated by light and down-regulated by auxin in the outer tissues of the maize mesocotyl. *Plant Physiol,* 131**,** 803-13.

COOPER, G. R., BROSTROM, C. O. & BROSTROM, M. A. 1997. Analysis of the endoplasmic reticular Ca2+ requirement for alpha1-antitrypsin processing and transport competence. *Biochem J,* 325 (Pt 3)**,** 601-8.

CORBETT, E. F., MICHALAK, K. M., OIKAWA, K., JOHNSON, S., CAMPBELL, I. D., EGGLETON, P., KAY, C. & MICHALAK, M. 2000. The conformation of calreticulin is influenced by the endoplasmic reticulum luminal environment. *J Biol Chem,* 275**,** 27177-85.

CORBETT, E. F., OIKAWA, K., FRANCOIS, P., TESSIER, D. C., KAY, C., BERGERON, J. J. M., THOMAS, D. Y., KRAUSE, K. H. & MICHALAK, M. 1999. Ca2+ regulation of interactions between endoplasmic reticulum chaperones. *Journal of Biological Chemistry,* 274**,** 6203-6211.

COSSON, P. & LETOURNEUR, F. 1994. Coatomer interaction with di-lysine endoplasmic reticulum retention motifs. *Science,* 263**,** 1629-31.

CUNNEA, P. M., MIRANDA-VIZUETE, A., BERTOLI, G., SIMMEN, T., DAMDIMOPOULOS, A. E., HERMANN, S., LEINONEN, S., HUIKKO, M. P., GUSTAFSSON, J. A., SITIA, R. & SPYROU, G. 2003. ERdj5, an endoplasmic reticulum (ER)-resident protein containing DnaJ and thioredoxin domains, is expressed in secretory cells or following ER stress. *J Biol Chem,* 278**,** 1059-66.

CUOZZO, J. W. & KAISER, C. A. 1999. Competition between glutathione and protein thiols for disulphide-bond formation. *Nat Cell Biol,* 1**,** 130-5.

DELAUNAY, A., PFLIEGER, D., BARRAULT, M. B., VINH, J. & TOLEDANO, M. B. 2002. A thiol peroxidase is an H2O2 receptor and redox-transducer in gene activation. *Cell,* 111**,** 471-81.

DENIC, V., QUAN, E. M. & WEISSMAN, J. S. 2006. A luminal surveillance complex that selects misfolded glycoproteins for ER-associated degradation. *Cell,* 126**,** 349-59.

DEPUYDT, M., LEONARD, S. E., VERTOMMEN, D., DENONCIN, K., MORSOMME, P., WAHNI, K., MESSENS, J., CARROLL, K. S. & COLLET, J. F. 2009. A periplasmic reducing system protects single cysteine residues from oxidation. *Science,* 326**,** 1109-11.

DIAS-GUNASEKARA, S., GUBBENS, J., VAN LITH, M., DUNNE, C., WILLIAMS, J. A., KATAKY, R., SCOONES, D., LAPTHORN, A., BULLEID, N. J. & BENHAM, A. M. 2005. Tissue-specific expression and dimerization of the endoplasmic reticulum oxidoreductase Ero1beta. *J Biol Chem,* 280**,** 33066-75.

DOUGAN, S. K., HU, C. C., PAQUET, M. E., GREENBLATT, M. B., KIM, J., LILLEY, B. N., WATSON, N. & PLOEGH, H. L. 2011. Derlin-2-deficient mice reveal an essential role for protein dislocation in chondrocytes. *Mol Cell Biol,* 31**,** 1145-59.

EDMAN, J. C., ELLIS, L., BLACHER, R. W., ROTH, R. A. & RUTTER, W. J. 1985. Sequence of protein disulphide isomerase and implications of its relationship to thioredoxin. *Nature,* 317**,** 267-70.

EIAMPHUNGPORN, W., SOONSANGA, S., LEE, J. W. & HELMANN, J. D. 2009. Oxidation of a single active site suffices for the functional inactivation of the dimeric Bacillus subtilis OhrR repressor in vitro. *Nucleic Acids Res,* 37**,** 1174-81.

FAGIOLI, C. & SITIA, R. 2001. Glycoprotein quality control in the endoplasmic reticulum. Mannose trimming by endoplasmic reticulum mannosidase I times the proteasomal degradation of unassembled immunoglobulin subunits. *J Biol Chem,* 276**,** 12885-92.

FASS, D. 2008. The Erv family of sulfhydryl oxidases. *Biochimica Et Biophysica Acta-Molecular Cell Research,* 1783**,** 557-566.

FRAND, A. R. & KAISER, C. A. 1998. The ERO1 gene of yeast is required for oxidation of protein dithiols in the endoplasmic reticulum. *Mol Cell,* 1**,** 161-70.

FRAND, A. R. & KAISER, C. A. 1999. Ero1p oxidizes protein disulfide isomerase in a pathway for disulfide bond formation in the endoplasmic reticulum. *Mol Cell,* 4**,** 469-77.

FRAND, A. R. & KAISER, C. A. 2000. Two pairs of conserved cysteines are required for the oxidative activity of Ero1p in protein disulfide bond formation in the endoplasmic reticulum. *Mol Biol Cell,* 11**,** 2833-43.

FREEDMAN, R. B., BULLEID, N. J., HAWKINS, H. C. & PAVER, J. L. 1989. Role of protein disulphide-isomerase in the expression of native proteins. *Biochem Soc Symp,* 55**,** 167-92.

FUCHS, S., DE LORENZO, F. & ANFINSEN, C. B. 1967. Studies on the mechanism of the enzymic catalysis of disulfide interchange in proteins. *J Biol Chem,* 242**,** 398-402.

GEISZT, M., WITTA, J., BAFFI, J., LEKSTROM, K. & LETO, T. L. 2003. Dual oxidases represent novel hydrogen peroxide sources supporting mucosal surface host defense. *FASEB J,* 17**,** 1502-4.

GILBERT, J., OU, W., SILVER, J. & BENJAMIN, T. 2006. Downregulation of protein disulfide isomerase inhibits infection by the mouse polyomavirus. *J Virol,* 80**,** 10868-70.

GILLECE, P., PILON, M. & ROMISCH, K. 2000. The protein translocation channel mediates glycopeptide export across the endoplasmic reticulum membrane. *Proc Natl Acad Sci U S A,* 97**,** 4609-14.

GOLDBERGER, R. F., EPSTEIN, C. J. & ANFINSEN, C. B. 1963. Acceleration of reactivation of reduced bovine pancreatic ribonuclease by a microsomal system from rat liver. *J Biol Chem,* 238**,** 628-35.

GROSS, E., KASTNER, D. B., KAISER, C. A. & FASS, D. 2004. Structure of Ero1p, source of disulfide bonds for oxidative protein folding in the cell. *Cell,* 117**,** 601-10.

GROSS, E., SEVIER, C. S., HELDMAN, N., VITU, E., BENTZUR, M., KAISER, C. A., THORPE, C. & FASS, D. 2006. Generating disulfides enzymatically: reaction products and electron acceptors of the endoplasmic reticulum thiol oxidase Ero1p. *Proc Natl Acad Sci U S A,* 103**,** 299-304.

HALL, A., NELSON, K., POOLE, L. B. & KARPLUS, P. A. 2011. Structure-based insights into the catalytic power and conformational dexterity of peroxiredoxins. *Antioxid Redox Signal,* 15**,** 795-815.

HANSEN, H. G., SCHMIDT, J. D., SOLTOFT, C. L., RAMMING, T., GEERTZ-HANSEN, H. M., CHRISTENSEN, B., SORENSEN, E. S., JUNCKER, A. S., APPENZELLER-HERZOG, C. & ELLGAARD, L. 2012. Hyperactivity of the ero1alpha oxidase elicits endoplasmic reticulum stress but no broad antioxidant response. *J Biol Chem,* 287**,** 39513-23.

HARDING, H. P., ZHANG, Y., ZENG, H., NOVOA, I., LU, P. D., CALFON, M., SADRI, N., YUN, C., POPKO, B., PAULES, R., STOJDL, D. F., BELL, J. C., HETTMANN, T., LEIDEN, J. M. & RON, D. 2003. An integrated stress response regulates amino acid metabolism and resistance to oxidative stress. *Mol Cell,* 11**,** 619-33.

HAYNES, C. M., TITUS, E. A. & COOPER, A. A. 2004. Degradation of misfolded proteins prevents ER-derived oxidative stress and cell death. *Mol Cell,* 15**,** 767-76.

HELDMAN, N., VONSHAK, O., SEVIER, C. S., VITU, E., MEHLMAN, T. & FASS, D. 2010. Steps in reductive activation of the disulfide-generating enzyme Ero1p. *Protein Sci,* 19**,** 1863-76.

HILLSON, D. A. & FREEDMAN, R. B. 1980. Resolution of protein disulphide-isomerase and glutathione-insulin transhydrogenase activities by covalent chromatography. *Biochem J,* 191**,** 373-88.

HOLMGREN, A. & MORGAN, F. J. 1976. Enzyme reduction of disulfide bonds by thioredoxin. The reactivity of disulfide bonds in human choriogonadotropin and its subunits. *Eur J Biochem,* 70**,** 377-83.

HOLMGREN, A., SODERBERG, B. O., EKLUND, H. & BRANDEN, C. I. 1975. Three-dimensional structure of Escherichia coli thioredoxin-S2 to 2.8 A resolution. *Proc Natl Acad Sci U S A,* 72**,** 2305-9.

HOLST, B., TACHIBANA, C. & WINTHER, J. R. 1997. Active site mutations in yeast protein disulfide isomerase cause dithiothreitol sensitivity and a reduced rate of protein folding in the endoplasmic reticulum. *J Cell Biol,* 138**,** 1229-38.

HOOBER, K. L., JONEJA, B., WHITE, H. B., 3RD & THORPE, C. 1996. A sulfhydryl oxidase from chicken egg white. *J Biol Chem,* 271**,** 30510-6.

HOSOKAWA, N., TREMBLAY, L. O., YOU, Z., HERSCOVICS, A., WADA, I. & NAGATA, K. 2003. Enhancement of endoplasmic reticulum (ER) degradation of misfolded Null Hong Kong alpha1-antitrypsin by human ER mannosidase I. *J Biol Chem,* 278**,** 26287-94.

HOSOKAWA, N., WADA, I., HASEGAWA, K., YORIHUZI, T., TREMBLAY, L. O., HERSCOVICS, A. & NAGATA, K. 2001. A novel ER alpha-mannosidase-like protein accelerates ER-associated degradation. *EMBO Rep,* 2**,** 415-22.

HWANG, C., SINSKEY, A. J. & LODISH, H. F. 1992. Oxidized redox state of glutathione in the endoplasmic reticulum. *Science,* 257**,** 1496-502.

IMMENSCHUH, S., BAUMGART-VOGT, E., TAN, M., IWAHARA, S., RAMADORI, G. & FAHIMI, H. D. 2003. Differential cellular and subcellular localization of heme-binding protein 23/peroxiredoxin I and heme oxygenase-1 in rat liver. *J Histochem Cytochem,* 51**,** 1621-31.

INABA, K., MASUI, S., IIDA, H., VAVASSORI, S., SITIA, R. & SUZUKI, M. 2010. Crystal structures of human Ero1alpha reveal the mechanisms of regulated and targeted oxidation of PDI. *EMBO J,* 29**,** 3330-43.

JACKSON, M. R., NILSSON, T. & PETERSON, P. A. 1993. Retrieval of transmembrane proteins to the endoplasmic reticulum. *J Cell Biol,* 121**,** 317-33.

JEONG, W., PARK, S. J., CHANG, T. S., LEE, D. Y. & RHEE, S. G. 2006. Molecular mechanism of the reduction of cysteine sulfinic acid of peroxiredoxin to cysteine by mammalian sulfiredoxin. *J Biol Chem,* 281**,** 14400-7.

JESSOP, C. E. & BULLEID, N. J. 2004. Glutathione directly reduces an oxidoreductase in the endoplasmic reticulum of mammalian cells. *J Biol Chem,* 279**,** 55341-7.

JIN, D. Y., TIE, J. K. & STAFFORD, D. W. 2007. The conversion of vitamin K epoxide to vitamin K quinone and vitamin K quinone to vitamin K hydroquinone uses the same active site cysteines. *Biochemistry,* 46**,** 7279-83.

KIKKERT, M., DOOLMAN, R., DAI, M., AVNER, R., HASSINK, G., VAN VOORDEN, S., THANEDAR, S., ROITELMAN, J., CHAU, V. & WIERTZ, E. 2004. Human HRD1 is an E3 ubiquitin ligase involved in degradation of proteins from the endoplasmic reticulum. *J Biol Chem,* 279**,** 3525-34.

KIM, S., SIDERIS, D. P., SEVIER, C. S. & KAISER, C. A. 2012. Balanced Ero1 activation and inactivation establishes ER redox homeostasis. *J Cell Biol,* 196**,** 713-25.

KSENZENKO, M., KONSTANTINOV, A. A., KHOMUTOV, G. B., TIKHONOV, A. N. & RUUGE, E. K. 1983. Effect of electron transfer inhibitors on superoxide generation in the cytochrome bc1 site of the mitochondrial respiratory chain. *FEBS Lett,* 155**,** 19-24.

KUGE, S., JONES, N. & NOMOTO, A. 1997. Regulation of yAP-1 nuclear localization in response to oxidative stress. *EMBO J,* 16**,** 1710-20.

KULP, M. S., FRICKEL, E. M., ELLGAARD, L. & WEISSMAN, J. S. 2006. Domain architecture of protein-disulfide isomerase facilitates its dual role as an oxidase and an isomerase in Ero1p-mediated disulfide formation. *J Biol Chem,* 281**,** 876-84.

KUSSMAUL, L. & HIRST, J. 2006. The mechanism of superoxide production by NADH:ubiquinone oxidoreductase (complex I) from bovine heart mitochondria. *Proc Natl Acad Sci U S A,* 103**,** 7607-12.

LABOISSIERE, M. C., STURLEY, S. L. & RAINES, R. T. 1995. The essential function of protein-disulfide isomerase is to unscramble non-native disulfide bonds. *J Biol Chem,* 270**,** 28006-9.

LAMANTIA, M. L. & LENNARZ, W. J. 1993. The essential function of yeast protein disulfide isomerase does not reside in its isomerase activity. *Cell,* 74**,** 899-908.

LAPPI, A. K., LENSINK, M. F., ALANEN, H. I., SALO, K. E., LOBELL, M., JUFFER, A. H. & RUDDOCK, L. W. 2004. A conserved arginine plays a role in the catalytic cycle of the protein disulphide isomerases. *J Mol Biol,* 335**,** 283-95.

LEE, W., CHOI, K. S., RIDDELL, J., IP, C., GHOSH, D., PARK, J. H. & PARK, Y. M. 2007. Human peroxiredoxin 1 and 2 are not duplicate proteins: the unique presence of CYS83 in Prx1 underscores the structural and functional differences between Prx1 and Prx2. *J Biol Chem,* 282**,** 22011-22.

LILLEY, B. N. & PLOEGH, H. L. 2004. A membrane protein required for dislocation of misfolded proteins from the ER. *Nature,* 429**,** 834-40.

LODISH, H. F. & KONG, N. 1990. Perturbation of Cellular Calcium Blocks Exit of Secretory Proteins from the Rough Endoplasmic-Reticulum. *Journal of Biological Chemistry,* 265**,** 10893-10899.

LODISH, H. F., KONG, N. & WIKSTROM, L. 1992. Calcium is required for folding of newly made subunits of the asialoglycoprotein receptor within the endoplasmic reticulum. *J Biol Chem,* 267**,** 12753-60.

LYLES, M. M. & GILBERT, H. F. 1991. Catalysis of the oxidative folding of ribonuclease A by protein disulfide isomerase: dependence of the rate on the composition of the redox buffer. *Biochemistry,* 30**,** 613-9.

MAINARDI, J. L., HUGONNET, J. E., RUSCONI, F., FOURGEAUD, M., DUBOST, L., MOUMI, A. N., DELFOSSE, V., MAYER, C., GUTMANN, L., RICE, L. B. & ARTHUR, M. 2007. Unexpected inhibition of peptidoglycan LD-transpeptidase from Enterococcus faecium by the beta-lactam imipenem. *J Biol Chem,* 282**,** 30414-22.

MARCINIAK, S. J., YUN, C. Y., OYADOMARI, S., NOVOA, I., ZHANG, Y., JUNGREIS, R., NAGATA, K., HARDING, H. P. & RON, D. 2004. CHOP induces death by promoting protein synthesis and oxidation in the stressed endoplasmic reticulum. *Genes Dev,* 18**,** 3066-77.

MARGITTAI, E., LOW, P., STILLER, I., GRECO, A., GARCIA-MANTEIGA, J. M., PENGO, N., BENEDETTI, A., SITIA, R. & BANHEGYI, G. 2012. Production of H(2)O(2) in the endoplasmic reticulum promotes in vivo disulfide bond formation. *Antioxid Redox Signal,* 16**,** 1088-99.

MASUI, S., VAVASSORI, S., FAGIOLI, C., SITIA, R. & INABA, K. 2011. Molecular bases of cyclic and specific disulfide interchange between human ERO1alpha protein and protein-disulfide isomerase (PDI). *J Biol Chem,* 286**,** 16261-71.

MATSUSHIMA, S., IDE, T., YAMATO, M., MATSUSAKA, H., HATTORI, F., IKEUCHI, M., KUBOTA, T., SUNAGAWA, K., HASEGAWA, Y., KURIHARA,

T., OIKAWA, S., KINUGAWA, S. & TSUTSUI, H. 2006. Overexpression of mitochondrial peroxiredoxin-3 prevents left ventricular remodeling and failure after myocardial infarction in mice. *Circulation,* 113**,** 1779-86.

MAY, D., ITIN, A., GAL, O., KALINSKI, H., FEINSTEIN, E. & KESHET, E. 2005. Ero1-L alpha plays a key role in a HIF-1-mediated pathway to improve disulfide bond formation and VEGF secretion under hypoxia: implication for cancer. *Oncogene,* 24**,** 1011-20.

MCCRACKEN, A. A. & BRODSKY, J. L. 1996. Assembly of ER-associated protein degradation in vitro: dependence on cytosol, calnexin, and ATP. *J Cell Biol,* 132**,** 291-8.

MELDOLESI, J. & POZZAN, T. 1998. The endoplasmic reticulum Ca2+ store: a view from the lumen. *Trends Biochem Sci,* 23**,** 10-4.

MEZGHRANI, A., FASSIO, A., BENHAM, A., SIMMEN, T., BRAAKMAN, I. & SITIA, R. 2001. Manipulation of oxidative protein folding and PDI redox state in mammalian cells. *EMBO J,* 20**,** 6288-96.

MIMURA, N., YUASA, S., SOMA, M., JIN, H., KIMURA, K., GOTO, S., KOSEKI, H. & AOE, T. 2008. Altered quality control in the endoplasmic reticulum causes cortical dysplasia in knock-in mice expressing a mutant BiP. *Mol Cell Biol,* 28**,** 293-301.

MOLINARI, M., CALANCA, V., GALLI, C., LUCCA, P. & PAGANETTI, P. 2003. Role of EDEM in the release of misfolded glycoproteins from the calnexin cycle. *Science,* 299**,** 1397-400.

MOLLER, J. V., OLESEN, C., WINTHER, A. M. & NISSEN, P. 2010. The sarcoplasmic Ca2+-ATPase: design of a perfect chemi-osmotic pump. *Q Rev Biophys,* 43**,** 501-66.

MOLTENI, S. N., FASSIO, A., CIRIOLO, M. R., FILOMENI, G., PASQUALETTO, E., FAGIOLI, C. & SITIA, R. 2004. Glutathione limits Ero1-dependent oxidation in the endoplasmic reticulum. *J Biol Chem,* 279**,** 32667-73.

MOORE, S. F. & MACKENZIE, A. B. 2009. NADPH oxidase NOX2 mediates rapid cellular oxidation following ATP stimulation of endotoxin-primed macrophages. *J Immunol,* 183**,** 3302-8.

MUNRO, S. & PELHAM, H. R. 1987. A C-terminal signal prevents secretion of luminal ER proteins. *Cell,* 48**,** 899-907.

NELSON, K. J., PARSONAGE, D., HALL, A., KARPLUS, P. A. & POOLE, L. B. 2008. Cysteine pK(a) values for the bacterial peroxiredoxin AhpC. *Biochemistry,* 47**,** 12860-8.

NGUYEN, V. D., SAARANEN, M. J., KARALA, A. R., LAPPI, A. K., WANG, L., RAYKHEL, I. B., ALANEN, H. I., SALO, K. E., WANG, C. C. & RUDDOCK, L. W. 2011. Two endoplasmic reticulum PDI peroxidases increase the efficiency of the use of peroxide during disulfide bond formation. *J Mol Biol,* 406**,** 503-15.

NGUYEN, V. D., WALLIS, K., HOWARD, M. J., HAAPALAINEN, A. M., SALO, K. E., SAARANEN, M. J., SIDHU, A., WIERENGA, R. K., FREEDMAN, R. B., RUDDOCK, L. W. & WILLIAMSON, R. A. 2008. Alternative conformations of the x region of human protein disulphide-isomerase modulate exposure of the substrate binding b' domain. *J Mol Biol,* 383**,** 1144-55.

NIGAM, S. K., GOLDBERG, A. L., HO, S., ROHDE, M. F., BUSH, K. T. & SHERMAN, M. 1994. A set of endoplasmic reticulum proteins possessing properties of molecular chaperones includes Ca(2+)-binding proteins and members of the thioredoxin superfamily. *J Biol Chem,* 269**,** 1744-9.

NILSSON, T., JACKSON, M. & PETERSON, P. A. 1989. Short cytoplasmic sequences serve as retention signals for transmembrane proteins in the endoplasmic reticulum. *Cell,* 58**,** 707-18.

NILSSON, T., RABOUILLE, C., HUI, N., WATSON, R. & WARREN, G. 1996. The role of the membrane-spanning domain and stalk region of N-acetylglucosaminyltransferase I in retention, kin recognition and structural maintenance of the Golgi apparatus in HeLa cells. *J Cell Sci,* 109 (Pt 7)**,** 1975-89.

ODA, Y., OKADA, T., YOSHIDA, H., KAUFMAN, R. J., NAGATA, K. & MORI, K. 2006. Derlin-2 and Derlin-3 are regulated by the mammalian unfolded protein response and are required for ER-associated degradation. *J Cell Biol,* 172**,** 383-93.

OKUDA-SHIMIZU, Y. & HENDERSHOT, L. M. 2007. Characterization of an ERAD pathway for nonglycosylated BiP substrates, which require Herp. *Mol Cell,* 28**,** 544-54.

OSTERGAARD, H., TACHIBANA, C. & WINTHER, J. R. 2004. Monitoring disulfide bond formation in the eukaryotic cytosol. *J Cell Biol,* 166**,** 337-45.

PAGANI, M., FABBRI, M., BENEDETTI, C., FASSIO, A., PILATI, S., BULLEID, N. J., CABIBBO, A. & SITIA, R. 2000. Endoplasmic reticulum oxidoreductin 1-lbeta (ERO1-Lbeta), a human gene induced in the course of the unfolded protein response. *J Biol Chem,* 275**,** 23685-92.

PAGANI, M., PILATI, S., BERTOLI, G., VALSASINA, B. & SITIA, R. 2001. The C-terminal domain of yeast Ero1p mediates membrane localization and is essential for function. *FEBS Lett,* 508**,** 117-20.

PAULING, L. & COREY, R. B. 1951a. Atomic coordinates and structure factors for two helical configurations of polypeptide chains. *Proc Natl Acad Sci U S A,* 37**,** 235-40.

PAULING, L. & COREY, R. B. 1951b. The pleated sheet, a new layer configuration of polypeptide chains. *Proc Natl Acad Sci U S A,* 37**,** 251-6.

PAULSEN, C. E. & CARROLL, K. S. 2009. Chemical dissection of an essential redox switch in yeast. *Chem Biol,* 16**,** 217-25.

PESKIN, A. V., LOW, F. M., PATON, L. N., MAGHZAL, G. J., HAMPTON, M. B. & WINTERBOURN, C. C. 2007. The high reactivity of peroxiredoxin 2 with H(2)O(2) is not reflected in its reaction with other oxidants and thiol reagents. *J Biol Chem,* 282**,** 11885-92.

PHALEN, T. J., WEIRATHER, K., DEMING, P. B., ANATHY, V., HOWE, A. K., VAN DER VLIET, A., JONSSON, T. J., POOLE, L. B. & HEINTZ, N. H. 2006. Oxidation state governs structural transitions in peroxiredoxin II that correlate with cell cycle arrest and recovery. *J Cell Biol,* 175**,** 779-89.

POLLARD, M. G., TRAVERS, K. J. & WEISSMAN, J. S. 1998. Ero1p: a novel and ubiquitous protein with an essential role in oxidative protein folding in the endoplasmic reticulum. *Mol Cell,* 1**,** 171-82.

RAJAGOPALAN, S., XU, Y. & BRENNER, M. B. 1994. Retention of unassembled components of integral membrane proteins by calnexin. *Science,* 263**,** 387-90.

RAMOS, A. M., FERNANDEZ, C., AMRAN, D., SANCHO, P., DE BLAS, E. & ALLER, P. 2005. Pharmacologic inhibitors of PI3K/Akt potentiate the apoptotic action of the antileukemic drug arsenic trioxide via glutathione depletion and increased peroxide accumulation in myeloid leukemia cells. *Blood,* 105**,** 4013-20.

REDDIE, K. G., SEO, Y. H., MUSE III, W. B., LEONARD, S. E. & CARROLL, K. S. 2008. A chemical approach for detecting sulfenic acid-modified proteins in living cells. *Mol Biosyst,* 4**,** 521-31.

RUTKEVICH, L. A., COHEN-DOYLE, M. F., BROCKMEIER, U. & WILLIAMS, D. B. 2010. Functional relationship between protein disulfide isomerase family members during the oxidative folding of human secretory proteins. *Mol Biol Cell,* 21**,** 3093-105.

SAARANEN, M. J., KARALA, A. R., LAPPI, A. K. & RUDDOCK, L. W. 2010. The role of dehydroascorbate in disulfide bond formation. *Antioxid Redox Signal,* 12**,** 15-25.

SCHERENS, B., DUBOIS, E. & MESSENGUY, F. 1991. Determination of the sequence of the yeast YCL313 gene localized on chromosome III. Homology with the protein disulfide isomerase (PDI gene product) of other organisms. *Yeast,* 7**,** 185-93.

SCHEUNER, D. & KAUFMAN, R. J. 2008. The unfolded protein response: a pathway that links insulin demand with beta-cell failure and diabetes. *Endocr Rev,* 29**,** 317-33.

SCHNEIDER, C. A., RASBAND, W. S. & ELICEIRI, K. W. 2012. NIH Image to ImageJ: 25 years of image analysis. *Nat Methods,* 9**,** 671-5.

SCHULMAN, S., WANG, B., LI, W. & RAPOPORT, T. A. 2010. Vitamin K epoxide reductase prefers ER membrane-anchored thioredoxin-like redox partners. *Proc Natl Acad Sci U S A,* 107**,** 15027-32.

SCHUTZE, M. P., PETERSON, P. A. & JACKSON, M. R. 1994. An N-terminal double-arginine motif maintains type II membrane proteins in the endoplasmic reticulum. *EMBO J,* 13**,** 1696-705.

SEO, Y. H. & CARROLL, K. S. 2009. Profiling protein thiol oxidation in tumor cells using sulfenic acid-specific antibodies. *Proc Natl Acad Sci U S A,* 106**,** 16163-8.

SEVIER, C. S. & KAISER, C. A. 2006. Disulfide transfer between two conserved cysteine pairs imparts selectivity to protein oxidation by Ero1. *Mol Biol Cell,* 17**,** 2256-66.

SEVIER, C. S. & KAISER, C. A. 2008. Ero1 and redox homeostasis in the endoplasmic reticulum. *Biochim Biophys Acta,* 1783**,** 549-56.

SEVIER, C. S., QU, H., HELDMAN, N., GROSS, E., FASS, D. & KAISER, C. A. 2007. Modulation of cellular disulfide-bond formation and the ER redox environment by feedback regulation of Ero1. *Cell,* 129**,** 333-44.

SOLDA, T., GALLI, C., KAUFMAN, R. J. & MOLINARI, M. 2007. Substrate-specific requirements for UGT1-dependent release from calnexin. *Mol Cell,* 27**,** 238-49.

SOMLYO, A. P., BOND, M. & SOMLYO, A. V. 1985. Calcium content of mitochondria and endoplasmic reticulum in liver frozen rapidly in vivo. *Nature,* 314**,** 622-5.

SONG, Y., DRIESSENS, N., COSTA, M., DE DEKEN, X., DETOURS, V., CORVILAIN, B., MAENHAUT, C., MIOT, F., VAN SANDE, J., MANY, M. C. & DUMONT, J. E. 2007. Roles of hydrogen peroxide in thyroid physiology and disease. *J Clin Endocrinol Metab,* 92**,** 3764-73.

SUN, J. & TRUMPOWER, B. L. 2003. Superoxide anion generation by the cytochrome bc1 complex. *Arch Biochem Biophys,* 419**,** 198-206.

SWANTON, E. & BULLEID, N. J. 2003. Protein folding and translocation across the endoplasmic reticulum membrane. *Mol Membr Biol,* 20**,** 99-104.

TAVENDER, T. J. & BULLEID, N. J. 2010. Peroxiredoxin IV protects cells from oxidative stress by removing H2O2 produced during disulphide formation. *J Cell Sci,* 123**,** 2672-9.

TAVENDER, T. J., SHEPPARD, A. M. & BULLEID, N. J. 2008. Peroxiredoxin IV is an endoplasmic reticulum-localized enzyme forming oligomeric complexes in human cells. *Biochem J,* 411**,** 191-9.

TAVENDER, T. J., SPRINGATE, J. J. & BULLEID, N. J. 2010. Recycling of peroxiredoxin IV provides a novel pathway for disulphide formation in the endoplasmic reticulum. *EMBO J,* 29**,** 4185-97.

TIAN, F., ZHOU, X., WIKSTROM, J., KARLSSON, H., SJOLAND, H., GAN, L. M., BOREN, J. & AKYUREK, L. M. 2009. Protein disulfide isomerase increases in myocardial endothelial cells in mice exposed to chronic hypoxia: a stimulatory role in angiogenesis. *Am J Physiol Heart Circ Physiol,* 297**,** H1078-86.

TOKUHIRO, K., IKAWA, M., BENHAM, A. M. & OKABE, M. 2012. Protein disulfide isomerase homolog PDILT is required for quality control of sperm membrane protein ADAM3 and male fertility [corrected]. *Proc Natl Acad Sci U S A,* 109**,** 3850-5.

TU, B. P., HO-SCHLEYER, S. C., TRAVERS, K. J. & WEISSMAN, J. S. 2000. Biochemical basis of oxidative protein folding in the endoplasmic reticulum. *Science,* 290**,** 1571-4.

TU, B. P. & WEISSMAN, J. S. 2002. The FAD- and O(2)-dependent reaction cycle of Ero1-mediated oxidative protein folding in the endoplasmic reticulum. *Mol Cell,* 10**,** 983-94.

USHIODA, R., HOSEKI, J., ARAKI, K., JANSEN, G., THOMAS, D. Y. & NAGATA, K. 2008. ERdj5 is required as a disulfide reductase for degradation of misfolded proteins in the ER. *Science,* 321**,** 569-72.

VAN LITH, M., HARTIGAN, N., HATCH, J. & BENHAM, A. M. 2005. PDILT, a divergent testis-specific protein disulfide isomerase with a non-classical SXXC motif that engages in disulfide-dependent interactions in the endoplasmic reticulum. *J Biol Chem,* 280**,** 1376-83.

VAN LITH, M., TIWARI, S., PEDIANI, J., MILLIGAN, G. & BULLEID, N. J. 2011. Real-time monitoring of redox changes in the mammalian endoplasmic reticulum. *J Cell Sci,* 124**,** 2349-56.

VAN MONTFORT, R. L., CONGREVE, M., TISI, D., CARR, R. & JHOTI, H. 2003. Oxidation state of the active-site cysteine in protein tyrosine phosphatase 1B. *Nature,* 423**,** 773-7.

VAN, P. N., PETER, F. & SOLING, H. D. 1989. Four intracisternal calcium-binding glycoproteins from rat liver microsomes with high affinity for calcium. No

indication for calsequestrin-like proteins in inositol 1,4,5-trisphosphate-sensitive calcium sequestering rat liver vesicles. *J Biol Chem,* 264**,** 17494-501.

WAGNER, E., LUCHE, S., PENNA, L., CHEVALLET, M., VAN DORSSELAER, A., LEIZE-WAGNER, E. & RABILLOUD, T. 2002. A method for detection of overoxidation of cysteines: peroxiredoxins are oxidized in vivo at the active-site cysteine during oxidative stress. *Biochem J,* 366**,** 777-85.

WAHLMAN, J., DEMARTINO, G. N., SKACH, W. R., BULLEID, N. J., BRODSKY, J. L. & JOHNSON, A. E. 2007. Real-time fluorescence detection of ERAD substrate retrotranslocation in a mammalian in vitro system. *Cell,* 129**,** 943-55.

WAJIH, N., HUTSON, S. M. & WALLIN, R. 2007. Disulfide-dependent protein folding is linked to operation of the vitamin K cycle in the endoplasmic reticulum. A protein disulfide isomerase-VKORC1 redox enzyme complex appears to be responsible for vitamin K1 2,3-epoxide reduction. *J Biol Chem,* 282**,** 2626-35.

WANG, L., LI, S. J., SIDHU, A., ZHU, L., LIANG, Y., FREEDMAN, R. B. & WANG, C. C. 2009. Reconstitution of human Ero1-Lalpha/protein-disulfide isomerase oxidative folding pathway in vitro. Position-dependent differences in role between the a and a' domains of protein-disulfide isomerase. *J Biol Chem,* 284**,** 199-206.

WIERTZ, E. J., TORTORELLA, D., BOGYO, M., YU, J., MOTHES, W., JONES, T. R., RAPOPORT, T. A. & PLOEGH, H. L. 1996. Sec61-mediated transfer of a membrane protein from the endoplasmic reticulum to the proteasome for destruction. *Nature,* 384**,** 432-8.

WILSON, D. W., LEWIS, M. J. & PELHAM, H. R. 1993. pH-dependent binding of KDEL to its receptor in vitro. *J Biol Chem,* 268**,** 7465-8.

WOOD, M. J., STORZ, G. & TJANDRA, N. 2004. Structural basis for redox regulation of Yap1 transcription factor localization. *Nature,* 430**,** 917-21.

WU, M. M., GRABE, M., ADAMS, S., TSIEN, R. Y., MOORE, H. P. & MACHEN, T. E. 2001. Mechanisms of pH regulation in the regulated secretory pathway. *J Biol Chem,* 276**,** 33027-35.

YE, Y., MEYER, H. H. & RAPOPORT, T. A. 2001. The AAA ATPase Cdc48/p97 and its partners transport proteins from the ER into the cytosol. *Nature,* 414**,** 652-6.

YE, Y., SHIBATA, Y., KIKKERT, M., VAN VOORDEN, S., WIERTZ, E. & RAPOPORT, T. A. 2005. Recruitment of the p97 ATPase and ubiquitin ligases to the site of retrotranslocation at the endoplasmic reticulum membrane. *Proc Natl Acad Sci U S A,* 102**,** 14132-8.

YE, Y., SHIBATA, Y., YUN, C., RON, D. & RAPOPORT, T. A. 2004. A membrane protein complex mediates retro-translocation from the ER lumen into the cytosol. *Nature,* 429**,** 841-7.

ZAPUN, A., DARBY, N. J., TESSIER, D. C., MICHALAK, M., BERGERON, J. J. M. & THOMAS, D. Y. 1998. Enhanced catalysis of ribonuclease B folding by the interaction of calnexin or calreticulin with ERp57. *Journal of Biological Chemistry,* 273**,** 6009-6012.

ZITO, E., MELO, E. P., YANG, Y., WAHLANDER, A., NEUBERT, T. A. & RON, D. 2010. Oxidative protein folding by an endoplasmic reticulum-localized peroxiredoxin. *Mol Cell,* 40**,** 787-97.

Appendix 1 .

Size exclusion gel filtration calibration curve.

Before analysing Ero1α by size exclusion gel filtration chromatography, a calibration curve was calculated using proteins of known molecular weight. Cytochrome C (12.3 kDa), ribonuclease A (13.7 kDa), ovalbumin (43 kDa), bovine serum albumin (67 kDa) and thyroglobulin (669 kDa) were loaded onto the column and their elution volumes recorded. Blue dextran was loaded onto the column to calculate the void volume of 7.8 ml. The column volume is 24 ml.The Kav value for each elution volume was calculated using the equation:

$$Kav = \frac{\text{Volume of elution} - \text{Void volume}}{\text{Column volume} - \text{Void volume}}$$

The Kav value was plotted against the log of the molecular weight for each protein and the line of best fit was drawn (Appendix 1), with the equation:

$$y = -0.3106x + 1.8825$$

where y is the Kav value and x is the log value of the molecular weight. This equation was then used to calculate the molecular weight of Ero1α after obtaining its elution volume.

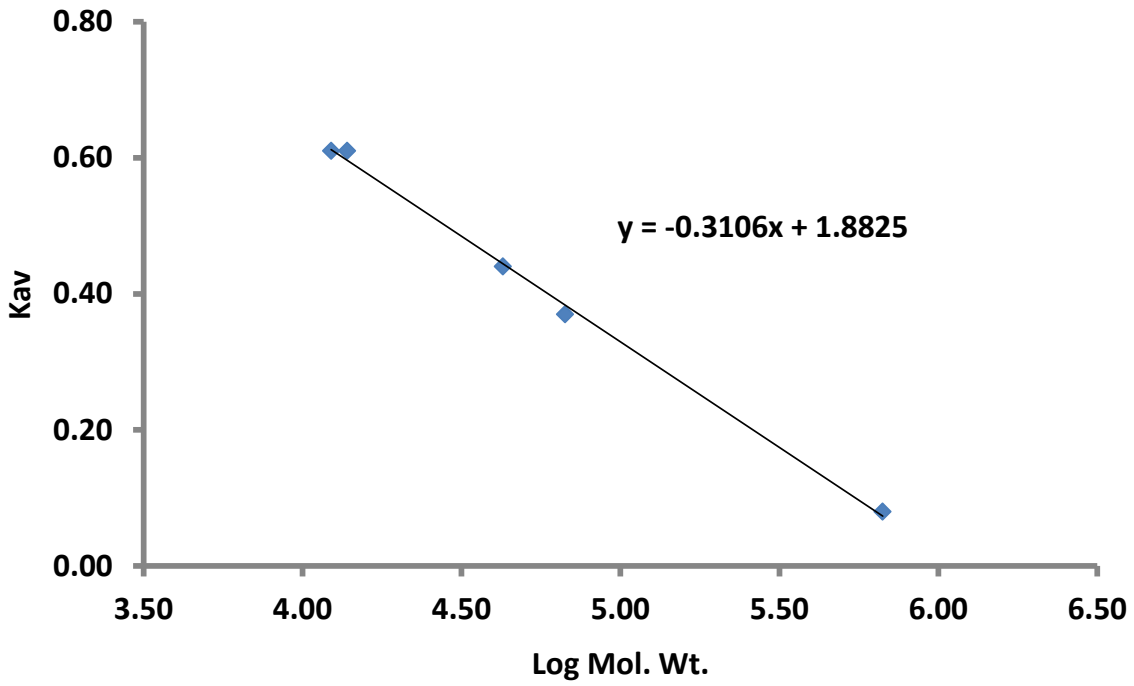

Appendix 2.

PDI wild type and binding mutant purification.

Wild type PDI was expressed and purified as described in Chapter 2.4.2. Analysis of samples taken before and after induction show that PDI expression is induced by IPTG (Appendix 2A, Lanes 1 & 2) as PDI can be seen as a band running at approximately 55 kDa. Cells were lysed and centrifuged at high speed to remove insoluble matter (Lane 3). This clarified lysate was then loaded onto a HisTrap column, and a sample of unbound material from the flowthrough was taken (Lane 4). Comparatively little PDI remains unbound, whereas the majority of *E. coli* proteins are unbound. After a linear gradient elution with up to 500 mM imidazole, bound material is released and contains PDI. Lanes 5 and 6 correspond to protein containing fractions which were eluted.

In addition to the wild type PDI enzyme, a PDI binding mutant used in previous studies (Nguyen et al., 2008) was purified from a plasmid vector kindly gifted by Prof. Lloyd Ruddock. This binding mutant contains a His-tag and three point mutations that abolish binding of PDI to substrates (I272A, D346A, D348A). The plasmid was expressed in Origami B (DE3) pLysS *E. coli* cells. The 55 kDa band that appears post-induction (comparing Appendix 2B, lanes 1 and 2) corresponds to the molecular weight of PDI. Cells were lysed (lane 3) and clarified by centrifugation (lane 4). After washing the column, A number of contaminating bands persisted after HisTrap elution (lanes 6 – 8). Size exclusion gel filtration was able to remove a number of these contaminants although one contaminating band exists at approximately 26 kDa (Appendix 2C). This may be a cleavage product or a remaining *E. coli* protein.

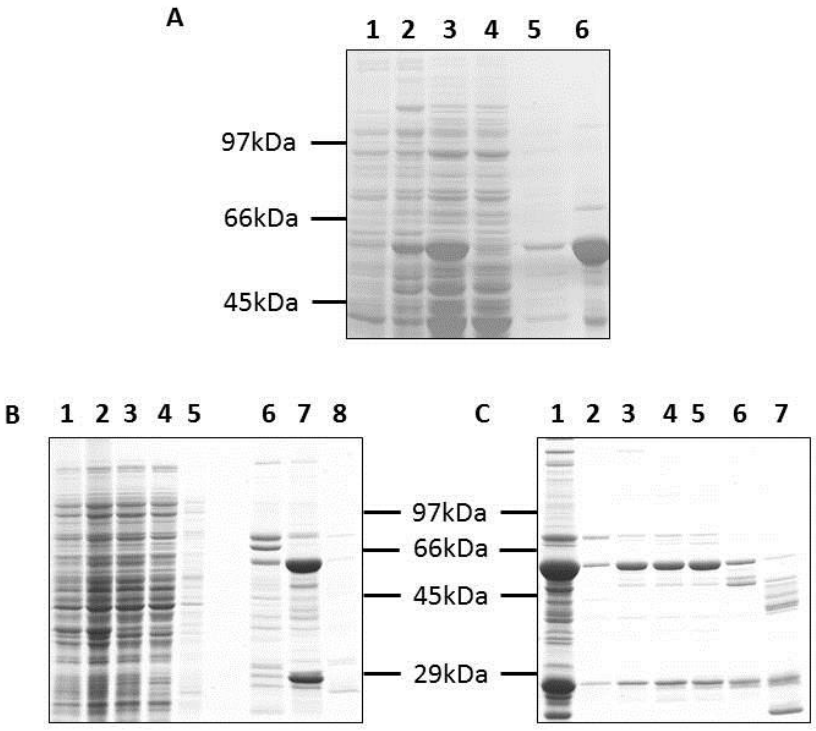

Appendix 2 – SDS-PAGE analysis of the expression and purification of wild type PDI and PDI binding mutant. A – Wild type PDI was expressed in Origami *E. coli* bacteria with samples taken before and after induction with IPTG (lanes 1 and 2). Cells were lysed and clarified (lane 3) before loading onto a HisTrap column. Unbound material (lane 4) contained little PDI; PDI was eluted in imidazole-containing buffer (lanes 5 & 6). B – Expression and purification of the PDI binding mutant by nickel affinity. The PDI binding mutant was purified using a HisTrap column. Samples were taken before and after induction (lanes 1 & 2), and clarifying the cell lysate (lane 3). Material remaining unbound to the nickel-agarose column contained little PDI (lane 4). The column was washed (lane 5) prior to elution with imidazole-containing buffer. Protein-containing fractions were run to determine which contained the PDI mutant (lanes 6, 7 & 8). C – Removal of contaminants from the PDI binding mutant preparation by size-exclusion gel filtration. Fractions containing PDI from the HisTrap purification were pooled and concentrated (lane 1) before passing through the gel filtration column. Samples from the protein containing fractions were analysed by SDS-PAGE (lanes 2 – 7).